THE UNIVERSITY OF MICHIGAN

INDUSTRY PROGRAM OF THE COLLEGE OF ENGINEERING

A STUDY OF TARGET TEMPERATURES IN THE FOCUS OF A CYLINDRICAL PARABOLIC SOLAR CONCENTRATOR

Milan H. Cobble

A dissertation submitted in partial fulfillment
of the requirements for the degree of
Doctor of Philosophy in the
University of Michigan
1958

August, 1958

IP-310

enson

UMR1242

Doctoral Committee:

Professor R. Clay Porter, Chairman
Professor Floyd N. Calhoun
Associate Professor Glenn V. Edmonson
Professor William W. Hagerty, University of Delaware
Associate Professor Jesse L. York

PREFACE

Future generations will almost certainly be forced to utilize solar radiation to supply some of their energy requirements.

To be able to predict the temperature that objects will achieve when heated by solar energy would seem both desirable and a necessary prerequisite to intelligent utilization of this energy. In the field of direct solar energy utilization there are three natural classifications: (1) No concentration, which is characterized typically by black plates under glass, in which the state of knowledge is well-developed; (2) Medium concentration, characterized typically by singly-curved mirrors, in which there is literally no information; (3) High concentration, characterized by solar furnaces, in which the mirrors are typically formed from doubly-curved surfaces, which is in a state of knowledge between that of (1) and (2). This dissertation attempts to fill in some of the gaps in knowledge in the medium concentration area.

The author wishes to gratefully acknowledge the aid of those who contributed to the completion of this thesis. Acknowledgment is given to Mr. E. B. Shand of the Corning Glass Works, who gave information on the properties of pyrex glass. I wish also to thank the Doctoral Committee which aided in defining the subject matter that this thesis was to investigate, Mr. Norman Foster of the United States Weather Bureau, who took time from his duties to calibrate the pyrheliometer at the United States Bureau of Standards in Washington, D. C., and Mr. Dan Boehm for his advice and aid in machining parts of the pyrheliometer and the concentrator. Special thanks are due my wife, Nancy, for the typing of the original draft of the thesis.

TABLE OF CONTENTS

TABLE OF CONTENTS (CONT'D)

LIST OF TABLES

LIST OF TABLES (CONT'D)

LIST OF FIGURES

LIST OF FIGURES (CONT'D)

LIST OF PLATES

NOMENCLATURE

A_{cy} = Area of cylindrical target, ft^2

A_{cyn} = Normal area of cylinder, ft^2

A_{gli} = Inside area of thin hollow glass cylinder, ft^2

A_{glo} = Outside area of thin hollow glass cylinder, ft^2

A_{nm} = Area of mirror normal to radiation, ft^2

$A_{nm'}$ = Area of mirror normal to radiation without target, ft^2

A_p = Area of plate target, ft^2

A_{pn} = Area of plate target normal to radiation, ft^2

c = Specific heat, $Btu/lb_m\,^\circ R$

C = Fraction of mirror exposed to radiation, dimensionless

C_a = Natural convection coefficient for flat plate, $Btu/hr\ ft^2\,^\circ R^{1.25}$

C_b = Forced convection coefficient for flat plate, $Btu/hr\ ft^2\,^\circ R$

C_c = Natural convection coefficient for cylinder, $Btu/hr\ ft^2\,^\circ R^{1.25}$

C_d = Forced convection coefficient for cylinder, $Btu/hr\ ft^2\,^\circ R$

C_e = Equivalent combined conduction and convection coefficient, $Btu\ ft/hr\ ft^2\,^\circ R^{1.258}$

d = Prefix, indicating differential, dimensionless

D = Diameter of a circular tube of equal exposed surface as a flat plate, ft

D_{cy} = Diameter of cylindrical target, ft

D_{gli} = Inside diameter of thin hollow glass cylinder, ft

D_{glo} = Outside diameter of thin hollow glass cylinder, ft

F_a = Configuration factor, a function of the configuration of the surfaces involved, dimensionless

F_e = A factor to allow for the departure of the surfaces involved from complete blackness, a function of the emissivities ϵ_p and ϵ_{gli} as well as the configuration of the surfaces, dimensionless

g = Acceleration of gravity, 4.17×10^8 ft/hr^2

h = Film coefficient, Btu/hr ft^2 °R

H_s = Radiation rate from the sun as determined by pyrheliometer, Btu/hr ft^2

H_{sk} = Radiation rate from the sky as determined by pyrheliometer, Btu/hr ft^2

H_T = Total radiation rate as determined by pyrheliometer, Btu/hr ft^2

K_c = Equivalent conductivity, Btu ft/hr ft^2 °R

K_f = Conductivity at film temperature, Btu ft/hr ft^2 °R

K_m = Mean conductivity, Btu ft/hr ft^2 °R

L = Characteristic length, ft

m = Mass, lb_m

M_f = Modulus at film temperature

n = Relative aperture, dimensionless

N_f = Modulus at film temperature

N_{Gr} = Grashof Number, dimensionless

N_{Nu} = Nusselt Number, dimensionless

N_{Pr} = Prandtl Number, dimensionless

N_{Re} = Reynolds Number, dimensionless

Q_a = Rate of energy addition, Btu/hr

Q_c = Rate of energy loss by convection, Btu/hr

Q_ℓ = Rate of energy loss, Btu/hr

Q_r = Rate of energy loss by radiation, Btu/hr

Q_s = Rate of energy addition from the sun, Btu/hr

Q_{sd} = Rate of energy addition from the sun direct, Btu/hr

Q_{si} = Rate of energy addition from the sun indirect, Btu/hr

Q_{sk} = Rate of energy addition from the sky, Btu/hr

Q_{skd} = Rate of energy addition from the sky direct, Btu/hr

Q_{ski} = Rate of energy addition from the sky indirect, Btu/hr

Q_u = Rate of energy utilization, Btu/hr

R = Reflectivity of mirror for solar radiation, dimensionless

T_{cy} = Temperature of cylindrical target, °R

T_f = Film temperature, °R

T_{gli} = Temperature of inside surface of thin hollow glass cylinder, °R

T_{glo} = Temperature of outside surface of thin hollow glass cylinder, °R

T_o = Temperature of air, °R

T_p = Temperature of plate target, °R

T_s = Temperature of surroundings, °R

V = Velocity of air, ft/hr

$\frac{\alpha}{2}$ = Angle subtended by 1/2 sun's diameter

α_{sk} = Absorbtivity for sky radiation, dimensionless

α_{si} = Absorbtivity for indirect solar radiation, dimensionless

α_{sn} = Absorbtivity for normal solar radiation, dimensionless

α_{sd} = Absorbtivity for direct solar radiation, dimensionless

β_f = Coefficient of volumetric expansion at T_f, $\frac{1}{°R}$

ΔT = Temperature difference, °R

ϵ = Emissivity, dimensionless

ϵ_{glo} = Emissivity of outside surface of thin hollow glass cylinder, dimensionless

ϵ_p = Emissivity of target plate, dimensionless

θ = Time, hr

μ_f = Viscosity at T_f, $lb_m/hr\ ft$

ν_f = Kinematic viscosity at T_f, ft^2/hr

σ = Stefan-Boltzmann constant, $.173 \times 10^{-8}$ $Btu/hr\ ft^2\ ^\circ R^4$

$\tau_r\tau_a$ = Transmission factor through glass, dimensionless

τ_a = Absorbtivity factor of glass, dimensionless

τ_{asd} = Absorbtivity factor of glass for sun direct radiation, dimensionless

τ_{asi} = Absorbtivity factor of glass for sun indirect radiation, dimensionless

τ_{ask} = Absorbtivity factor of glass for sky radiation, dimensionless

τ_{askn} = Absorbtivity factor of glass for normal sky radiation, dimensionless

τ_r = Reflection factor of glass, dimensionless

τ_{rsd} = Reflection factor of glass for sun direct radiation, dimensionless

τ_{rsi} = Reflection factor of glass for sun indirect radiation, dimensionless

τ_{rsk} = Reflection factor of glass for sky radiation, dimensionless

τ_{rskn} = Reflection factor of glass for normal sky radiation, dimensionless

INTRODUCTION

Solar concentrators have an ancient heritage. According to the literature they have been in use for over two thousand years. In the past it was sufficient to know that it was possible, by shaping certain metals in a prescribed manner, to heat and indeed to melt most existing materials.

It is conceivable that in the future we may be forced to utilize some of the sun's energy to replace, at least in part, some of our energy requirements now supplied by our dwindling supply of fossile fuels. However, efficient utilization of this energy must be preceded by investigation and research into the temperatures that can be attained by a target placed at the focus of a solar concentrator.

The field of solar energy utilization has three natural subdivisions. The first subdivision is that of no concentration, typified by flat plate absorbers. The field has been well investigated and the theory, as developed by H. C. Hottel and B. B. Woertz is well substantiated by numerous investigators. The second category concerns medium concentration which has an ideal upper limit of concentration of approximately 215 times. This category is represented by the parabolic cylinder. No theory exists for this category. The third subdivision is that of high concentration and is typified in use by the solar furnaces. These are usually paraboloids of revolution that are in theory capable of concentrating radiation some 46,100 times under ideal conditions. The best work to date in this area is an analysis "Theoretical Considerations On the Performance Considerations of Solar Furnaces" by

E. Loh, P. Duwez, N. Hiester, and T. Tietz. This report is concerned with the calculation of the heat flux and the maximum temperature obtainable at the focus, and ignores convection.

In this investigation, which was concerned with the second category under steady state conditions, a theoretical equation was proposed that relates the time rate of energy addition per unit area to the time rate of energy loss per unit area for a flat plate placed at the focus of a parabolic cylinder. The solution of this equation determined the temperature of the plate. The validity of the equation was checked experimentally by heating a plate in the focus of a concentrator and measuring the temperature rise of the plate above the surroundings under various conditions and comparing this temperature rise to the theoretical value.

It was quickly apparent that, with a target exposed to air, the convection losses due to winds were excessive; thus, it seemed a good idea to cover the target with a thin hollow glass cylinder. To further reduce the losses, the space between the plate and the surrounding glass cylinder was evacuated. A theoretical equation was developed to predict the temperature of a flat plate for various time rates of energy input per unit area to the plate. To determine a plate temperature from this equation, two other equations were proposed, one that predicts the temperature of the outside surface of the thin hollow glass cylinder, and one that predicts the temperature of the inside surface of the thin hollow glass cylinder. All three equations were checked by comparing the predicted temperature rise to the actual temperature rise obtained during tests.

A theoretical equation was also developed for the case of a cylindrical target surrounded by a thin hollow glass cylinder in which the intervening space was air. As in the previous cases, the temperature rise of the cylindrical plate predicted by the theory was checked experimentally.

To give a comparison between having air in the space between the target and the surrounding thin hollow glass cylinder or having a vacuum, an experimental test was made for a flat plate using different time rates of energy input per unit area for both cases.

A test was conducted with a flat plate as a target subjected to various total radiation rates in (Btu/hr ft^2) when the target was covered by no glass cylinder, one glass cylinder, two glass cylinders and, finally, three glass cylinders. This experiment indicated the advantage of using glass cylinders to obtain high equilibrium temperatures.

FLAT PLATE THEORY

General Equation

The differential equation of an object heated by radiation assuming infinite conductivity and zero conduction loss by supports is:

$$Q_a = cm\frac{dT}{d\theta} + hA_p \left[T_p - T_o\right] + \sigma\epsilon_p A_p \left[T_p^4 - T_s^4\right] + Q_u \qquad (1)$$

Under steady state conditions $dT/d\theta = 0$, and if the time rate of energy utilization is zero $Q_u = 0$, Equation (1) reduces to the following form:

$$Q_a = hA_p \left[T_p - T_o\right] + \sigma\epsilon_p A_p \left[T_p^4 - T_s^4\right] \qquad (2)$$

If Equation (2) is divided by the plate area A_p, the following equation results:

$$\frac{Q_a}{A_p} = h \left[T_p - T_o\right] + \sigma\epsilon_p \left[T_p^4 - T_s^4\right] \qquad (3)$$

The right hand term of Equation (#) is equal to the time rate of energy loss per unit area or

$$\frac{Q_\ell}{A_p} = h \left[T_p - T_o\right] + \sigma\epsilon_p \left[T_p - T_s^4\right] \qquad (4)$$

and therefore:

$$\frac{Q_a}{A_p} = \frac{Q_\ell}{A_p} \qquad (5)$$

The time rate of energy addition to the plate is equal to the sum of the sun and sky components as measured by a pyrheliometer, so

$$Q_a = Q_s + Q_{sk} \qquad (6)$$

Each component travels to the plate by a direct path from the sun or sky or by an indirect path from the sun or sky to the mirror and then to the plate. Therefore:

$$Q_a = Q_{sd} + Q_{si} + Q_{skd} + Q_{ski} \tag{7}$$

The direct component as shown by Hottel[1] is a function of the time rate of radiation per unit area from the sun, the area receiving radiation and an absorbtivity factor of the plate for this radiation; thus:

$$Q_{sd} = H_s A_{pn} \alpha_{sn} \tag{8}$$

The indirect component from the sun is a function of the time rate of radiation per unit area from the sun, the area of the mirror normal to this radiation, the fraction of the mirror exposed, the reflectivity of the mirror, and the absorbtivity of the plate for this radiation, thus:

$$Q_{si} = H_s A_{nm} CR\alpha_{si} \tag{9}$$

The sky components together represent less than 1% of the time rate of radiation per unit area to the plate when using a fully exposed mirror. It is fortunate that this is so because it is virtually impossible to state accurately the sky contribution to the plate. However, we may look at the limiting values of this contribution and then make a reasonable estimate.

If a perfectly reflecting mirror were placed in back of the plate so that the sky could see only sky or mirror, the contribution for this idealized case would be a function of the product of the time rate

---

(1) Hoyt C. Hottel and B. B. Woertz, "The Performance of Flat Plate Solar Heat Collectors," Transactions American Society of Mechanical Engineers, 1942, vol. 64, pp. 91-104.

of sky radiation per unit area, the total area of the plate, and the absorbtivity of the plate for this radiation, or

$$Q_{skd} + Q_{ski} = H_{sk} A_p \alpha_{sk} \tag{10}$$

In terms of the normal area of the plate this becomes

$$Q_{skd} + Q_{ski} = H_{sk} A_{pn} \alpha_{sk} \times \frac{A_p}{A_{pn}} \approx 2 H_{sk} A_{pn} \alpha_{sk} \tag{11}$$

However, actually the sky radiation is brightest near the sun, the direction in which it is determined, and diminishes in every direction from the sun. In addition, the back side of the plate has for its view only a small fraction that is mirror, that is its view factor of the mirror is less than unity. Also, the radiation from the sky via the mirror is diminished by the amount of radiation absorbed by the mirror. Thus, the contribution of the sky lies between these extremes:

$$0 < Q_{skd} + Q_{ski} \lessapprox 2 H_{sk} A_{pn} \alpha_{sk} \tag{12}$$

On substitution of α_{skn} for α_{sk} the sky contribution will be allowed for by

$$Q_{skd} + Q_{ski} = H_{sk} A_{pn} \alpha_{skn} \tag{13}$$

Summing the contributions

$$Q_a = H_s A_{pn} \alpha_{sn} + H_s A_{nm} CR \alpha_{si} + H_{sk} A_{pn} \alpha_{skn} \tag{14}$$

Dividing Equation (14) by A_p

$$\frac{Q_a}{A_p} = \frac{H_s A_{pn} \alpha_{sn} + H_s A_{nm} CR \alpha_{si} + H_{sk} A_{pn} \alpha_{skn}}{A_p} \tag{15}$$

Substitution in Equation (5) results in

$$\frac{H_s A_{pn}\alpha_{sn} + H_s A_{nm} CR\alpha_{si} + H_{sk} A_{pn}\alpha_{skn}}{A_p} = H\left[T_p - T_o\right] + \sigma\epsilon_p\left[T_p^4 - T_s^4\right] \qquad (16)$$

Equation (16) may be rearranged to yield

$$T_p = \left[T_s^4 + \frac{1}{\sigma\epsilon_p}\left[\left[\frac{H_s A_{pn}\alpha_{sn} + H_s A_{nm} CR\alpha_{si} + H_{sk} A_{pn}\alpha_{skn}}{A_p}\right] - h\left[T_p - T_o\right]\right]\right]^{\frac{1}{4}} \qquad (17)$$

Subtracting T_o from each side gives

$$T_p - T_o = \left[T_s^4 + \frac{1}{\sigma\epsilon_p}\left[\left[\frac{H_s A_{pn}\alpha_{sn} + H_s A_{nm} CR\alpha_{si} + H_{sk} A_{pn}\alpha_{skn}}{A_p}\right] - h\left[T_p - T_o\right]\right]\right]^{\frac{1}{4}} - T_o \qquad (18)$$

Using the results of Equation (15) in Equation (18)

$$T_p - T_o = \sqrt[4]{T_s^4 + \frac{1}{\sigma\epsilon_p}\left[\frac{Q_a}{A_p} - h\left[T_p - T_o\right]\right]} - T_o \qquad (19)$$

Equations (18) and (19) relate the temperature rise of the plate above the surroundings, in terms of the variables pertinent to a solar concentrator. Equation (18) can be applied to any parabolic cylindrical mirror, for any value of A_{nm}'/A_{pn} equal to or less than the value determined by the following equation developed in the appendix:

$$C = \frac{A_{nm}'}{A_{tr}} = \frac{A_{pn} + A_{nm}}{A_{pn}} \leq \frac{n\left[1 - \frac{n^2}{16} - \frac{n}{2}\tan\frac{\alpha}{2}\right]}{2\tan\frac{\alpha}{2}\left(1 + \frac{n^2}{16}\right)^2} \qquad (20)$$

Experimental Verification (Flat Plate #1)

The validity of Equation (16) to predict the steady state temperature attained in a solar concentrator will be determined by comparing the theoretical temperature rise T_p-T_o , to the actual temperature rise for a given plate in a controlled experiment.

Equation (16) states

$$\frac{H_s A_{pn} \alpha_{sn} + H_s A_{nm} CR \alpha_{si} + H_{sk} A_{pn}}{A_p} = h \left[T_p-T_o\right] + \sigma \epsilon_p \left[T_p^4-T_s^4\right] \tag{16}$$

or

$$\frac{Q_a}{A_p} = \frac{Q_\ell}{A_p} \tag{5}$$

The right hand equation may be put as

$$\frac{Q_\ell}{A_p} = h \left[T_p-T_o\right] + \sigma \epsilon_p \left[T_p^4-T_s^4\right] \tag{4}$$

or

$$\frac{Q_\ell}{A_p} = \frac{Q_c}{A_p} + \frac{Q_r}{A_p} \tag{21}$$

where

$$\frac{Q_c}{A_p} = h \left[T_p-T_o\right] \tag{22}$$

and

$$\frac{Q_r}{A_p} = \sigma \epsilon_p \left[T_p^4-T_s^4\right] \tag{23}$$

Since $\epsilon_p = .96$

$$\frac{Q_r}{A_p} = .173 \times .96 \left[\left(\frac{T_p}{100}\right)^4 - \left(\frac{T_s}{100}\right)^4\right] \tag{24}$$

or

$$\frac{Q_r}{A_p} = .1661 \left[\left(\frac{T_p}{100}\right)^4 - \left(\frac{T_s}{100}\right)^4 \right] \tag{25}$$

In evaluating h of Equation (22), two boundary conditions are assumed. A least loss condition is assumed for no wind (natural convection), and a maximum loss is assumed to occur with a wind velocity of four miles per hour.

Taking the case of natural convection first, in the laminar range, Jakob's correlation for vertical planes, horizontal and vertical cylinders, a block and a sphere is used to calculate h in range of

$$N_{Gr} \cdot N_{Pr} = 10^4 \text{ to } 10^3$$

The equation(2) states

$$N_{Nu} = .555(N_{Gr}N_{Pr})^{\frac{1}{4}} \tag{26}$$

or

$$h = .555 \frac{k_f}{L} \left(\frac{g\beta_f L^3 \Delta T}{\nu_f^2}\right)^{\frac{1}{4}} \left(\frac{c\mu}{k}\right)_f^{\frac{1}{4}} \tag{27}$$

For convenience, Equation (27) is put in the following form:

$$h = C_a \Delta T^{\frac{1}{4}} = C_a \left[T_p - T_o\right]^{\frac{1}{4}} \tag{28}$$

where

$$C_a = .555 \frac{k_f}{L} \left(\frac{g\beta_f L^3}{\nu_f^2}\right)^{\frac{1}{4}} \left(\frac{c\mu}{k}\right)^{\frac{1}{4}} \tag{29}$$

Table I gives the steps in evaluating C_a for film temperatures from 0-600°F. The values obtained are plotted in Figure 1. This graph enables one to determine h from Equation (28) when T_p and T_o are known, since the film temperature $T_f = \frac{T_p + T_o}{2}$ will be known, and C_a can then be determined from Figure 1.

(2) Max Jakob, Heat Transfer, John Wiley & Sons, Inc., New York, 1949, vol. I, p. 530.

To arrive at values of h for forced convection, H. Reiher's equation as stated in Jakob's Heat Transfer, Volume I, is used. This equation is for forced convection perpendicular to flat plates for Reynold's numbers from 4000-15000. The equation(3) states

$$N_{Nu} = .205\ N_{Re}^{.731} \tag{30}$$

or

$$h = .205\ \frac{k_f}{D}\left(\frac{VD}{\nu_f}\right)^{.731} = C_b \tag{31}$$

where D is equal to the diameter of a circular tube of equal exposed surface as the plate.

Equation (31) is solved for film temperatures from 0°-600°F in Table II. The results are plotted in Figure 1. With the aid of the graph, the forced convection coefficient can be determined when T_p and T_o are known, since the film temperature will be known also

$$T_f = \frac{T_p + T_o}{2}$$

At the same time that Equation (22) is solved for the least loss and maximum loss conditions, Equation (23) is solved for the least loss and maximum loss conditions. It may reasonably be assumed that the sky temperature $\left[T_s\right]$ is equal to or less than the temperature of the air $\left[T_o\right]$. Data from the University of California indicates that on a clear night the effective temperature of the sky may run as low as 420°R. It is assumed for the daytime conditions that $T_s = T_o = 520°R$ for the least loss condition and that $T_s = 490°R$ for the maximum loss condition. The temperature $\left[T_s\right]$ includes the influence of the sky, earth, mirror and the sun (the target has an extremely small view of the sun).

(3) Ibid, p. 560, 562.

To evaluate the time rate of energy addition per unit area of plate, Equation (15) must be evaluated.

$$\frac{Q_a}{A_p} = \frac{H_s A_{pn} \alpha_{sn} + H_s A_{nm} CR \alpha_{si} + H_{sk} A_{pn} \alpha_{skn}}{A_p} \tag{15}$$

where the following values apply

$$\frac{A_{pn}}{A_p} = .461$$

$$\alpha_{sn} = .98$$

$$\frac{A_{nm}}{A_p} = 17.492$$

$$\alpha_{si} = .961$$

$$R = .70$$

$$\alpha_{skn} = .98$$

Thus

$$\frac{Q_a}{A_p} = H_s(.461)(.98) + H_s(17.492)C(.70)(.961) + H_{sk}(.461)(.98) \tag{32}$$

or

$$\frac{Q_a}{A_p} = .4518\ H_s + 11.76\ CH_s + .04518\ H_{sk} \tag{33}$$

The total time rate or radiation per unit area is equal to the sum of the sun contribution plus the sky contribution and may be expressed as

$$H_T = H_s + H_{sk} \tag{34}$$

or

$$H_s = H_T - H_{sk} \tag{35}$$

From data obtained during the experimental verification

$$H_s = \frac{H_T - H_{sk}}{H_T} \times H_T \sim .9\ H_T \tag{36}$$

and

$$H_{sk} = \frac{H_T - H_s}{H_T} \times H_T \sim .1\ H_T \tag{37}$$

The substitution of Equation (36) and Equation (37) into Equation (33) results in

$$\frac{Q_a}{A_p} = \underset{\text{(sun direct)}}{.4066\ H_T} + \underset{\text{(sun indirect)}}{10.59\ H_T C} + \underset{\text{(sky)}}{.04518\ H_T} \tag{38}$$

or

$$\frac{Q_a}{A_p} = \left[.4518 + 10.59C\right] H_T \tag{39}$$

and thus, since $Q_a/A_p = Q_\ell/A_p$

$$\left[.4518 + 10.59C\right] H_T = h\left[T_p - T_o\right] + .1661\left[\left(\frac{T_p}{100}\right)^4 - \left(\frac{T_s}{100}\right)^4\right] \tag{40}$$

or

$$\frac{Q_a}{A_p} = h\left[T_p - T_o\right] + .1661\left[\left(\frac{T_p}{100}\right)^4 - \left(\frac{T_s}{100}\right)^4\right] \tag{41}$$

Equation (40) can be rearranged to yield

$$T_p = 100\sqrt[4]{\left(\frac{T_s}{100}\right)^4 + \frac{1}{.1661}\left[\left[.4518+10.59C\right] H_T - h\left[T_p - T_o\right]\right]} \tag{42}$$

or using the results of Equation (41)

$$T_p = 100\sqrt[4]{\left(\frac{T_s}{100}\right)^4 + \frac{1}{.1661}\left[\frac{Q_a}{A_p} - h\left[T_p - T_o\right]\right]} \tag{43}$$

Subtracting T_o from both sides of Equation (43)

$$T_p - T_o = 100 \sqrt[4]{\left(\frac{T_s}{100}\right)^4 + \frac{1}{.1661}\left[\frac{Q_a}{A_p} - h\left[T_p - T_o\right]\right]} - T_o \qquad (44)$$

or

$$T_p - T_o = 100 \sqrt[4]{\left(\frac{T_s}{100}\right)^4 + \frac{1}{.1661}\left[\left[.4518 + 10.59C\right] H_T - h\left[T_p - T_o\right]\right]} - T_o \qquad (45)$$

In Table III, using the assumptions that $T_o = 520°R$, that there is natural convection, and that $T_s = T_o$ for minimum loss conditions, Equation (44) is solved for nine assumed plate temperatures. These temperature rises of the plate above the surroundings are plotted against Q_a/A_p in Figure 2 as the lower solid line which shows the theoretical temperature rise of the plate under various Q_a/A_p inputs to the plate for conditions of natural convection.

In Table IV, using the assumptions that $T_o = 520°R$, that there is forced convection (wind 4 m.p.h.), and that $T_s = 490°R$ for maximum loss conditions, Equation (45) is solved for Q_a/A_p for nine assumed plate temperatures. These temperature rises above the surroundings are plotted against Q_a/A_p in Figure 2 as the upper solid line which shows the theoretical temperature rise of the plate under various Q_a/A_p inputs to the plate under conditions of forced convection.

The experimental verification is made during the test runs by using Equation (39) to transfer pyrheliometer readings into Q_a/A_p values, and recording the actual temperature rise of the plate above the surroundings. The steps are shown in Table V. The temperature

rises of the plate $T_p - T_o$ are plotted against Q_a/A_p in Figure 2 to show contrast with the theoretical values that appear as solid lines.

Table I

Flat Plate #1, in Air, Free Convection Coefficient, C_a

T_f	k_f	ν_f	$(N_{Pr})_f$	L	$\frac{g\beta_f}{\nu_f^2}$	$\frac{g\beta_f}{\nu_f^2}(N_{Pr})_f$	$\frac{g\beta_f}{\nu_f^2}(N_{Pr})_f L^3$	$C_a = .555\frac{K_f}{L}\left[\left(\frac{g\beta_f L^3}{\nu_f^2}\right)(N_{Pr})\right]_f^{1/4}$
°F	$\frac{\text{Btu ft}}{\text{hr ft}^2\text{F}}$	$\frac{\text{ft}^2}{\text{hr}}$		ft	$\frac{1}{\text{ft}^3\text{F}}$	$\frac{1}{\text{ft}^3\text{F}}$	$\circ\frac{1}{\text{F}}$	$\frac{\text{Btu}}{\text{hr ft}^2\text{F}^{5/4}}$
0	.0130	.4614	.731	.375	4.256×10^6	3.111×10^6	1.640×10^5	.3871
100	.0157	.6507	.706	.375	1.758×10^6	1.240×10^6	6.544×10^4	.3711
200	.0182	.8649	.690	.375	8.442×10^5	5.825×10^5	3.182×10^4	.3511
300	.0205	1.1052	.682	.375	4.491×10^5	3.063×10^5	1.615×10^4	.3419
400	.0228	1.3611	.677	.375	2.616×10^5	1.771×10^5	9.338×10^3	.3317
500	.0250	1.6453	.672	.375	1.604×10^5	1.078×10^5	5.684×10^3	.3213
600	.0272	1.9503	.668	.375	1.034×10^5	6.907×10^4	3.642×10^3	.3128

Table II

Flat Plate #1, in Air, Forced Convection Coefficient, C_b

T_f	k_f	ν_f	V	D	$(N_{Re})_f$	$(N_{Re})_f^{.731}$	$C_b = .205\frac{k_f}{D}(N_{Re})^{.731}$
°F	$\frac{\text{Btu ft}}{\text{hr ft}^2\text{F}}$	$\frac{\text{ft}^2}{\text{hr}}$	$\frac{\text{ft}}{\text{hr}}$	ft			$\frac{\text{Btu}}{\text{hr ft}^2\text{°F}}$
0	.0130	.4614	21120	.1259	5691.2	556.0	11.77
100	.0157	.6507	21120	.1259	4035.2	432.4	11.05
200	.0182	.8649	21120	.1259	3036.1	351.2	10.41
300	.0205	1.052	21120	.1259	2376.0	293.6	9.80
400	.0228	1.3611	21120	.1259	1929.2	252.0	9.35
500	.0250	1.6453	21120	.1259	1596.0	219.5	8.93
600	.0272	1.9503	21120	.1259	1346.4	193.8	8.58

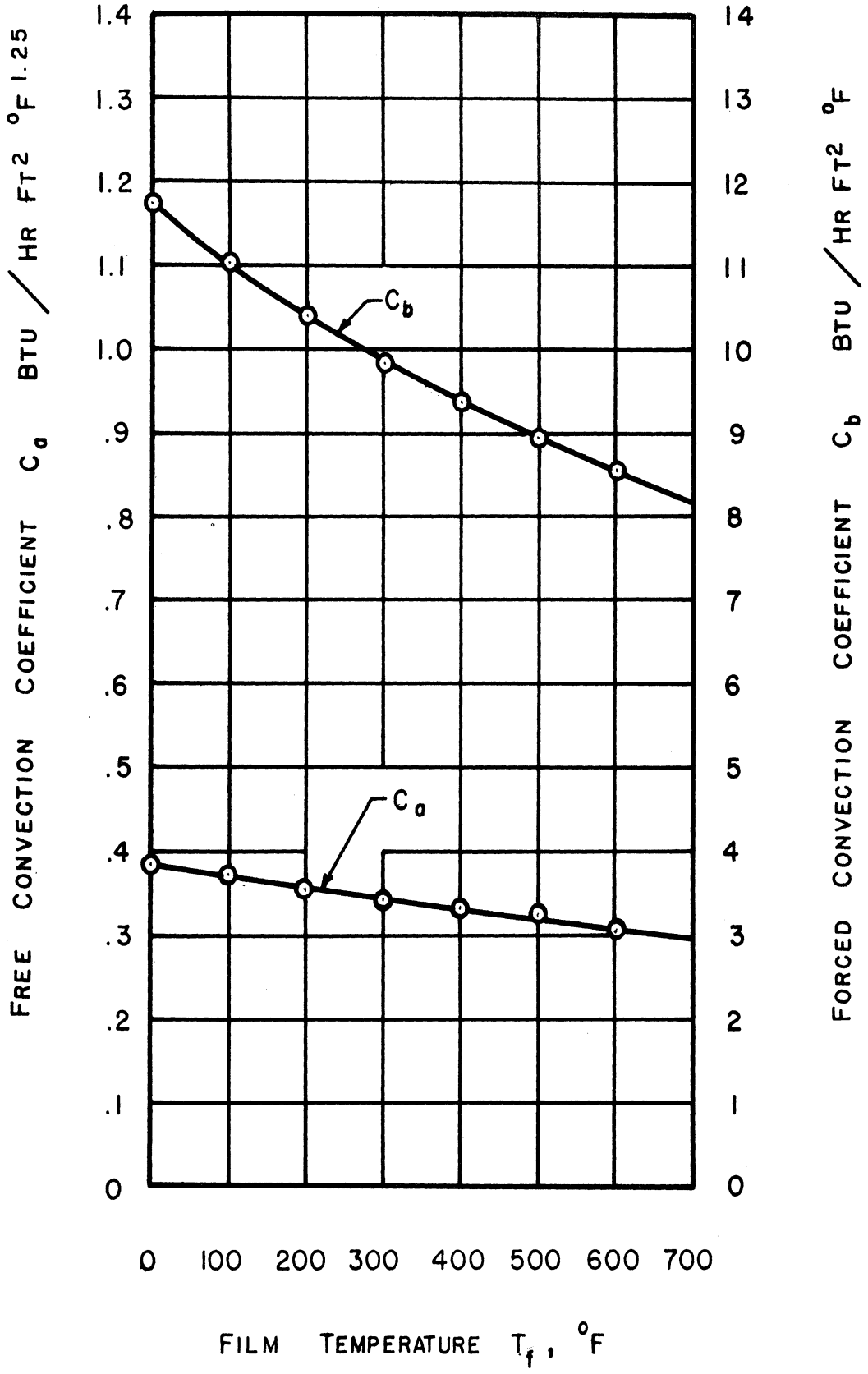

Figure 1. Plot of Coefficients C_a and C_b for the Determination of h for Flat Plate No. 1 in Air.

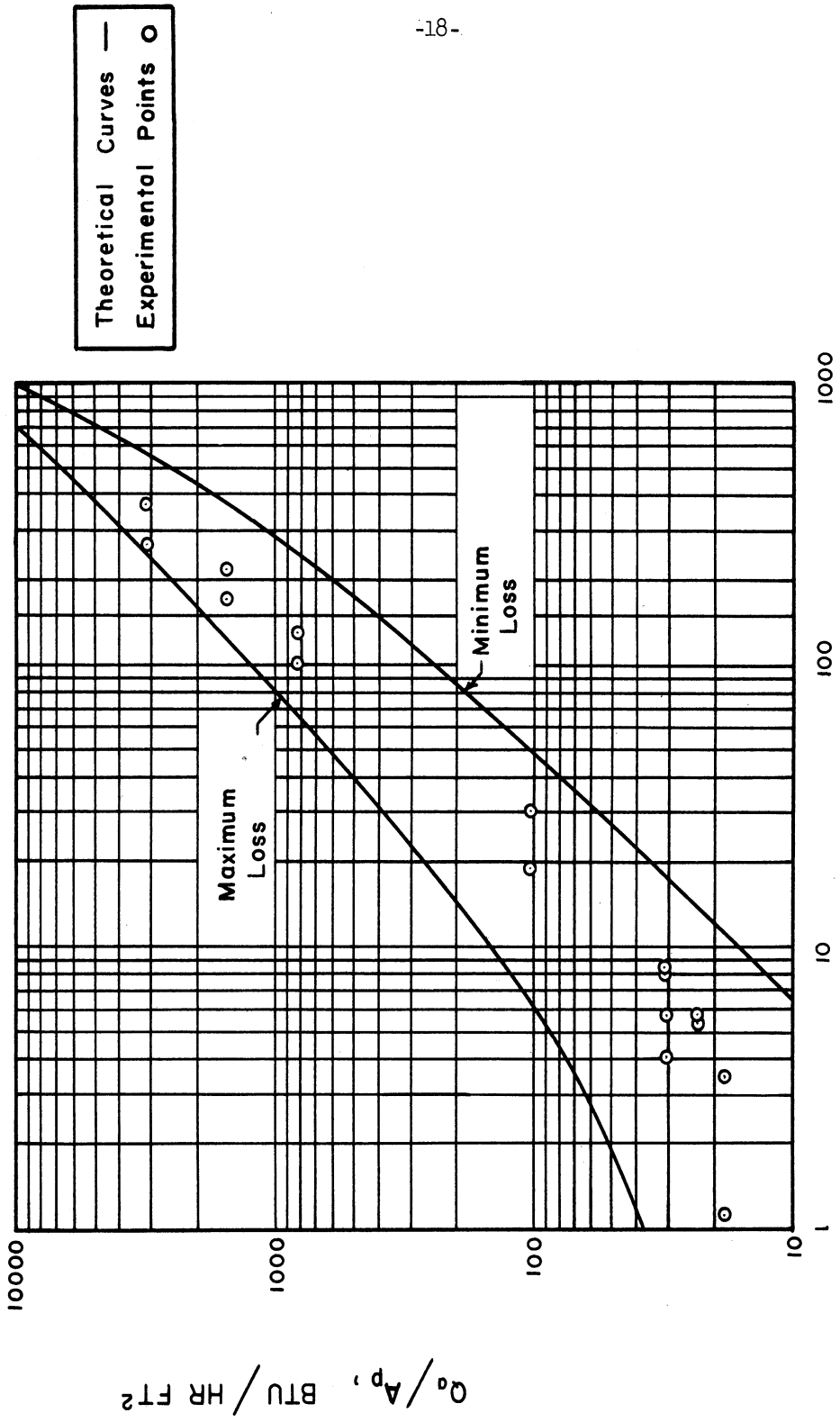

Figure 2. Theoretical and Experimental Plot of $(T_p - T_o)$ vs. Q_a/A_p for Flat Plate No. 1 in Air.

Table III

Flat Plate #1, in Air, Minimum Loss Calculations

$\Delta T = T_p - T_o$ °F	T_p °R	$T_f = \frac{T_p + T_o}{2}$ °R	T_f °F	C_a $\frac{Btu}{hr\ ft^2\ °F^{5/4}}$	h $\frac{Btu}{hr\ ft^2\ °F}$	$\frac{Q_a}{A_p}$ $\frac{Btu}{hr\ ft^2}$
1	521	520.5	60.5	.378	.378	1.32
5	525	522.5	62.5	.377	.564	7.56
10	530	525	65	.376	.669	16.31
30	550	535	75	.373	.873	56.73
50	570	545	85	.371	.987	103.17
100	620	570	110	.368	1.163	240.35
200	720	620	160	.360	1.352	595.65
400	920	720	260	.346	1.546	1677.51
800	1320	920	460	.327	1.742	6312.93

Table IV

Flat Plate #1, in Air, Maximum Loss Calculations

$\Delta T = T_p - T_o$ °F	T_p °R	$T_f = \frac{T_p + T_o}{2}$ °R	T_f °F	C_b $\frac{Btu}{hr\ ft^2\ °F}$	h $\frac{Btu}{hr\ ft^2\ °F}$	$\frac{Q_a}{A_p}$ $\frac{Btu}{hr\ ft^2}$
1	521	520.5	60.5	11.32	11.32	37.95
5	525	522.5	62.5	11.31	11.31	86.98
10	530	525	65	11.30	11.30	148.31
30	550	535	75	11.23	11.23	393.14
50	570	545	85	11.17	11.17	638.08
100	620	570	110	10.98	10.98	1247.7
200	720	620	160	10.69	10.69	2488.6
400	920	720	260	10.08	10.08	5126
600	1120	820	360	9.50	9.50	8218

Table V

Flat Plate #1, in Air, Experimental Data

Pyrheliometer millivolts [Test]	H_T $\frac{Btu}{hr\,ft^2}$	C	10.59C H_T $\frac{Btu}{hr\,ft^2}$	.4518 H_T $\frac{Btu}{hr\,ft^2}$	$\frac{Q_a}{A_p}$ $\frac{Btu}{hr\,ft^2}$	$T_p - T_o$ °F [Test]
7.15	283	1	2997	127.9	3125	270 -376
6.72	266	.5	1408	120.2	1528	171 -221
6.72	266	.25	704.2	120.2	824.4	102 -130
5.80	230	0	0	104.0	104.0	19 - 30
1.04	41.2	0	0	18.6	18.6	1.1- 3.4
1.75	69.3	0	0	31.3	31.3	8 - 8.3
1.30	51.5	0	0	23.3	23.3	5.3- 5.7
1.69	66.9	0	0	30.2	30.2	4.1-- 6.7

OUTSIDE SURFACE OF THIN HOLLOW GLASS CYLINDER SURROUNDING TARGET

General Equation

For steady state conditions with no time rate of energy utilization, the time rate of energy absorbed per unit area equals the time rate of energy loss per unit area or

$$\frac{Q_a}{A_{glo}} = \frac{Q_\ell}{A_{glo}} \tag{1}$$

Where

$$\frac{Q_\ell}{A_{glo}} = h\left[T_{glo}-T_o\right] + \sigma\epsilon_{glo}\left[T_{glo}^4-T_s^4\right] \tag{2}$$

The time rate of energy addition is the sum of four factors and is stated as

$$Q_a = Q_{sd} + Q_{si} + Q_{skd} + Q_{ski} \tag{3}$$

The sun direct component $\left[Q_{sd}\right]$ is a function of the time rate of direct sun radiation per unit area, the transmission factor through the glass, the area of the target that receives radiation, and the absorbtivity of the target for radiation. Under the assumptions that the target for radiation within the glass cylinder is a flat plate and that the time rate of energy loss by the plate is equal to the time rate of energy loss by the outside surface of the glass cylinder the sun direct component is

$$Q_{sd} = H_s\tau_{rsd}\tau_{asi}A_{pn}\alpha_{sd} \tag{4}$$

The sun indirect component $\left[Q_{si}\right]$ is a function of the time rate of direct sun radiation per unit area, the area of the mirror

normal to the radiation, the fraction of the mirror exposed, the reflectivity of the mirror, the transmission factor of the glass, and the absorbtivity of the target for this radiation, and can be stated

$$Q_{si} = H_s C A_{nm} R \tau_{rsi} \tau_{asi} \alpha_{si} \tag{5}$$

The sky components are treated together. If the glass cylinder and target were placed in front of a perfectly reflecting mirror so that the combination could see only mirror or sky, the time rate of energy added from these two sources would be a function of the product of the time rate of energy addition from the sky, the transmission coefficient through the glass, the area of the target, and the absorbtivity of the target for sky radiation; thus

$$Q_{skd} + Q_{ski} = H_{sk} \tau_{rsk} \tau_{ask} A_p \alpha_{sk} \tag{6}$$

For the same reasons advanced in the case of the flat plate, the actual contribution from both components is

$$0 < Q_{skd} + Q_{ski} \leq H_{sk} \tau_{rsk} \tau_{ask} A_p \alpha_{sk} \tag{7}$$

It is assumed that approximately this can be expressed as:

$$Q_{skd} + Q_{ski} = H_{sk} \tau_{rsk} \tau_{ask} A_{pn} \alpha_{skn} \tag{8}$$

Thus summing up the contributions:

$$Q_a = H_s \tau_{rsd} \tau_{asd} A_{pn} \alpha_{sd} + H_s C A_{nm} R \tau_{rsi} \tau_{asi} \alpha_{si} + H_{sk} \tau_{rsk} \tau_{ask} A_{pn} \alpha_{skn} \tag{9}$$

Or, when divided by the outside area of the cylinder

$$\frac{Q_a}{A_{glo}} = \frac{H_s \tau_{rsd} \tau_{asd} A_{pn} \alpha_{sd} + H_s C A_{nm} R \tau_{rsi} \tau_{asi} \alpha_{si} + H_{sk} \tau_{rsk} \tau_{ask} A_{pn} \alpha_{skn}}{A_{glo}} \tag{10}$$

Substituting in Equation (1) results in

$$\frac{H_s \tau_{rsd} \tau_{asd} A_{pn} \alpha_{sd} + H_s C A_{nm} R \tau_{rsi} \tau_{asi} \alpha_{si} + H_{sk} \tau_{rsk} \tau_{ask} A_{pn} \alpha_{skn}}{A_{glo}} =$$

$$h \left[T_{glo} - T_o\right] + \sigma \epsilon_{glo} \left[T_{glo}^4 - T_s^4\right] \tag{11}$$

Equation (11) may be rewritten as

$$T_{glo} = \left[T_s^4 + \frac{1}{\sigma \epsilon_{glo}} \left[\frac{H_s \tau_{rsd} \tau_{asd} A_{pn} \alpha_{sd} + H_s C A_{nm} R \tau_{rsi} \tau_{asi} \alpha_{si} +}{A_{glo}}\right.\right. \tag{12}$$

$$\left.\left.\frac{H_{sk} \tau_{rsk} \tau_{ask} A_{pn} \alpha_{skn}}{A_{glo}} - h \left[T_{glo} - T_o\right]\right]\right]^{\frac{1}{4}}$$

Subtracting T_o from both sides yields

$$T_{glo} - T_o = \sqrt[4]{\text{Above}} - T_o \tag{13}$$

Using the results of Equation (10) in Equation (13) gives

$$T_{glo} - T_o = \sqrt[4]{T_s^4 + \frac{1}{\sigma \epsilon_{glo}} \left[\frac{Q_a}{A_{glo}} - h \left[T_{glo} - T_o\right]\right]} - T_o \tag{14}$$

Equation (13) and Equation (14) are the theoretical equations relating the temperature rise of the outside surface of a thin glass cylinder surrounding a plate target in terms of factors that pertain to a solar concentrator.

Experimental Verification (Flat Plate #2)

Equation (14) will be checked by calculating the theoretical temperature rise of the surface above the air temperature $T_{glo}-T_o$ under given Q_a/A_{glo} values and comparing the theoretical temperature rise to that obtained in experiment.

The equation concerning losses states

$$\frac{Q_\ell}{A_{glo}} = h\left[T_{glo}-T_o\right] + \sigma\epsilon_{glo}\left[T_{glo}^4-T_s^4\right] \tag{2}$$

The time rate of energy loss per unit cylinder area is the sum of a convection loss and a radiation loss term

$$\frac{Q_\ell}{A_{glo}} = \frac{Q_c}{A_{glo}} + \frac{Q_r}{A_{glo}} \tag{15}$$

where

$$\frac{Q_c}{A_{glo}} = h\left[T_{glo}-T_o\right] \tag{16}$$

and

$$\frac{Q_r}{A_{glo}} = \sigma\epsilon_{glo}\left[T_{glo}^4-T_s^4\right] \tag{17}$$

which for the glass cylinder with $\epsilon_{glo} = .925$ becomes

$$\frac{Q_r}{A_{glo}} = .173 \times .925\left[\left(\frac{T_{glo}}{100}\right)^4-\left(\frac{T_s}{100}\right)^4\right] \tag{18}$$

$$\frac{Q_r}{A_{glo}} = .1600\left[\left(\frac{T_{glo}}{100}\right)^4-\left(\frac{T_s}{100}\right)^4\right] \tag{19}$$

and

$$\frac{Q_\ell}{A_{glo}} = h\left[T_{glo}-T_o\right] + .1600\left[\left(\frac{T_{glo}}{100}\right)^4-\left(\frac{T_s}{100}\right)^4\right] \tag{2a}$$

As in the case of the flat plate, Equation (13) will be evaluated for a least loss condition (natural convection) and a maximum loss condition (4 m.p.h.).

McAdams recommends in the region of laminar flow $\left[10^4 < N_{Gr}N_{Pr} < 10^9\right]$ the following equation[4] for natural convection:

$$N_{Nu} = .59(N_{Gr}N_{Pr})^{\frac{1}{4}} \tag{20}$$

or

$$h = .59\,\frac{k_f}{L}\left(\frac{g\beta_f L^3\Delta T N_{Pr}}{\nu_f^2}\right)^{\frac{1}{4}} \tag{21}$$

This equation is put in the following form:

$$h = .59\,\frac{k_f}{L}\left(ML^3\Delta T\right)^{\frac{1}{4}} \tag{22}$$

where

$$M = \frac{g\beta_f N_{Pr}}{\nu_f^2} \tag{23}$$

Equation (22) is in turn put in the following form:

$$h = C_c\Delta T^{\frac{1}{4}} = C_c(T_{glo}-T_o)^{\frac{1}{4}} \tag{24}$$

where

$$C_c = .59\,\frac{k_f}{L}\left(ML^3\right)^{\frac{1}{4}} \tag{25}$$

---

(4) W. H. McAdams, Heat Transmission, McGraw-Hill Book Co., New York, 1954, p. 172.

Equation (25) is solved to obtain C_c for film temperatures $T_f = \frac{T_{glo} + T_o}{2}$ from 0° to 600°F. The steps are shown in Table VI and the values of C_c resulting are plotted in Figure 3 against film temperature. By means of this graph h can be found for any film temperature with the aid of Equation (24).

In the forced convection range, for flow of air normal to single cylinders in the range of Reynold's numbers from 4000-40,000, the recommended McAdams equation(5) is

$$N_{Nu} = .174\ (N_{Re})^{.618} \tag{26}$$

or

$$h = .174\ \frac{K_f}{D_{glo}}\ \left(\frac{VD_{glo}}{\nu_f}\right)^{.618} = C_d \tag{27}$$

Equation (27) is solved to obtain C_d for film temperatures from 0° to 600°F and the steps are shown in Table VII. The values of C_d obtained are plotted in Figure 3 against film temperature.

Dealing with the time rate of energy addition per unit area, Equation (10) states

$$\frac{Q_a}{A_{glo}} = \frac{H_s \tau_{rsd} \tau_{asd} A_{pn} \alpha_{sd} + H_s C A_{nm} R \tau_{rsi} \tau_{asi} \alpha_{si} + H_{sk} \tau_{rsk} \tau_{ask} A_{pn} \alpha_{skn}}{A_{glo}} \tag{10}$$

Dietz has shown that up to an angle of incidence of 50° the overall transmittance $\left[\tau_r \tau_a\right]$ is barely changed; for this reason,

---

(5) Ibid, p. 260.

normal incidence factors will be used.[6] For Equation (10) the following values hold for this experiment:

$$\frac{A_{pn}}{A_{glo}} = .0657$$

$$\tau_{rsd} \approx \tau_{rsi} \approx \tau_{rsk} \approx \tau_r = .93$$

$$\tau_{asd} \approx \tau_{asi} \approx \tau_{ask} \approx \tau_a = .98$$

$$\alpha_{sd} = .98$$

$$\alpha_{si} = .961$$

$$\alpha_{skn} = .98$$

$$\frac{A_{nm}}{A_{glo}} = 1.969$$

$$R = .70$$

Therefore,

$$\frac{Q_a}{A_{glo}} = H_s(.93)(.98)(.0657)(.98) + H_sC(1.969)(.70)(.93)(.98)(.961) + H_{sk}(.0657)(.93)(.98)(.98) \quad (28)$$

or

$$\frac{Q_a}{A_{glo}} = .05868\ H_s + 1.208CH_s + .005868\ H_{sk} \quad (29)$$

---

(6) Albert G. H. Dietz, "Diathermanous Materials and Properties of Surfaces," Space Heating with Solar Energy, Proceedings of a Course-Symposium of Massachusetts Institute of Technology, 1954, p. 40.

Since $H_s \sim .9H_T$ and $H_{sk} \sim .1H_T$, Equation (29) simplifies to

$$\frac{Q_a}{A_{glo}} = \left[.05868 + 1.0870\ C\right] H_T \tag{30}$$

and

$$\frac{Q_a}{A_{glo}} = \frac{Q_\ell}{A_{glo}} \tag{1}$$

thus

$$\left[.05868 + 1.0870\ C\right] H_T = h\left[T_{glo}-T_o\right] + .1600\left[\left(\frac{T_{glo}}{100}\right)^4-\left(\frac{T_s}{100}\right)^4\right] \tag{31}$$

Equation (31) can be rearranged to give

$$T_{glo} = 100\sqrt[4]{\left(\frac{T_s}{100}\right)^4 + \frac{1}{.1600}\left[\left[.05868+1.0870C\right] H_T - h\left[T_{glo}-T_o\right]\right]} \tag{32}$$

Subtracting T_o from each side yields

$$T_{glo}-T_o = 100\sqrt[4]{\text{Above}} - T_o \tag{33}$$

or utilizing Equation (30)

$$T_{glo}-T_o = 100\sqrt[4]{\left(\frac{T_s}{100}\right)^4 + \frac{1}{.1600}\left[\frac{Q_a}{A_{glo}} - h\left[T_{glo}-T_o\right]\right]} - T_o \tag{34}$$

Equation (34) was solved for Q_a/A_{glo} values for the least loss conditions by assuming $T_s = T_o = 520°R$ and assuming natural convection

for various assumed T_{glo} values. The steps are shown in Table VIII. Equation (33) was solved for Q_a/A_{glo} values for maximum loss conditions by assuming $T_o = 520°R$, $T_s = 490°R$ and assuming a wind velocity of 4 m.p.h. The steps are shown in Table IX.

The theoretical values of Q_a/A_{glo} are plotted for the least loss and maximum loss against the temperature rise $\left[T_{glo}-T_o\right]$ as solid lines in Figure 4.

The verification of Equation (34) is made by using Equation (30) to transfer H_T readings into Q_a/A_{glo} values and recording the actual temperature rise of the outside surface of the glass cylinder. The steps are shown in Table X. The actual temperature rises of the outside surface $\left[T_{glo}-T_o\right]$ are plotted vs. Q_a/A_{glo} as circles in Figure 4 to show comparison with the theoretical values that are shown as solid lines.

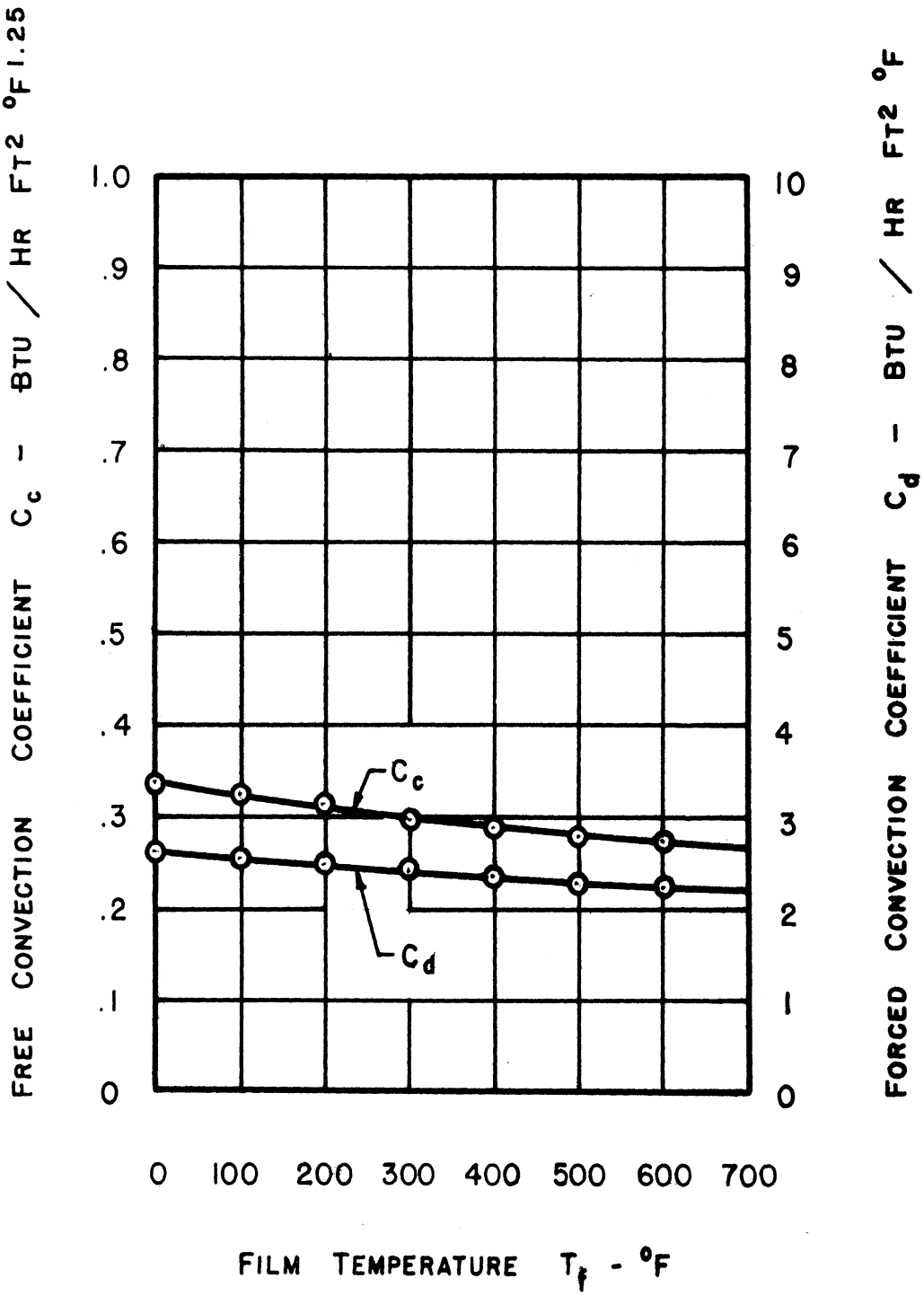

Figure 3. Plot of Coefficients C_c and C_d vs. T for the Determination of h for Glass Cylinder in Air, Outside Surface.

Table VI

Glass Cylinder, in Air, Outside Surface, Free Convection Coefficient, C_c

T_f	k_f	L	M	ML^3	$[ML^3]^{1/4}$	$C_c = \frac{.59}{L} k_f [ML^3]^{1/4}$
F	$\frac{\text{Btu ft}}{\text{hr ft}^2\text{F}}$	ft	$\frac{1}{\text{ft}^3\text{F}}$	$\frac{1}{\text{F}}$	$\frac{1}{\text{F}}^{1/4}$	$\frac{\text{Btu}}{\text{hr ft}^2\text{F}^{5/4}}$
0	.0130	.833	3.111×10^6	1.800×10^6	36.63	.3371
100	.0157	.833	1.240×10^6	7.176×10^5	29.11	.3237
200	.0182	.833	5.825×10^5	3.371×10^5	24.10	.3106
300	.0205	.833	3.063×10^5	1.773×10^5	20.52	.2977
400	.0225	.833	1.771×10^5	1.025×10^5	17.89	.2887
500	.0250	.833	1.078×10^5	6.238×10^4	15.80	.2797
600	.0272	.833	6.907×10^4	3.997×10^4	14.14	.2723

Table VII

Glass Cylinder, in Air, Outside Surface, Forced Convection Coefficient, C_d

T_f	k_f	ν_f	D_o	(N_{Re})	$(N_{Re})^{.618}$	$C_d = .174\frac{k_f}{D_o} N_{Re}^{.618}$
°F	$\frac{\text{Btu ft}}{\text{hr ft}^2\text{F}}$	$\frac{\text{ft}^2}{\text{hr}}$	ft			$\frac{\text{Btu}}{\text{hr ft}^2\text{F}}$
0	.0130	.4614	.333	15258	385.0	2.613
100	.0157	.6507	.333	10819	311.3	2.551
200	.0182	.8649	.333	8140	261.1	2.480
300	.0205	1.1050	.333	6371	224.4	2.401
400	.0225	1.3611	.333	5172	197.3	2.348
500	.0250	1.6453	.333	4279	175.5	2.290
600	.0272	1.9503	.333	3610	158.0	2.244

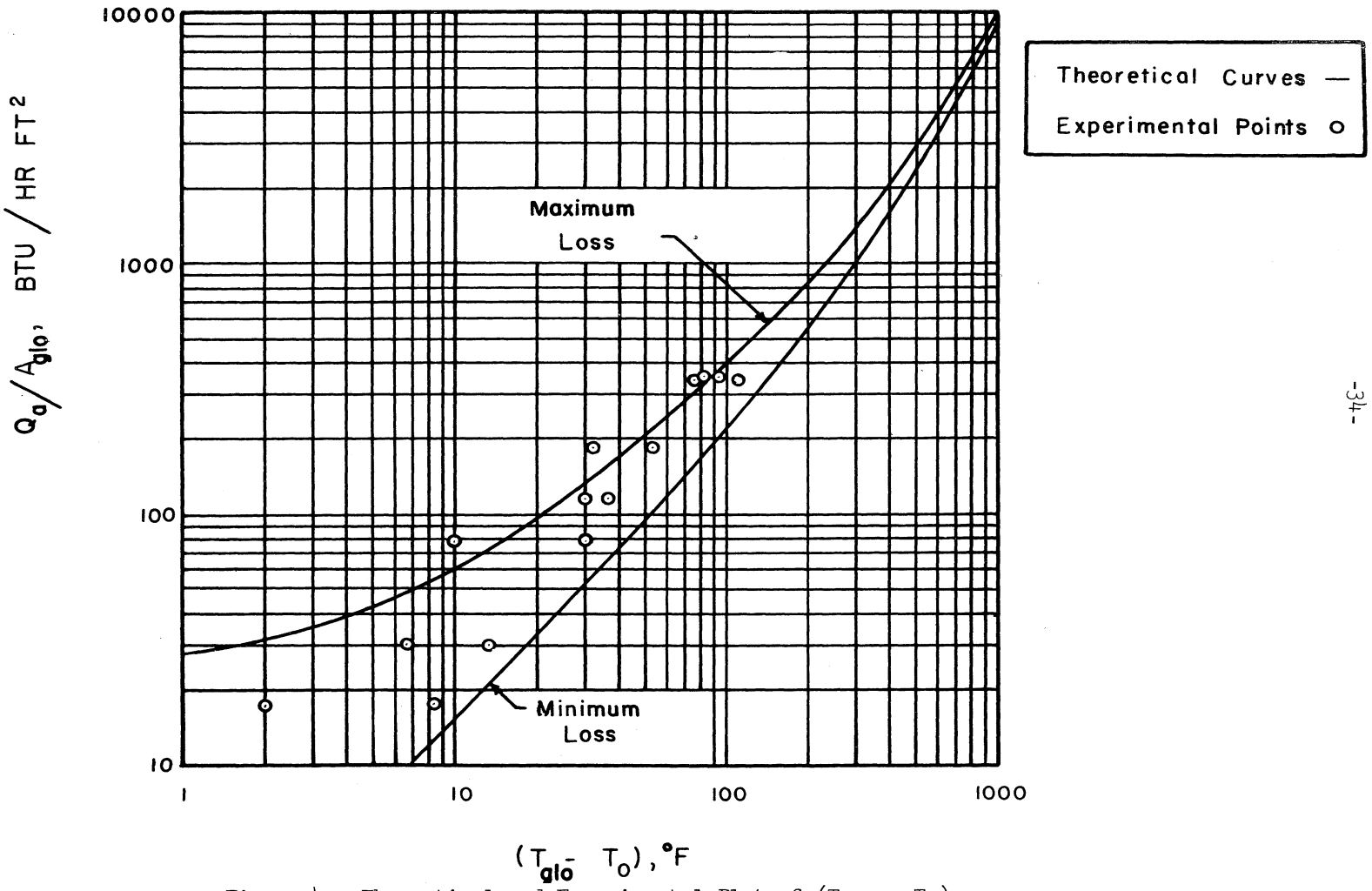

Figure 4. Theoretical and Experimental Plot of $(T_{glo} - T_o)$ vs. Q_a/A_{glo} for Glass Cylinder, in Air, Outside Surface.

Table VIII

Glass Cylinder, in Air, Outside Surface, Minimum Loss Calculations

$\Delta T = T_{glo} - T_o$ °F	T_{glo} °R	$T_f = \frac{T_{glo} + T_o}{2}$ °R	T_f °F	C_c $\frac{Btu}{hr\,ft^2\,°F^{5/4}}$	h $\frac{Btu}{hr\,ft^2\,°F}$	$\frac{Q_a}{A_{glo}}$ $\frac{Btu}{hr\,ft^2}$
1	521	520.5	60.5	.327	.327	1.23
5	525	522.5	62.5	.326	.489	7.00
10	530	525	65	.325	.578	15.04
30	550	535	75	.324	.759	52.18
50	570	545	85	.323	.859	94.86
100	620	570	110	.320	1.012	220.6
200	720	620	160	.314	1.181	549.2
400	920	720	260	.300	1.341	1566
600	1120	820	360	.291	1.44	3265
800	1320	820	460	.282	1.500	5941
1000	1520	1020	560	.275	1.546	8970

Table IX

Glass Cylinder, in Air, Outside Surface, Maximum Loss Calculations

$\Delta T = T_{glo} - T_o$ °F	T_{glo} °R	$T_f = \frac{T_{glo}+T_o}{2}$ °R	T_f °F	C_d $\frac{Btu}{hr\ ft^2\ °F}$	h $\frac{Btu}{hr\ ft^2\ °F}$	$\frac{Q_a}{A_{glo}}$ $\frac{Btu}{hr\ ft^2}$
1	521	520.5	60.5	2.57	2.57	28.22
5	525	522.5	62.5	2.565	2.565	42.14
10	530	525	65	2.56	2.56	59.62
30	550	535	75	2.55	2.55	130.7
50	570	545	85	2.54	2.54	203.7
100	620	570	110	2.52	2.52	396.2
200	720	620	160	2.48	2.48	833.8
400	920	720	260	2.41	2.41	2018
600	1120	820	360	2.35	2.35	3719
800	1320	920	460	2.29	2.29	6597
1000	1520	1020	560	2.24	2.24	10690

Table X

Glass Cylinder, in Air, Outside Surface, Flat Plate #2 Target, Experimental Data

Pyrheliometer millivolts [Test]	H_T $\frac{Btu}{hr\ ft^2}$	C	1.0870 C H_T $\frac{Btu}{hr\ ft^2}$	.05868 H_T $\frac{Btu}{hr\ ft^2}$	$\frac{Qa}{Aglo}$ $\frac{Btu}{hr\ ft^2}$	$[T_{glo}-T_o]$ °F [Test]
7.6	301	1	327.2	17.66	344.86	75 -110
7.7	305	1	331.5	17.90	349.40	82 - 92
7.7	305	.5	165.8	17.90	183.70	32 - 53
5.2	206	.5	103	12.09	115.09	30 - 36
6.0	238	.25	64.68	13.97	78.65	10 - 30
2.31	91.5	.25	24.87	5.37	30.24	6.7-13.3
7.5	297	0	0	17.43	17.43	2 - 8.3

INSIDE SURFACE OF THIN HOLLOW GLASS CYLINDER SURROUNDING TARGET

General Equation

In proposing a theoretical equation to predict the inside surface temperature of a glass cylinder covering a target to be heated by radiation, it is assumed that the time rate of energy absorbed by the glass cylinder in the steady state equals the time rate of energy received and lost by the plate, and the time rate of energy loss by the inside as well as the outside surface of the cylinder, or

$$(Q_a)_p = (Q_\ell)_p = (Q_\ell)_{gli} = (Q_\ell)_{glo} \tag{1}$$

The heat transfer loss per unit length through a cylindrical shell of infinite length is

$$\frac{Q_\ell}{L} = \frac{2\pi K_m \Delta T}{\ln \frac{D_{glo}}{D_{gli}}} \tag{2}$$

If $A_{glo} = \pi L D_{glo}$ (assuming adiabatic ends) then

$$\frac{Q_\ell}{A_{glo}} = \frac{Q_\ell}{\pi L D_{glo}} = \frac{2\pi L K_m \Delta T}{\pi L D_{glo} \ln \frac{D_{glo}}{D_{gli}}} = \frac{2K_m \left[T_{gli} - T_{glo}\right]}{D_{glo} \ln \frac{D_{glo}}{D_{gli}}} \tag{3}$$

Thus, to determine the inside surface temperature of the glass, one solves the following equation for previously derived, assuming a flat plate target.

$$T_{glo} = \sqrt[4]{T_s^4 + \frac{1}{\sigma \epsilon_{glo}} \left[\frac{H_s \tau_{rsd} \tau_{asd} A_{pn} \alpha_{sd} + H_s C A_{nm} R \tau_{rsi} \tau_{asi} \alpha_{si} + \frac{H_{sk} \tau_{rsk} \tau_{ask} A_{pn} \alpha_{skn}}{A_{glo}} - h \left[T_{glo} - T_o\right]}{A_{glo}} \right]} \tag{4}$$

Then utilizing the following equation for steady state

$$\frac{Q_a}{A_{glo}} = \frac{Q_\ell}{A_{glo}} \tag{5}$$

and since

$$\frac{Q_a}{A_{glo}} = \frac{H_s \tau_{rsd} \tau_{asd} A_{pn} \alpha_{sd} + H_s C A_{nm} R \tau_{rsi} \tau_{asi} \alpha_{si} +}{A_{glo}}$$

$$\frac{H_{sk} \tau_{rsk} \tau_{ask} A_{pn} \alpha_{skn}}{A_{glo}} \tag{6}$$

By substituting the results of Equation (3) and Equation (6) in Equation (5) one obtains

$$\frac{H_s \tau_{rsd} \tau_{asd} A_{pn} \alpha_{sd} + H_s C A_{nm} R \tau_{rsi} \tau_{asi} \alpha_{si} + H_{sk} \tau_{rsk} \tau_{ask} A_{pn} \alpha_{skn} =}{A_{glo}}$$

$$\frac{2 K_m \left[T_{gli} - T_{glo}\right]}{D_{glo} \ln \frac{D_{glo}}{D_{gli}}} \tag{7}$$

This equation can then be solved for T_{gli} when T_{glo} from Equation (4) is known.

Equation (7) can be put in an alternate form:

$$T_{gli} = \left[\frac{H_s \tau_{rsd} \tau_{asd} A_{pn} \alpha_{sd} + H_s C A_{nm} R \tau_{rsi} \tau_{asi} \alpha_{si} +}{A_{glo}} \right.$$

$$\left. \frac{H_{sk} \tau_{rsk} \tau_{ask} A_{pn} \alpha_{skn}}{A_{glo}} \right] \frac{D_{glo} \ln \frac{D_{glo}}{D_{gli}}}{2 K_m} + T_{glo} \tag{8}$$

Subtracting T_o from both sides yields

$$T_{gli}-T_o = \left[\text{Above}\right] D_{glo} \frac{\ln \frac{D_{glo}}{D_{gli}}}{2 K_m} + T_{glo}-T_o \qquad (9)$$

Equation (9) expresses the theoretical temperature difference between the inside surface of the thin hollow glass cylinder and the surroundings when the target is a flat plate where the temperature of the outside surface is given by Equation (4).

Experimental Verification (Flat Plate #2)

The equation to be evaluated for experimental verification when the target is a flat plate inside a glass cylinder is

$$\frac{H_s \tau_{rsd} \tau_{asd} A_{pn} \alpha_{sd} + H_s C A_{nm} R \tau_{rsi} \tau_{asi} \alpha_{si} + H_{sk} \tau_{rsk} \tau_{ask} A_{pn} \alpha_{skn}}{A_{glo}} = \frac{2 K_m \left[T_{gli}-T_{glo}\right]}{D_{glo} \ln \frac{D_{glo}}{D_{gli}}} \qquad (7)$$

Using the flat plate previously designated, Equation (7) becomes

$$\left[.05868 + 1.0870\ C\right] H_T = \frac{2 K_m \left[T_{gli}-T_{glo}\right]}{D_{glo} \ln \frac{D_{glo}}{D_{gli}}} \qquad (10)$$

or, since

$$\frac{Q_a}{A_{glo}} = \frac{Q_\ell}{A_{glo}} \qquad (5)$$

where

$$\frac{Q_a}{A_{glo}} = \left[.05868 + 1.0870\ C\right] H_T \qquad (11)$$

and

$$\frac{Q_\ell}{A_{glo}} = \frac{2\ K_m \left[T_{gli}-T_{glo}\right]}{D_{glo}\ \ln \frac{D_{glo}}{D_{gli}}} \tag{3}$$

therefore:

$$\frac{Q_a}{A_{glo}} = \frac{2\ K_m \left[T_{gli}-T_{glo}\right]}{D_{glo}\ \ln \frac{D_{glo}}{D_{gli}}} \tag{12}$$

The following values pertain to Equation (12):

K_m = .6774 Btu ft/hr ft^2 °F

D_{glo} = 4/12 ft

D_{gli} = 3.75/12 ft

$$\frac{Q_a}{A_{glo}} = 62.97 \left[T_{gli}-T_{glo}\right] \tag{13}$$

Equation (13) can be written

$$\frac{Q_a}{A_{glo}} = 62.97 \left[(T_{gli}-T_o) - (T_{glo}-T_o)\right] \tag{14}$$

Substitution of the results of Equation (14) and Equation (11) in Equation (5) results in

$$\left[.05868 + 1.0870\ C\right] H_T = 62.97 \left[(T_{gli}-T_o) - (T_{glo}-T_o)\right] \tag{15}$$

Equation (15) can be rearranged to

$$T_{gli}-T_o = \frac{1}{62.97} \left[.05868 + 1.0870\ C\right] H_T + (T_{glo}-T_o) \tag{16}$$

or, using the result of Equation (5)

$$T_{gli}-T_o = \frac{1}{62.97} \frac{Q_a}{A_{glo}} + (T_{glo}-T_o) \tag{17}$$

Where $T_{glo}-T_o$ is determined from

$$T_{glo}-T_o = \sqrt[4]{T_s^4 + \frac{1}{.1600}\left[\frac{Q_a}{A_{glo}} - h\left[T_{glo}-T_o\right]\right]} - T_o \qquad (18)$$

Equation (18) can be evaluated for any Q_a/A_{glo} for this glass cylinder by use of Figure 4.

Equation (17) was solved for the theoretical temperature rise of the inside surface of the glass by assuming various Q_a/A_{glo} values and determining the temperature rise of the glass $\left[T_{glo}-T_o\right]$ for the least loss conditions previously mentioned by using Figure 4. A series of computations are shown in Table XI.

Equation (17) was solved for the theoretical temperature rise of the inside surface of the glass for the maximum loss conditions by using Figure 4 to determine $\left[T_{glo}-T_o\right]$ for various assumed values of Q_a/A_{glo}. A series of these computations appear in Table XII.

The theoretical $\left[T_{gli}-T_o\right]$ values for the least loss and maximum loss conditions are plotted against Q_a/A_{glo} values as solid lines in Figure 5.

The experimental verification is made by using Equation (11) to transfer H_T values obtained in the test to Q_a/A_{glo} values, and also recording the actual temperature rise of the inside surface of the glass cylinder above the surroundings $\left[T_{gli}-T_o\right]$. The steps are shown in Table XIII. The temperature rises of the inside surface $\left[T_{gli}-T_o\right]$ are plotted vs. Q_a/A_{glo} as circles in Figure 5 to show agreement with the theoretical values that appear as two solid black lines.

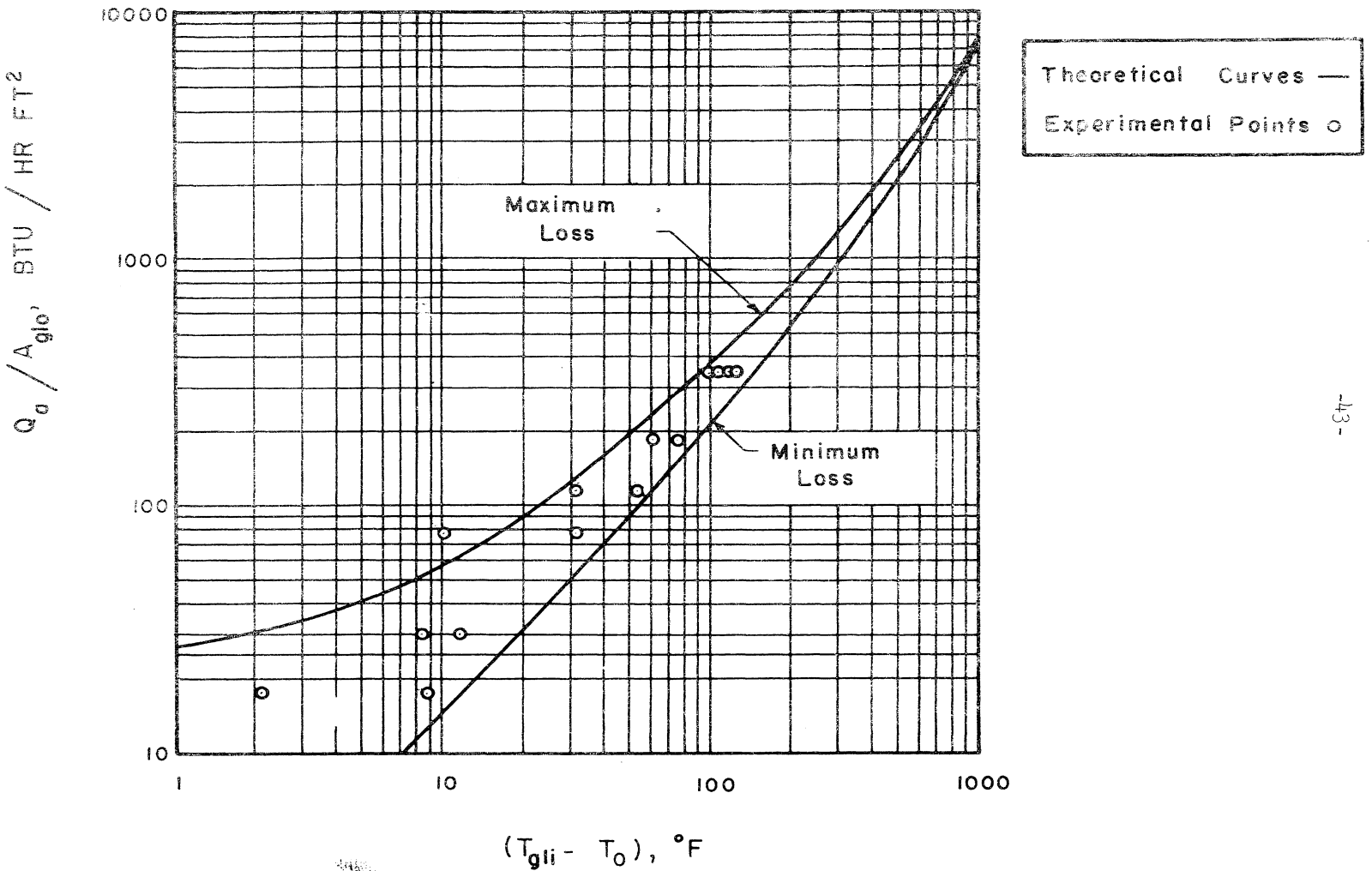

Figure 5. Theoretical and Experimental Plot of $(T_{gli} - T_o)$ vs. Q_a/A_{glo} for Glass Cylinder, in Air, Inside Surface.

Table XI

Glass Cylinder, in Air, Inside Surface, Minimum Loss Conditions

$\frac{Q_a}{A_{glo}}$ $\frac{Btu}{hr\,ft^2}$	$[T_{glo}-T_o]$ °R	$\frac{1}{62.97} \times \frac{Q_a}{A_{glo}}$ °R	$[T_{gli}-T_o]$ °R
1.23	1	.02	1.02
7.00	5	.11	5.11
15.04	30	.24	10.24
52.18	50	.83	30.83
94.86	70	1.51	51.51
220.6	100	3.50	103.50
549.2	200	8.72	208.72
1566	400	24.87	424.87
3265	600	51.85	651.85
5941	800	94.34	894.34
8970	1000	142.44	1142.44

Table XII

Glass Cylinder, in Air, Inside Surface, Maximum Loss Conditions

$\frac{Q_a}{A_{glo}}$ $\frac{Btu}{hr\ ft^2}$	$[T_{glo}-T_o]$ °R	$\frac{1}{62.97} \times \frac{Q_a}{A_{glo}}$ °R	$[T_{gli}-T_o]$ °R
24.75	0	.39	.39
28.22	1	.45	1.45
42.14	5	.67	5.67
59.62	10	.95	10.95
130.7	30	2.08	32.08
203.7	50	3.23	53.23
396.2	100	6.29	106.29
833.8	200	13.24	213.24
2018	400	32.05	432.05
3719	600	59.06	659.06
6597	800	104.76	904.76
10690	1000	169.78	1169.78

Table XIII

Glass Cylinder, in Air, Inside Surface, Flat Plate #2 Target, Experimental Data

Pyrheliometer millivolts [Test]	H_T $\frac{Btu}{hr\,ft^2}$	C	1.0870 C H_T $\frac{Btu}{hr\,ft^2}$	.05868 H_T $\frac{Btu}{hr\,ft^2}$	$\frac{Q_a}{A_{glo}}$ $\frac{Btu}{hr\,ft^2}$	$[T_{gli} - T_o]$ °F [Test]
7.6	301	1	327.2	17.66	344.86	99 -124
7.7	305	1	331.5	17.90	349.40	104 -117
7.7	305	.5	165.8	17.90	183.70	60 - 75
5.2	206	.5	103.0	12.09	115.09	31 - 53
6.0	238	.25	64.68	13.97	78.65	10 - 31
2.31	91.5	.25	24.87	5.37	30.24	8.3- 11.7
7.5	297	0	0	17.43	17.43	2.1- 877

FLAT PLATE UNDER A THIN HOLLOW GLASS CYLINDER IN VACUUM

General Equation

In the steady state condition

$$\frac{Q_a}{A_p} = \frac{Q_\ell}{A_p} \tag{1}$$

The equation for Q_a previously developed is

$$Q_a = H_s \tau_{rsd} \tau_{asd} A_{pn} \alpha_{sd} + H_s C A_{nm} R \tau_{rsi} \tau_{asi} \alpha_{si} + H_{sk} \tau_{rsk} \tau_{ask} A_{pn} \alpha_{skn} \tag{2}$$

When Equation (2) is divided by A_p

$$\frac{Q_a}{A_p} = \frac{H_s \tau_{rsd} \tau_{asd} A_{pn} \alpha_{sd} + H_s C A_{nm} R \tau_{rsi} \tau_{asi} \alpha_{si} + \frac{H_{sk} \tau_{rsk} \tau_{ask} A_{pn} \alpha_{skn}}{A_p}}{A_p} \tag{3}$$

Since there is no air for convection loss, the right hand of Equation (1) is concerned only with radiation loss and so

$$\frac{Q_\ell}{A_p} = \sigma F_a F_e \left[T_p^4 - T_{gli}^4 \right] \tag{4}$$

Thus substituting the results of Equation (3) and Equation (4) into Equation (1) results in

$$\frac{H_s \tau_{rsd} \tau_{asd} A_{pn} \alpha_{sd} + H_s C A_{nm} R \tau_{rsi} \tau_{asi} \alpha_{si} + H_{sk} \tau_{rsk} \tau_{ask} A_{pn} \alpha_{skn}}{A_p} = \sigma F_a F_e \left[T_p^4 - T_{gli}^4 \right] \tag{5}$$

Equation (5) can be rearranged to yield

$$T_p = \sqrt[4]{T_{gli}^4 + \frac{H_s \tau_{rsd} \tau_{asd} A_{pn} \alpha_{sd} + H_s C A_{nm} R \tau_{rsi} \tau_{asi} \alpha_{si} + H_{sk} \tau_{rsk} \tau_{ask} A_{pn} \alpha_{skn}}{\sigma F_a F_e A_p}} \tag{6}$$

Subtracting T_o from each side

$$T_p - T_o = \sqrt[4]{\text{Above}} - T_o \tag{7}$$

Where T_{gli} is obtained from the equation

$$T_{gli} = \left[\frac{H_s \tau_{rsd} \tau_{asd} A_{pn} \alpha_{sd} + H_s C A_{nm} R \tau_{rsi} \tau_{asi} \alpha_{si} + H_{sk} \tau_{rsk} \tau_{ask} A_{pn} \alpha_{skn}}{A_{glo}} \right] \tag{8}$$

$$\frac{D_{glo} \ln \frac{D_{glo}}{D_{gli}}}{2 K_m} + T_{glo}$$

and where T_{glo} is obtained from equation

$$T_{glo} = \sqrt[4]{T_s^4 + \frac{1}{\sigma \epsilon_{glo}} \left[\frac{H_s \tau_{rsd} \tau_{asd} A_{pn} \alpha_{sd} + H_s C A_{nm} R \tau_{rsi} \tau_{asi} \alpha_{si} +}{A_{glo}} \right.} \tag{9}$$

$$\left. \frac{H_{sk} \tau_{rsk} \tau_{ask} A_{pn} \alpha_{skn}}{A_{glo}} - h \left[T_{glo} - T_o \right] \right]$$

The limiting value to apply to the above equations is

$$C = \frac{A_{nm}'}{A_{tr}} = \frac{A_{pn} + A_{nm}}{A_{pn}} = \frac{n \left[1 - \frac{n^2}{16} - \frac{n}{2} \tan \frac{\alpha}{2} \right]}{2 \tan \frac{\alpha}{2} \left(1 + \frac{n^2}{16} \right)^2} \tag{10}$$

The ratio is developed in the appendix.

Experimental Verification

The equation to be evaluated is

$$\frac{H_s \tau_{rsd} \tau_{asd} A_{pn} \alpha_{sd} + H_s C A_{nm} R \tau_{rsi} \tau_{asi} \alpha_{si} + H_{sk} \tau_{rsk} \tau_{ask} A_{pn} \alpha_{skn}}{A_p} =$$

$$\sigma F_a F_e \left[T_p^4 - T_{gli}^4\right] \tag{5}$$

The left side may be obtained from previous calculations by multiplying numerator and denominator by A_{glo}, thus

$$\frac{H_s \tau_{rsd} \tau_{asd} A_{pn} \alpha_{sd} + H_s C A_{nm} R \tau_{rsi} \tau_{asi} \alpha_{si} + H_{sk} \tau_{rsk} \tau_{ask} A_{pn} \alpha_{skn}}{A_{glo}} \times \frac{A_{glo}}{A_p} =$$

$$\sigma F_a F_e \left[T_p^4 - T_{gli}^4\right] \tag{11}$$

Substituting the results of Equation (2) in Equation (11) and utilizing the fact that $A_{glo}/A_p = 7.107$, the following equation results:

$$7.107 \frac{Q_a}{A_{glo}} = \sigma F_a F_e \left[T_p^4 - T_{gli}^4\right] \tag{12}$$

From a previous development concerning the thin hollow glass cylinder

$$\frac{Q_a}{A_{glo}} = .05868\ H_s + 1.208\ CH_s + .005868\ H_{sk} \tag{13}$$

Substitution of the equality in Equation (13) in Equation (12) results in

$$7.107 \left[.05868\ H_s + 1.208\ CH_s + .005868\ H_{sk}\right] =$$

$$\sigma\ F_a F_e \left[T_p^4 - T_{gli}^4\right] \tag{14}$$

or

$$.417\ H_s + 8.58\ CH_s + .0417\ H_{sk} = \sigma F_a F_e \left[T_p^4 - T_{gli}^4\right] \qquad (15)$$

and since $H_s \sim .9\ H_T$, and $H_{sk} \sim .1\ H_T$

$$.376\ H_T + 7.726\ CH_T + .0376\ H_T = \sigma F_a F_e \left[T_p^4 - T_{gli}^4\right] \qquad (16)$$

Collecting terms this becomes

$$.417\ H_T + 7.726\ CH_T = \sigma F_a F_e \left[T_p^4 - T_{gli}^4\right] \qquad (17)$$

which, put in terms of steady state conditions, is

$$\frac{Q_a}{A_p} = \frac{Q_\ell}{A_p} \qquad (1)$$

where

$$\frac{Q_a}{A_p} = .417\ H_T + 7.726\ CH_T \qquad (18)$$

The time rate of energy loss per unit area is:

$$\frac{Q_\ell}{A_p} = \sigma F_a F_e \left[T_p^4 - T_{gli}^4\right] \qquad (19)$$

Substitution of this result in Equation (1) yields

$$\frac{Q_a}{A_p} = \sigma F_a F_e \left[T_p^4 - T_{gli}^4\right] \qquad (20)$$

In this case $F_a = 1$, and F_e is evaluated at a mean between that of a body that is small compared to its surroundings and a body that is large compared to its surroundings $F_e = .925$

$$\frac{Q_a}{A_p} = .1600 \left[\left(\frac{T_p}{100}\right)^4 - \left(\frac{T_{gli}}{100}\right)^4\right] \qquad (21)$$

Recalling the assumption that Q_a to the plate equals Q_a to the outside surface of the thin hollow glass cylinder

$$\frac{Q_a}{A_p} = \frac{Q_a}{A_{glo}} \times \frac{A_{glo}}{A_p} = 7.107 \frac{Q_a}{A_{glo}} \tag{22}$$

or

$$\frac{Q_a}{A_{glo}} = .1407 \frac{Q_a}{A_p} \tag{23}$$

Utilizing Equation (18) and Equation (21) in Equation (1) yields

$$\left[.417 + 7.726\ C\right] H_T = .1600 \left[\left(\frac{T_p}{100}\right)^4 - \left(\frac{T_{gli}}{100}\right)^4\right] \tag{24}$$

or utilizing the results of Equations (18) and (21)

$$\frac{Q_a}{A_p} = .1600 \left[\left(\frac{T_p}{100}\right)^4 - \left(\frac{T_{tli}}{100}\right)^4\right] \tag{21}$$

or, in terms of plate temperature

$$T_p = 100 \sqrt[4]{\left(\frac{T_{gli}}{100}\right)^4 + \frac{1}{.1600}\left[\frac{Q_a}{A_p}\right]} \tag{25}$$

Subtracting T_o from both sides yields

$$T_p - T_o = 100 \sqrt[4]{\left(\frac{T_{gli}}{100}\right)^4 + \frac{1}{.1600}\left[\frac{Q_a}{A_p}\right]} - T_o \tag{26}$$

which in alternate form is

$$T_p - T_o = 100 \sqrt[4]{\left(\frac{T_{gli}}{100}\right)^4 + \left[\frac{.417 + 7.726\ C}{.1600}\right] H_T} - T_o \tag{27}$$

T_{gli} may be determined from

$$T_{gli} - T_o = \frac{1}{62.97} \times \frac{Q_a}{A_{glo}} + (T_{glo} - T_o) \tag{28}$$

and where

$$T_{glo}-T_o = \sqrt[4]{T_s^4 + \frac{1}{.1600}\left[\frac{Q_a}{A_{glo}} - h\left[T_{glo}-T_o\right]\right]} - T_o \qquad (29)$$

The theoretical temperature rise of the plate $\left[T_p-T_o\right]$ using Equation (26) can be calculated by assuming various Q_a/A_p values under the assumptions T_o = 520°R, that Q_a/A_{glo} can be determined from Equation (23) and that T_{gli} can be determined for minimum loss and for maximum loss conditions from Figure 5. The graph represents the solution of Equation (28), which in turn is based on Equation (29).

Tabulated values in the solution of Equation (26) are shown in Table XIV for least loss conditions and in Table XV for maximum loss conditions. The values of $\left[T_p-T_o\right]$ vs. Q_a/A_p for each loss condition are plotted as solid lines in Figure 6.

The theoretical verification of the predicted temperature rise comes by using Equation (18) to transfer H_T values to Q_a/A_p under test conditions and recording the actual temperature rise of the plate. A series of test results are shown in Table XVI. The temperature rise $\left[T_p-T_o\right]$ is plotted vs. Q_a/A_p as circles in Figure 6 to show comparison with theory.

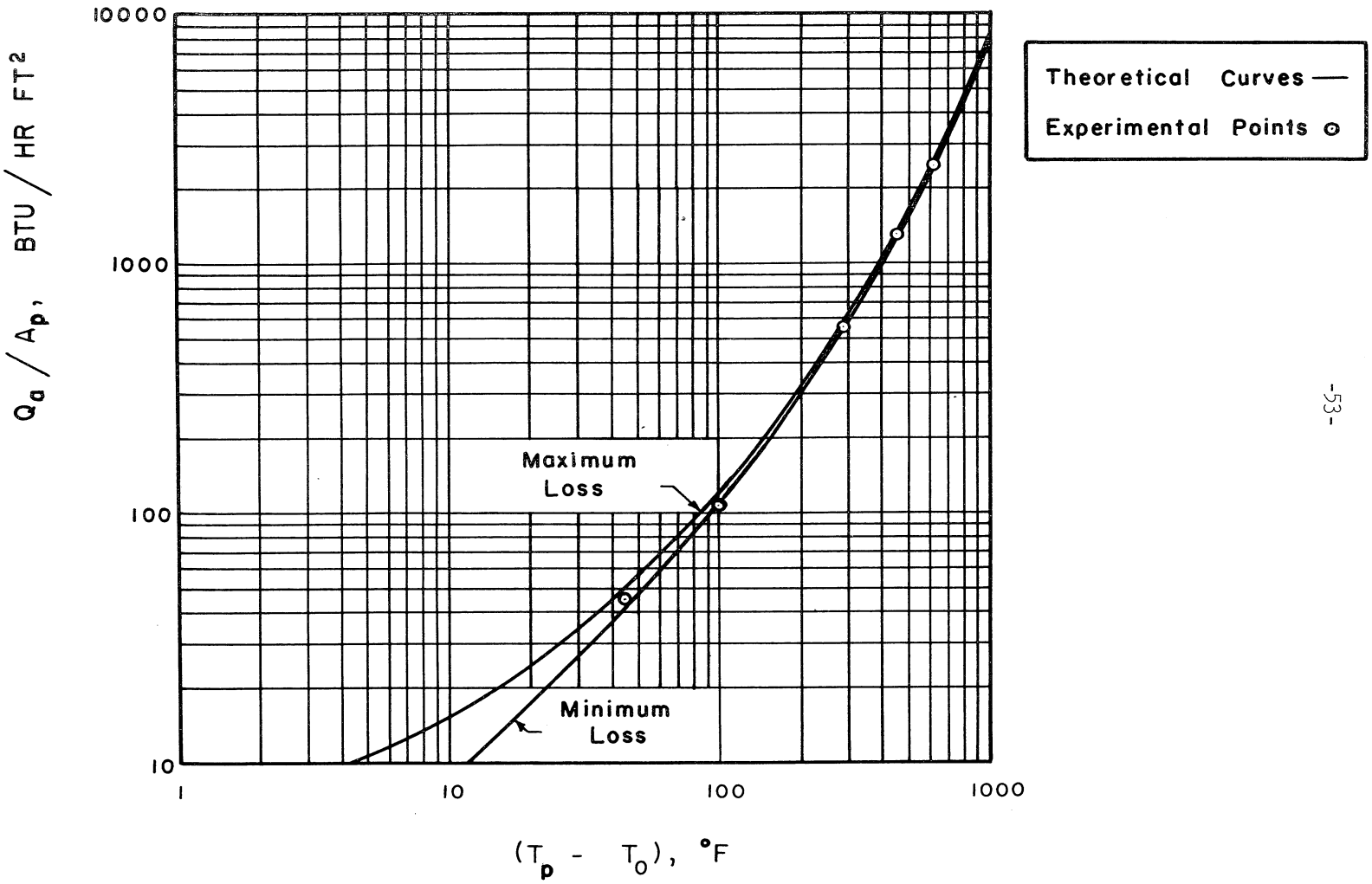

Figure 6. Theoretical and Experimental Plot of $(T_p - T_o)$ vs. Q_a/A_p for Flat Plate No. 2, Under Glass, in Vacuum.

Table XIV

Flat Plate #2, Under Glass, in Vacuum, Minimum Loss Conditions

$\frac{Q_a}{A_p}$ $\frac{Btu}{hr\ ft^2}$	$\frac{Q_a}{A_{glo}}$ $\frac{Btu}{hr\ ft^2}$	$[T_{gli} - T_o]$ °F	T_{gli} °R	$[T_p - T_o]$ °F
1	.1407	.1	520.1	1.2
7.107	1	.8	520.8	8.5
10	1.407	1.1	521.8	11.8
20	2.814	2.1	522.1	22.8
50	7.035	5	525	52.2
100	14.07	9	529	92.5
200	28.14	17	537	155.5
500	70.35	38	558	279.9
1000	140.7	68	588	408.9
2000	281.4	120	640	571
5000	703.5	240	760	844
100002	1407	385	905	1102

Table XV

Flat Plate #2, Under Glass, in Vacuum, Maximum Loss Conditions

$\frac{Q_a}{A_p}$ $\frac{Btu}{hr\,ft^2}$	$\frac{Q_a}{A_{glo}}$ $\frac{Btu}{hr\,ft^2}$	$[T_{gli} - T_o]$ °F	T_{gli} °R	$[T_p - T_o]$ °F
10	1.407	- 6.7	513.3	4.4
20	2.814	- 6.3	513.7	15.3
50	7.035	- 5.0	515	44.3
100	14.07	- 2.9	517.1	84.9
200	28.14	1.3	521.3	147.9
500	70.35	14	534	272
1000	140.7	34	554	400.9
2000	281.4	74	594	562
5000	703.5	180	700	834
10000	1407	325	845	1090

Table XVI

Flat Plate #2, Under Glass, in Vacuum, Experimental Data

Pyrheliometer millivolts [Test]	H_T $\frac{Btu}{hr\,ft^2}$	C	$7.726CH_T$ $\frac{Btu}{hr\,ft^2}$	$.4170\,H_T$ $\frac{Btu}{hr\,ft^2}$	$\frac{Q_a}{A_p}$ $\frac{Btu}{hr\,ft^2}$	$[T_p - T_o]$ °F [Test]
7.7	305	1	2356.43	127.19	2483.62	603
7.7	305	.5	1178.22	127.19	1305.41	452
6.0	238	.25	459.7	99.24	558.94	288
6.7	265	0	0	110.50	110.50	100
2.78	110	0	0	45.87	45.87	44

CYLINDER UNDER GLASS IN AIR

General Equation

In the steady state condition

$$\frac{Q_a}{A_{cy}} = \frac{Q_\ell}{A_{cy}} \tag{1}$$

The time rate of energy addition is the sum of four factors

$$Q_a = Q_{sd} + Q_{si} + Q_{skd} + Q_{ski} \tag{2}$$

The direct sun component is given by

$$Q_{sd} = H_s \tau_{rsd} \tau_{asd} A_{cyn} \alpha_{sd} \tag{3}$$

and the sun's indirect component is

$$Q_{si} = H_s C R A_{nm} \tau_{rsi} \tau_{asi} \alpha_{si} \tag{4}$$

The sky contribution is approximated by

$$Q_{skd} + Q_{ski} \approx H_{sk} \tau_{rsk} \tau_{ask} A_{cyn} \alpha_{skn} \tag{5}$$

Summing all contributions and dividing by A_{cy}

$$\frac{Q_a}{A_{cy}} = \frac{H_s \tau_{rsd} \tau_{asd} A_{cyn} \alpha_{sd} + H_s C R A_{nm} \tau_{rsi} \tau_{asi} \alpha_{si} +}{A_{cy}}$$

$$\frac{H_{sk} \tau_{rsk} \tau_{ask} A_{cyn} \alpha_{skn}}{A_{cy}} \tag{6}$$

The left side of Equation (1) can be expressed as the sum of the time rate of radiation and convection loss per unit area

$$\frac{Q_\ell}{A_{cy}} = \frac{Q_r}{A_{cy}} + \frac{Q_c}{A_{cy}} \tag{7}$$

The time rate of radiation loss per unit area can be expressed as

$$\frac{Q_r}{A_{cy}} = \sigma F_a F_e \left[T_{cy}^4 - T_{gli}^4\right] \tag{8}$$

The time rate of convection loss per unit area can be expressed as Beckman did for annular spaces by putting the time rate of energy loss per foot of annylys in the form of the conduction equation through cylindrical annulus(7).

$$\frac{Q_c}{L} = \frac{2\pi K_c \left[T_{cy} - T_{gli}\right]}{\ln \frac{D_{gli}}{D_{cy}}} \tag{9}$$

Multiplying by L and dividing by A_{cy}, the following is obtained:

$$\frac{Q_c}{A_{cy}} = \frac{2\pi L K_c \left[T_{cy} - T_{gli}\right]}{A_{cy} \ln \frac{D_{gli}}{D_{cy}}} \tag{10}$$

where K_c is an equivalent conductivity that accounts for both convection and conduction heat exchange. Thus

$$\frac{Q_\ell}{A_{cy}} = \sigma F_a F_e \left[T_{cy}^4 - T_{gli}^4\right] + \frac{2\pi L K_c \left[T_{cy} - T_{gli}\right]}{A_{cy} \ln \frac{D_{gli}}{D_{cy}}} \tag{11}$$

Substituting Equation (11) and Equation (6) in Equation (1) gives

$$\frac{H_s \tau_{rsd} \tau_{asd} A_{cyn} \alpha_{sd} + H_s CRA_{nm} \tau_{rsi} \tau_{asi} \alpha_{si} + H_{sk} \tau_{rsk} \tau_{ask} A_{cyn} \alpha_{skn}}{A_{cy}} =$$

$$\sigma F_a F_e \left[T_{cy}^4 - T_{gli}^4\right] + \frac{2\pi L K_c \left[T_{cy} - T_{gli}\right]}{A_{cy} \ln \frac{D_{gli}}{D_{cy}}} \tag{12}$$

---

(7) Jakob, Heat Transfer, pp. 539-542.

Equation (12) may be rearranged in the following form:

$$T_{cy} = \sqrt[4]{T_{gli}^4 + \frac{1}{\sigma F_a F_e}\left[\frac{H_s \tau_{rsd} \tau_{asd} A_{cyn} \alpha_{sd} + H_s CRA_{nm} \tau_{rsi} \tau_{asi} \alpha_{si} + H_{sk} \tau_{rsk} \tau_{ask} A_{cyn} \alpha_{skn}}{A_{cy}} - \frac{2\pi L K_c \left[T_{cy} - T_{gli}\right]}{A_{cy} \ln \frac{D_{gli}}{D_{cy}}}\right]} \quad (13)$$

Subtracting T_o from both sides

$$T_{cy} - T_o = \sqrt[4]{\text{Above}} - T_o \quad (14)$$

An alternate form of Equation (14) is

$$T_{cy} - T_o = \sqrt[4]{T_{gli}^4 \frac{1}{\sigma F_a F_e}\left[\frac{Q_a}{A_{cy}} - \frac{2\pi L K_c \left[T_{cy} - T_{gli}\right]}{A_{cy} \ln \frac{D_{gli}}{D_{cy}}}\right]} - T_o \quad (15)$$

Where T_{gli} is determined from

$$T_{gli} = \left[\frac{H_s \tau_{rsd} \tau_{asd} A_{cyn} \alpha_{sd} + H_s CRA_{mn} \tau_{rsi} \tau_{asi} \alpha_{si} + H_{sk} \tau_{rsk} \tau_{ask} A_{cyn} \alpha_{skn}}{A_{glo}}\right] \frac{D_{glo} \ln \frac{D_{glo}}{D_{gli}}}{2 K_m} + T_o \quad (16)$$

And T_{glo} is determined from the equation

$$T_{glo} = \sqrt[4]{T_s^4 + \frac{1}{\sigma \varepsilon_{glo}}\left[\frac{H_s \tau_{rsd} \tau_{asd} A_{cyn} \alpha_{sd}}{A_{glo}} + \frac{H_s CRA_{mn} \tau_{rsi} \tau_{asi} \alpha_{si} + H_{sk} \tau_{rsk} \tau_{ask} A_{cyn} \alpha_{skn}}{A_{glo}} - h\left[T_{glo} - T_o\right]\right]} \quad (17)$$

The limiting value of A_{nm} to be used with Equation (13) or (14) is determined from

$$C = \frac{A_{nm'}}{A_{tr}} = \frac{A_{cyn} + A_{nm}}{A_{cyn}} \leq \frac{n}{2 \sin \frac{\alpha}{2} \left(1 + \frac{n^2}{16}\right)} \qquad (18)$$

This equation is derived in the appendix.

Experimental Verification

The equation to be evaluated is

$$\frac{H_s \tau_{rsd} \tau_{asd} A_{cyn} \alpha_{sd} + H_s C R A_{nm} \tau_{rsi} \tau_{asi} \alpha_{si} + H_{sk} \tau_{rsk} \tau_{ask} A_{cyn} \alpha_{skn}}{A_{cy}} =$$

$$\sigma F_a F_e \left[T_{cy}^4 - T_{gli}^4\right] + \frac{2\pi L K_c \left[T_{cy} - T_{gli}\right]}{A_{cy} \ln \frac{D_{gli}}{D_{cy}}} \qquad (12)$$

The left side of Equation (12) is

$$\frac{Q_a}{A_{cy}} = \frac{H_s \tau_{rsd} \tau_{asd} A_{cyn} \alpha_{sd} + H_s C R A_{nm} \tau_{rsi} \tau_{asi} \alpha_{si} + H_{sk} \tau_{rsk} \tau_{ask} A_{cyn} \alpha_{skn}}{A_{cy}} \qquad (6)$$

where the following values apply:

$H_s = .9\ H_T$

$\tau_{rsd} \sim \tau_{rsi} \sim \tau_{rsk} = .93$

$\tau_{asd} \sim \tau_{asi} \sim \tau_{ask} = .98$

$\alpha_{sd} = .95$

$\alpha_{si} = .98$

$\alpha_{skn} = .95$

$\frac{A_{cyn}}{A_{cy}} = .2574$

$$\frac{A_{nm}}{A_{cy}} = 9.953$$

$$R = .70$$

$$H_{sk} = .1\ H_T$$

$$\frac{Q_a}{A_{cy}} = (.9\ H_T)(.93)(.98)(.2574)(.95) +$$
$$(.9\ H_T)(.70)(9.953)(C)(.93)(.98)(.98) +$$
$$(.1\ H_T)(.93)(.98)(.2574)(.95) \qquad (19)$$

$$\frac{Q_a}{A_{cy}} = .2006\ H_T + 5.601\ CH_T + .02229\ H_T \qquad (20)$$

$$\frac{Q_a}{A_{cy}} = .2229\ H_T + 5.601\ CH_T \qquad (21)$$

The time rate of energy loss per unit area may be expressed as the sum of two components

$$\frac{Q_\ell}{A_{cy}} = \frac{Q_r}{A_{cy}} + \frac{Q_c}{A_{cy}} \qquad (7)$$

in which the radiation component is

$$\frac{Q_r}{A_{cy}} = \sigma F_a F_e \left[T_{cy}^4 - T_{gli}^4\right] \qquad (8)$$

where

$$F_a = 1$$

$$F_e = .925$$

$$\sigma = .173 \times 10^{-8}\ \frac{Btu}{hr\ ft^2\ {}^\circ R^4}$$

$$\frac{Q_r}{A_{cy}} = .173 \times 1 \times .925 \left[\left(\frac{T_{cy}}{100}\right)^4 - \left(\frac{T_{gli}}{100}\right)^4\right] \qquad (22)$$

thus

$$\frac{Q_r}{A_{cy}} = .1600 \left[\left(\frac{T_{cy}}{100}\right)^4 - \left(\frac{T_{gli}}{100}\right)^4\right] \tag{23}$$

The convection loss term is

$$\frac{Q_c}{A_{cy}} = \frac{2\pi L K_c \left[T_{cy} - T_{gli}\right]}{A_{cy} \ln \frac{D_{gli}}{D_{cy}}} \tag{10}$$

The term K_c is an equivalent conductivity and is defined for a given diameter ratio across an annulus as by means of a special Nusselt No.

$$N_{Nu} = \frac{K_c}{K_f} = C\ (N_{Gr})^n \tag{24}$$

For a diameter ratio of $\frac{D_{gli}}{D_{cy}} = 1.714$ Equation (24)[8] is

$$\frac{K_c}{K_f} = .0685\ (N_{Gr})^{.258} \tag{25}$$

or

$$K_c = .0685\ K_f\ (N_{Gr})^{.258} \tag{26}$$

which can be put as

$$K_c = .0685\ K_f\ \left(\frac{g\beta f}{\nu_f^2} \times D_{cy}^3 \quad \Delta T\right)^{.258} \tag{27}$$

Equation (27) may be expressed for convenience as

$$K_c = .0685\ K_f\ (N_f\ D_{cy}^3\ \Delta T)^{.258} \tag{28}$$

where

$$N_f = \frac{g\beta f}{\nu_f 2} \tag{29}$$

---

(8) Ibid.

Equation (28) may in turn be written

$$K_c = C_e \, (\Delta T)^{.258} \tag{30}$$

where

$$C_e = .0685 \, K_f \, (N_f D_{cy}^{\,3})^{.258} \tag{31}$$

Equation (31) is solved for C_e with film temperatures ranging from 0° to 600°F in seven increments. The steps are in Table XVII. The results of this table are plotted in Figure 7. This plot enables C_e to be determined when the film temperature is known and consequently Equation (30) can be solved for K_c when the ΔT between the cylinder at the focus and the inside of the glass cylindrical cover is known.

With K_c determined, insertion of the following values in Equation (10) will yield:

$$L = .4271 \text{ ft}$$

$$\frac{D_{gli}}{D_{cy}} = 1.714$$

$$A_{cy} = .2968 \text{ ft}^2$$

$$\frac{Q_c}{A_{cy}} = \frac{2\pi \times .4271 \, K_c \left[T_{cy} - T_{gli}\right]}{.2968 \ln 1.714} = 16.78 \, K_c \left[T_{cy} - T_{gli}\right] \tag{32}$$

Insertion of the results of Equation (32) and Equation (23) in Equation (7) yields

$$\frac{Q_\ell}{A_{cy}} = .1600 \left[\left(\frac{T_{cy}}{100}\right)^4 - \left(\frac{T_{gli}}{100}\right)^4\right] + 16.78 \, K_c \left[T_{cy} - T_{gli}\right] \tag{33}$$

Since

$$\frac{Q_a}{A_{cy}} = \frac{Q_\ell}{A_{cy}} \tag{1}$$

$$\frac{Q_a}{A_{cy}} = .1600 \left[\left(\frac{T_{cy}}{100}\right)^4 - \left(\frac{T_{gli}}{100}\right)^4 \right] + 16.78 \left[T_{cy} - T_{gli} \right] \qquad (34)$$

Substitution of the results of Equation (21) yields

$$\left[.2229 + 5.601C \right] H_T = .1600 \left[\left(\frac{T_{cy}}{100}\right)^4 - \left(\frac{T_{gli}}{100}\right)^4 \right] + 16.78 \left[T_{cy} - T_{gli} \right] \qquad (35)$$

or

$$T_{cy} = 100 \sqrt[4]{\left(\frac{T_{gli}}{100}\right)^4 + \frac{1}{.1600} \left[\left[.2229 + 5.601C \right] H_T - 16.78 K_c \left[T_{cy} - T_{gli} \right] \right]} \qquad (36)$$

Subtracting T_o from both sides gives

$$T_{cy} - T_o = 100 \sqrt[4]{\text{Above}} - T_o \qquad (37)$$

or, in alternate form,

$$T_{cy} - T_o = 100 \sqrt[4]{\left(\frac{T_{gli}}{100}\right)^4 + \frac{1}{.1600} \left[\frac{Q_a}{A_{cy}} - 16.78 \left[T_{cy} - T_{gli} \right] \right]} - T_o \qquad (38)$$

Where T_{gli} is determined from

$$T_{gli} - T_o = \left[\frac{Q_a}{A_{glo}} \right] \frac{D_{glo} \ln \frac{D_{glo}}{D_{gli}}}{2 K_m} + (T_{glo} - T_o) \qquad (39)$$

or

$$T_{gli} - T_o = \left[\frac{Q_a}{A_{glo}} \right] \frac{1}{62.97} + (T_{glo} - T_o) \qquad (40)$$

and T_{glo} can be determined from

$$T_{glo} - T_o = 100 \sqrt[4]{\left(\frac{T_s}{100}\right)^4 + \frac{1}{.1600} \left[\frac{Q_a}{A_{glo}} - h \left[T_{glo} - T_o \right] \right]} - T_o \qquad (41)$$

It has been assumed that

$$(Q_a)_{cy} = (Q_\ell)_{cy} = (Q_a)_{gli} = (Q_a)_{glo} = (Q_\ell)_{glo} \tag{42}$$

Thus

$$\frac{Q_a}{A_{glo}} = \frac{Q_a}{A_{cy}} \times \frac{A_{cy}}{A_{glo}} = .203 \frac{Q_a}{A_{cy}} \tag{43}$$

Equation (38) can be solved for the theoretical temperature rise of the cylinder by assuming a value of $\left[T_{cy} - T_o\right]$. With Equation (43), $\frac{Q_a}{A_{glo}}$ can be determined and thus T_{gli} can be determined from Figure 5, which is a plotted solution of Equation (40). The T_{cy} is estimated and then $\left[T_{cy} - T_o\right]$ is calculated by means of Equation (38). This is a trial procedure that is continued until the estimated T_{cy} equals the calculated T_{cy}. This procedure includes determining K_c at the film temperature $\left[T_f = \frac{T_{cy} + T_{gli}}{2}\right]$.

A series of steps in the solution of Equation (38) are shown in Table XVIII for minimum loss conditions. And in Table XIX for maximum loss conditions. The solutions $\left[T_{cy} - T_o\right]$ in Table XVIII and Table XIX are plotted against $\frac{Q_a}{A_{cy}}$ in Figure 8 as two solid lines.

The experimental verification comes from using Equation (21) to translate H_T values as determined by a pyrheliometer into $\frac{Q_a}{A_{cy}}$ values. Table XX shows a series of H_T values, equivalent $\frac{Q_a}{A_{cy}}$, and the measured temperature rise of the cylinder $\left[T_{cy} - T_o\right]$ above the surrounding temperature. The experimental temperature rises $\left[T_{cy} - T_o\right]$ are plotted vs. $\frac{Q_a}{A_{cy}}$ in Figure 8 as circles to show contrast with the theoretical temperature rise above the surroundings of the cylinder.

Table XVII

Cylinder, Under Glass, in Air, Convection Coefficient, C_e

T_f °F	k_f $\frac{\text{Btu ft}}{\text{hr ft}^2\text{F}}$	N_f $\frac{1}{\text{ft}^3\text{R}}$	L ft	$N_f D_{cy}^3$ $\frac{1}{\text{R}}$	$\left[N_f D_{cy}^3\right]^{.258}$ $\left[\frac{1}{\text{R}}\right]^{.258}$	$C_e = .0685\, k_f \left[N_f D_{cy}^3\right]^{.258}$ $\frac{\text{Btu ft}}{\text{hr ft}^2\text{F}^{1.258}}$
0	.0130	4.256×10^6	.1823	2.578×10^4	13.74	.01224
100	.0157	1.758×10^6	.1823	1.065×10^4	10.94	.01176
200	.0182	8.442×10^5	.1823	5.114×10^3	9.054	.01129
300	.0205	4.491×10^5	.1823	2.721×10^3	7.694	.01080
400	.0228	2.616×10^5	.1823	1.585×10^3	6.693	.01045
500	.0250	1.604×10^5	.1823	9.717×10^2	5.899	.01010
600	.0272	1.034×10^5	.1823	6.264×10^2	5.267	.009812

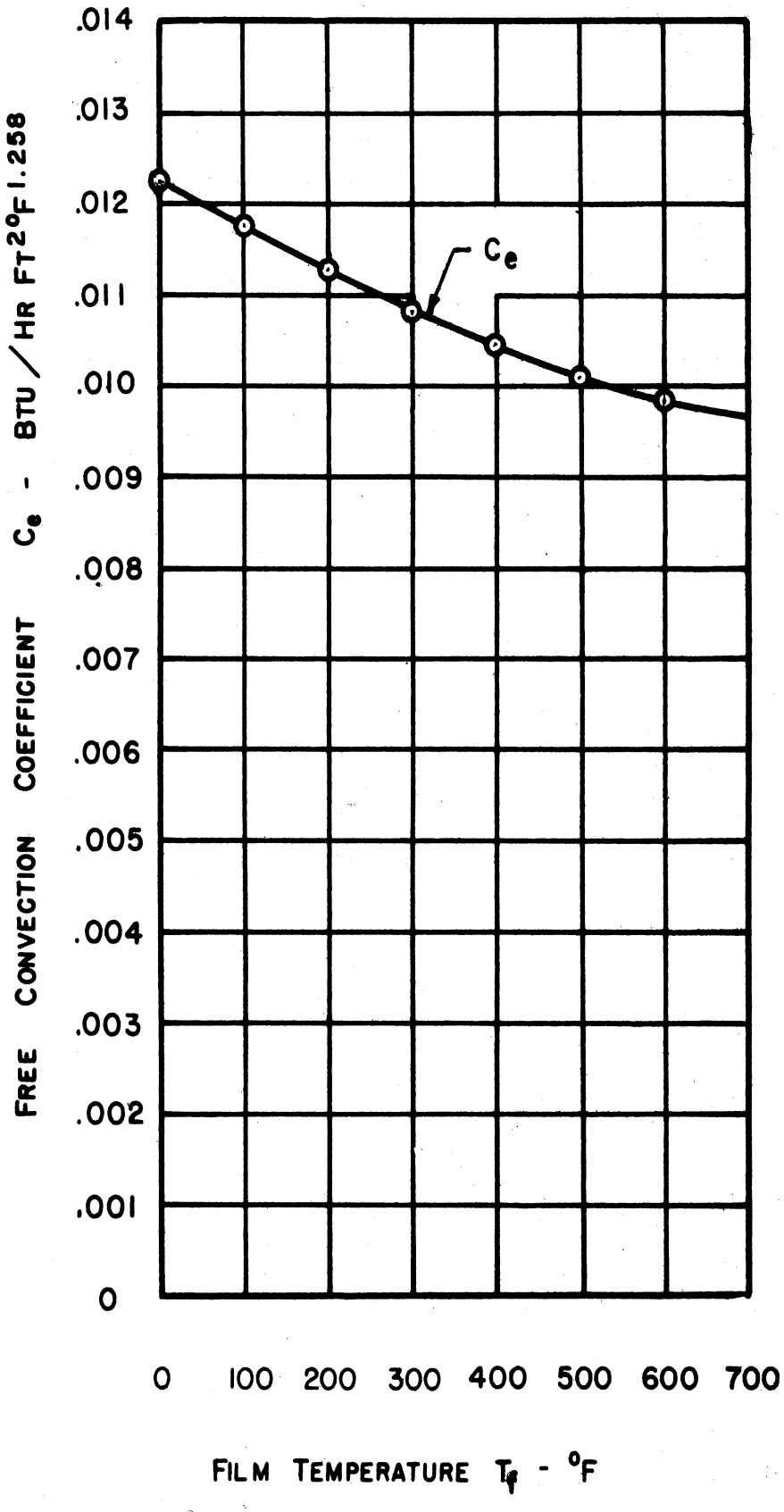

Figure 7. Plot of Coefficient C_e vs. T_f for the Determination of K_c for Cylinder, Under Glass, in Air.

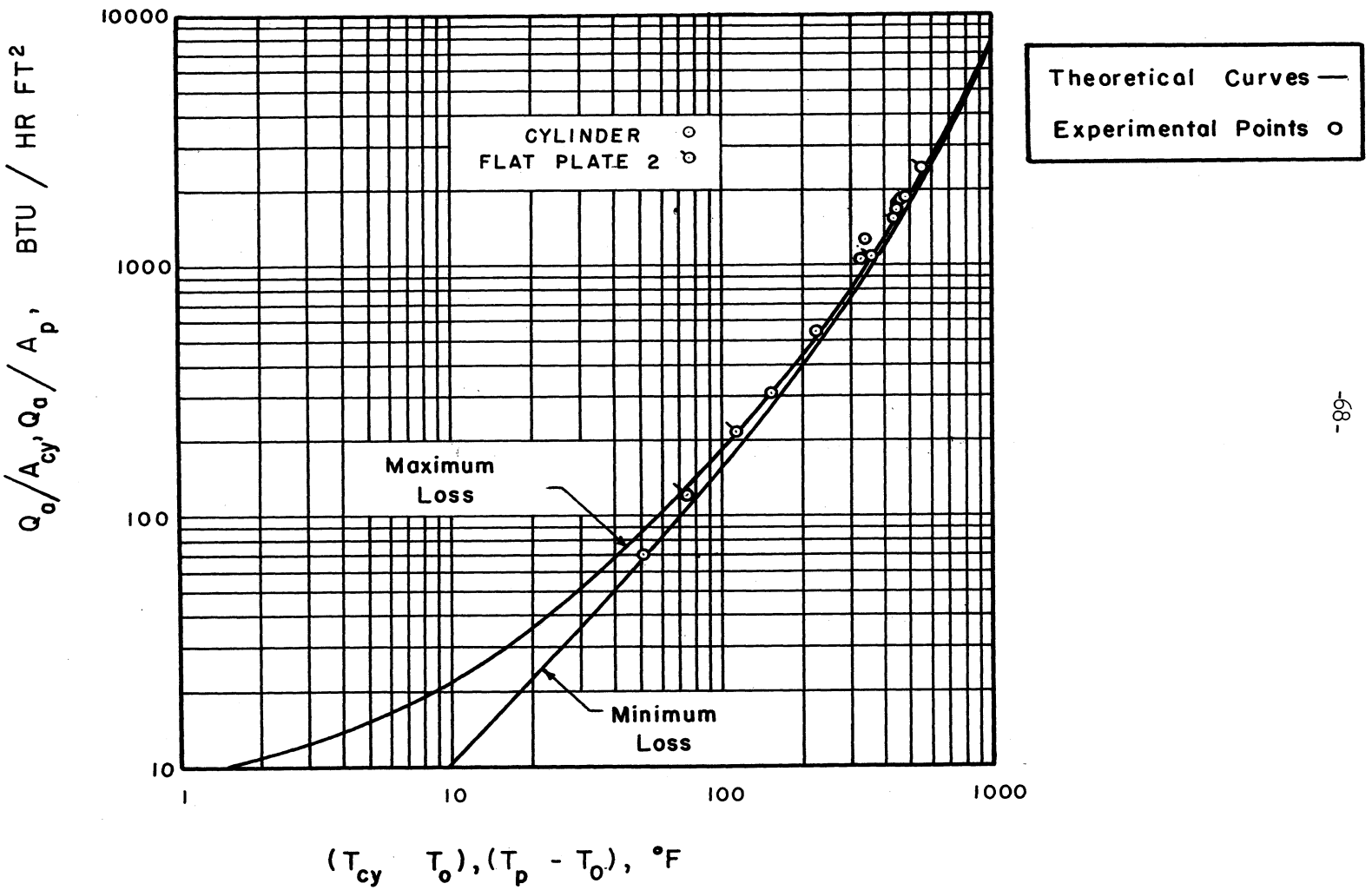

Figure 8. Theoretical and Experimental Plot of $(T_{cy} - T_o)$ vs. Q_a/A_{cy} for Cylinder, Under Glass, in Air. Experimental Comparison of Cylinder and Flat Plate No. 2.

Table XVIII

Cylinder, Under Glass, in Air, Minimum Loss Conditions

$\frac{Q_a}{A_{cy}}$ $\frac{Btu}{hr\,ft^2}$ [assumed]	$\frac{Q_a}{A_{glo}}$ $\frac{Btu}{hr\,ft^2}$	$[T_{gli}-T_o]$ °F	T_{gli} °R	T_{cy} °R [assumed]	T_f °F	C_e $\frac{Btu}{hr\,ft^2\,°F^{1.258}}$	$\frac{Q_a}{A_{cy}}$ $\frac{Btu}{hr\,ft^2}$ [calculated]	$[T_{cy}-T_o]$ °F
3	.609	.6	520.6	523.2	61.9	.01190	3.01	3.2
20	4.06	3.0	523	538	70.5	.01188	20.15	18
100	20.3	12.5	532.5	591	101.75	.01171	99.37	71
300	60.9	34	554	689	161.5	.01141	301.49	169
1000	203	92	612	891	291.5	.01081	1000.45	371
3000	609	218	738	1180	499	.01030	2993.43	660
10000	2030	480	1000	1623	853	.009	9992.53	1163

Table XIX

Cylinder, Under Glass, in Air, Maximum Loss Conditions

$\frac{Q_a}{A_{cy}}$ $\frac{Btu}{hr\,ft^2}$ [assumed]	$\frac{Q_a}{A_{glo}}$ $\frac{Btu}{hr\,ft^2}$	$[T_{gli} - T_o]$ °F	T_{gli} °R	T_{cy} °R [assumed]	T_f °F	C_e $\frac{Btu\,ft}{hr\,ft^2\,°F}$	$\frac{Q_a}{A_{cy}}$ $\frac{Btu}{hr\,ft^2}$ [calculated]	$[T_{cy} - T_o]$ °F
10	2.03	- 6.6	513.4	521.5	57.45	.01192	9.98	1.5
20	4.06	- 6	514	529	61.5	.01190	19.59	9
30	6.09	- 5.4	514.6	536	65.3	.01189	29.27	16
100	20.3	- 1.2	518.8	580	89.4	.01178	100.08	60
300	60.9	11	531	673	142	.01150	299.38	153
1000	203	50	570	872	261	.01097	998.88	352
3000	609	1152	672	1162	457	.01019	3003.85	642
10000	2030	410	930	1606	808	.009	9993,38	1086

Table XX

Cylinder, Under Glass, in Air, Experimental Data

Pyrheliometer millivolts [Test]	H_T $\frac{Btu}{hr\,ft^2}$	C	$5.601\,C\,H_T$ $\frac{Btu}{hr\,ft^2}$	$.2229\,H_T$ $\frac{Btu}{hr\,ft^2}$	$\frac{Q_a}{A_{cy}}$ $\frac{Btu}{hr\,ft^2}$	$[T_{cy}-T_o]$ °F [Test]
7.3	289	1	1618.69	64.42	1683.11	445
8.0	317	1	1775.52	70.66	1846.18	467
7.65	303	1	1697.10	67.54	1764.64	447
8.0	317	1	1775.52	70.66	1846.18	455
7.6	301	.875	1475.16	67.09	1542.25	440
7.4	293	.75	1230.82	65.31	1296.13	340
8.6	341	.5	954.97	76.01	1030.98	325
8.6	341	.25	477.49	76.01	553.50	222
8.6	341	.125	238.74	76.01	314.75	153
7.9	313	0	0	69.77	69.77	51

ADDITIONAL EXPERIMENTAL DATA

Effect of Replacing Air in Space Between Target and Surrounding Thin Hollow Glass Cylinder by a Vacuum

The experimental data for a flat plate heated in a vacuum has already been tabled in Table XVI. The results of this experiment are plotted against $\frac{Q_a}{A_p}$ in Figure 9.

Under the assumption that the air put in the space where a vacuum existed in the aforementioned test, the equation previously developed to evaluate the time rate of energy addition per unit area to the plate which for Plate II is

$$\frac{Q_a}{A_p} = .4170H_T + 7.726CH_T \qquad (1)$$

During the test, pyrheliometer readings were changed to H_T values and by means of Equation (1) were converted to $\frac{Q_a}{A_p}$ values. A series of these steps are shown in Table XXI as well as the temperature rise of the plate above the surroundings $\left[T_p - T_o\right]$. These temperature rises are plotted against $\frac{Q_a}{A_p}$ in Figure 9. With both curves plotted, Figure 9 shows the advantage of having a vacuum in the space between the target and the surrounding hollow glass cylinder.

Effect of Target Shape

To determine the effect of target shape on the temperature rise $\left[T_T - T_o\right]$ above the surroundings, the results of Table XXI for a flat plate heated within a hollow glass cylinder having air in the intervening space were plotted in Figure 8 which shows the theoretical

and experimental temperature rise of a cylinder heated within a hollow glass cylinder also having air in the intervening space. The experimental results for a cylinder are plotted with small circles while the results for the plate are plotted with circles having a single bar.

Effect of Placing Hollow Glass Cylinders Around the Target

A flat plate placed at the focus of the concentrator was tested for temperature rises of the plate under conditions of having 0, 1, 2 and then 3 glass covers surrounding the target. Table XXII shows the results of the test. Figure 10 shows a plot of the temperature rise of the plate vs. pyrheliometer readings.

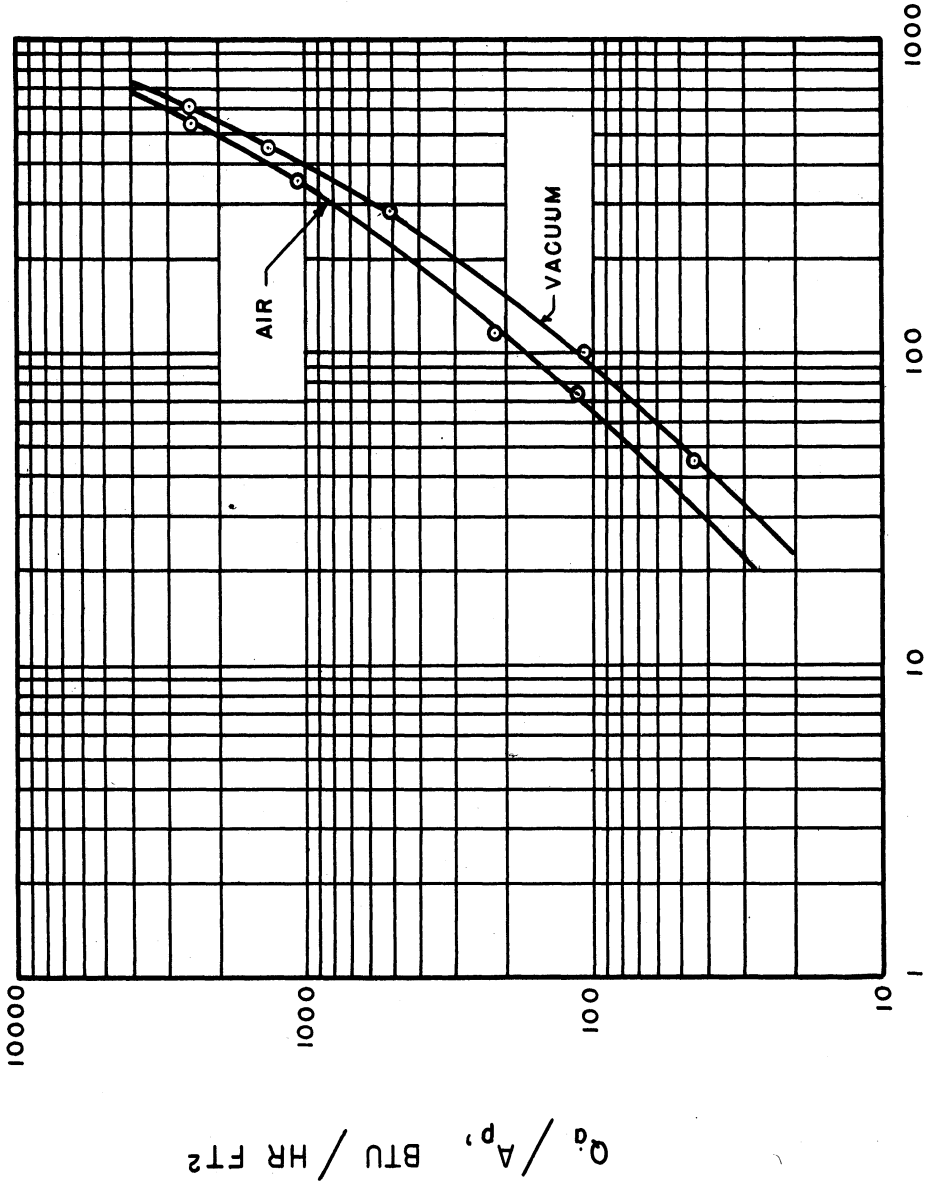

Figure 9. Experimental Comparison of Flat Plate No. 2, Under Conditions Utilizing Air and Vacuum, Under Glass.

Table XXI

Flat Plate #2, Under Glass, in Air, Experimental Data

Pyrheliometer millivolts [Test]	H_T $\frac{Btu}{hr\,ft^2}$	C	$7.726\,C\,H_T$ $\frac{Btu}{hr\,ft^2}$	$.4170\,H_T$ $\frac{Btu}{hr\,ft^2}$	$\frac{Q_a}{A_p}$ $\frac{Btu}{hr\,ft^2}$	$[T_p - T_o]$ °F [Test]
7.6	301	1	2325.53	125.51	2451.04	548
6.2	246	.5	950.30	102.58	1052.88	352
2.3	91.1	.25	175.96	37.99	213.95	113
7.2	289	0	0	120.51	120.51	73

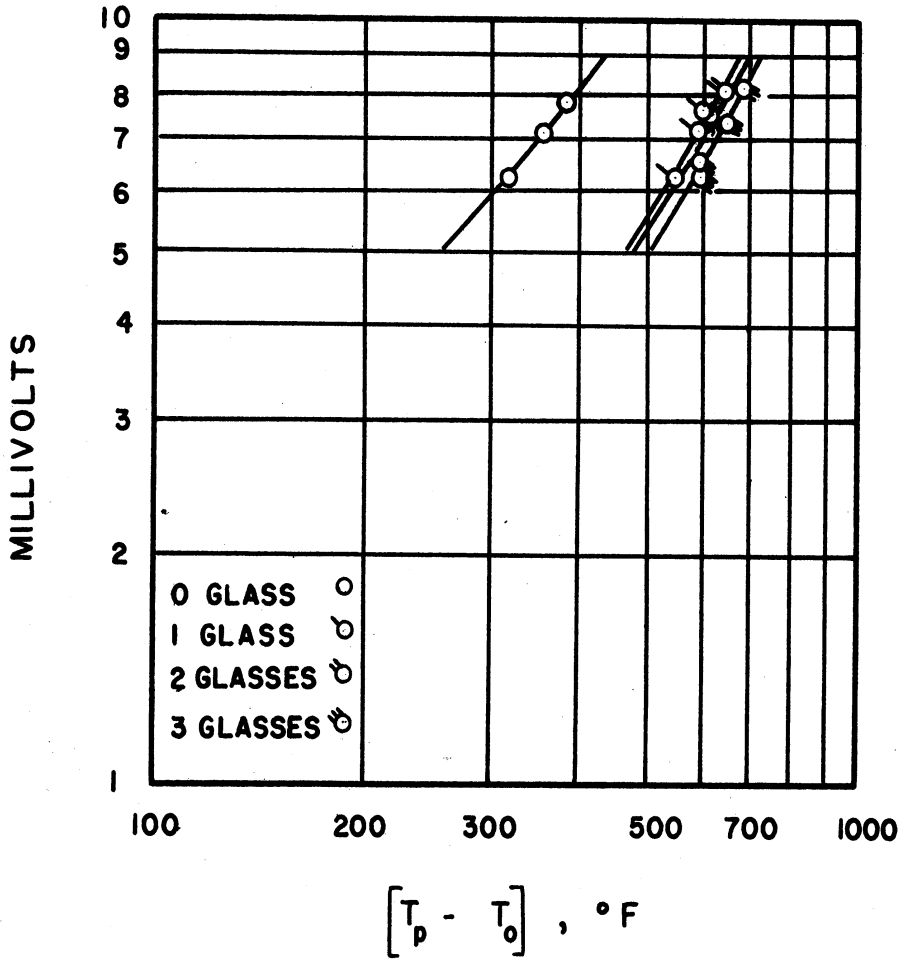

Figure 10. Plot of Pyrheliometer Readings vs. $(T_p - T_o)$ for Flat Plate No. 3, Using 0,1,2 or 3 Glasses.

Table XXII

Flat Plate #1, Under 0, 1, 2, 3 Glasses, Experimental Data

Glasses	Pyrheliometer millivolts	$[T_p - T_o]$ °F
0	7.8	384
0	7.1	355
0	6.2	319
1	7.6	601
1	7.1	591
1	6.3	540
2	8.0	641
2	7.5	610
2	6.5	591
3	8.1	685
3	7.4	648
3	6.2	595

SUMMARY

1. The steady state temperature rise above ambient temperature of a flat plate target placed at the focus of a parabolic solar concentrator can be determined from the equation

$$T_p - T_o = \sqrt[4]{T_s^4 + \frac{1}{\sigma\epsilon_p}\left[\frac{H_s A_{pn}\alpha_{sn} + H_s A_{nm} CR\alpha_{si} + \frac{H_{sk} A_{pn}\alpha_{skn}}{A_p} - h\left[T_p - T_o\right]}{A_p}\right]}} - T_o$$

This equation can be used to the upper limit imposed by the smallest target that will receive all the reflected radiation. This limit is

$$C = \frac{A_{nm}'}{A_{tr}} = \frac{A_{nm} + A_{pn}}{A_{pn}} = \frac{n\left[1 - \frac{n^2}{16} - \frac{n}{2}\tan\frac{\alpha}{2}\right]}{2\tan\frac{\alpha}{2}\left(1 + \frac{n^2}{16}\right)^2}$$

2. The steady state temperature rise above ambient temperature of a flat plate target placed at the focus when the target is covered by a thin hollow glass cylinder which has the space between the target and the glass cylinder evacuated can be determined from the equation

$$T_p - T_o = \sqrt[4]{T_{gli}^4 + \frac{H_s \tau_{rsd}\tau_{asd} A_{pn}\alpha_{sd}}{\sigma F_a F_e A_p} + \frac{H_s C A_{nm} R\tau_{rsi}\tau_{asi}\alpha_{si} + H_{sk}\tau_{rsk}\tau_{ask} A_{pn}\alpha_{skn}}{\sigma F_a F_e A_p}} - T_o$$

where T_{gli} is determined from

$$T_{gli} = \left[\frac{H_s \tau_{rsd} \tau_{asd} A_{pn} \alpha_{sd} + H_s C A_{nm} R \tau_{rsi} \tau_{asi} \alpha_{si}}{A_{glo}} + \right.$$

$$\left. \frac{H_{sk} \tau_{rsk} \tau_{ask} A_{pn} \alpha_{skn}}{A_{glo}} \right] \frac{D_{glo} \ln \frac{D_{glo}}{D_{gli}}}{2K_m} + T_{glo}$$

and where T_{glo} is determined from the equation

$$T_{glo} = \sqrt[4]{T_s^4 + \frac{1}{\sigma \epsilon_{glo}} \left[\frac{H_s \tau_{rsd} \tau_{asd} A_{pn} \alpha_{sd} + H_s C A_{nm} R \tau_{rsi} \tau_{asi} \alpha_{si}}{A_{glo}} + \right.}$$

$$\left. \frac{H_{sk} \tau_{rsk} \tau_{ask} A_{pn} \alpha_{skn}}{A_{glo}} - h \left[T_{glo} - T_o \right] \right]$$

The upper limiting value to apply to the above equation is

$$C = \frac{A_{nm}'}{A_{tr}} \Rightarrow \frac{A_{nm} + A_{pn}}{A_{pn}} = \frac{n \left[\frac{1-n^2}{16} - \frac{n}{2} \tan \frac{\alpha}{2} \right]}{2 \tan \frac{\alpha}{2} \left(1 + \frac{n^2}{16} \right)^2}$$

3. The steady state temperature rise above ambient temperature of a cylindrical target placed at the focus when the target is covered by a thin hollow glass cylinder, in which the space between the target and the glass cylinder is air, can be determined from the following equation:

$$T_{cy} - T_o = \sqrt[4]{T_{gli}^4 + \frac{1}{\sigma F_a F_e}\left[\frac{H_s \tau_{rsd} \tau_{asd} A_{cyn} \alpha_{sd}}{A_{cy}} + \frac{H_s C R A_{nm} \tau_{rsi} \tau_{asi} \alpha_{si}}{A_{cy}} + \frac{H_{sk} \tau_{rsk} \tau_{ask} A_{cyn} \alpha_{skn}}{A_{cy}} - \frac{2\pi L K_c \left[T_{cy} - T_{gli}\right]}{A_{cy} \ln \frac{D_{gli}}{D_{cy}}}\right]} - T_o$$

where T_{gli} is determined from

$$T_{gli} = \left[\frac{H_s \tau_{rsd} \tau_{asd} A_{cyn} \alpha_{sd}}{A_{glo}} + \frac{H_s C R A_{nm} \tau_{rsi} \tau_{asi} \alpha_{si}}{A_{glo}} + \frac{H_{sk} \tau_{rsk} \tau_{ask} A_{cyn} \alpha_{skn}}{A_{glo}}\right] \frac{D_{glo} \ln \frac{D_{glo}}{D_{gli}}}{2 K_m} + T_{glo}$$

and where T_{glo} is determined from the equation

$$T_{glo} = \sqrt[4]{T_s^4 + \frac{1}{\sigma \epsilon_{glo}}\left[\frac{H_s \tau_{rsd} \tau_{asd} A_{cyn} \alpha_{sd}}{A_{glo}} + \frac{H_s C R A_{nm} \tau_{rsi} \tau_{asi} \alpha_{si}}{A_{glo}} + \frac{H_{sk} \tau_{rsk} \tau_{ask} A_{cyn} \alpha_{skn}}{A_{glo}} - h\left[T_{glo} - T_o\right]\right]}$$

The equation may be used up to the limit of the width of the image that will fall on the smallest cylinder and can be determined from the equation

$$C = \frac{A_{nm}'}{A_{tr}} = \frac{A_{cyn} + A_{nm}}{A_{cyn}} \leq \frac{n}{2 \sin \frac{\alpha}{2}\left(1 + \frac{n^2}{16}\right)}$$

4. The geometry of the target is not significant when comparing a flat plate and a cylindrical target under conditions of the same time rate of energy input per unit area, when both are contained under a thin hollow glass cylinder.
5. Evacuation of the space between a target and a surrounding thin hollow glass cylinder results in a significant temperature rise for the same time rate of energy input per unit area above the temperature attained when air is left in the space.
6. The placing of one thin hollow glass cylinder over a flat plate target results in a very significant increase in temperature of the target for the same radiation rate over the temperature attained by a target exposed to the wind. The placing of two and three thin hollow glass covers results in further slight increases in temperature over the temperature attained using one glass cover under the same rate of radiation.

EQUIPMENT

Pyrheliometer

The intensity of solar radiation in Btu/hr ft^2 was evaluated by a pyrheliometer. The pyrheliometer shown in Plate II is similar to the thermoelectric pyrheliometer described by H. H. Kimball and H. E. Hobbs in an article "A New Form of Thermoelectric Recording Pyrheliometer."(9) This pyrheliometer is similar to the Eppley Pyrheliometer, which was built according to the specifications of the U. S. Weather Bureau. These specifications incorporate the principal features of an experimental model built by Kimball and Hobbs in 1923.

The heart of the pyrheliometer is shown in Figure 12 thermopile details. This heart consists of a thermopile of 36 thermocouples connected in series and made of iron-constantan thermocouples. The junctions are mounted so that the (1,3,5...) junctions maintain thermal contact with the inner ring but are electrically insulated from the ring; the (2,4,6...) junctions maintain thermal contact with the outer ring and are electrically insulated from the ring. Both rings have an area of 2.07 square inches. The inner ring is painted black in order to have a high absorbtivity for solar radiation, and the outer ring is painted white in order to have a much lower absorbtivity for solar radiation. The two colors have approximately the same emissivities at

(9) H. H. Kimball and H. E. Hobbs, "A New Form of Thermoelectric Recording Pyrheliometer," Monthly Weather Review, Vol. 51, No. 5, W. B. No. 806, May 1923, pp. 239-242.

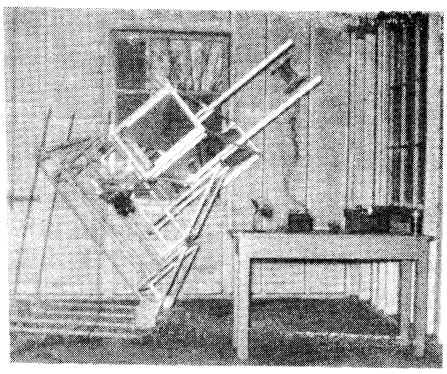

Figure a

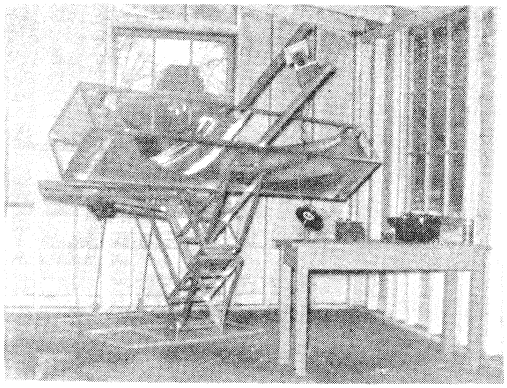

Figure b

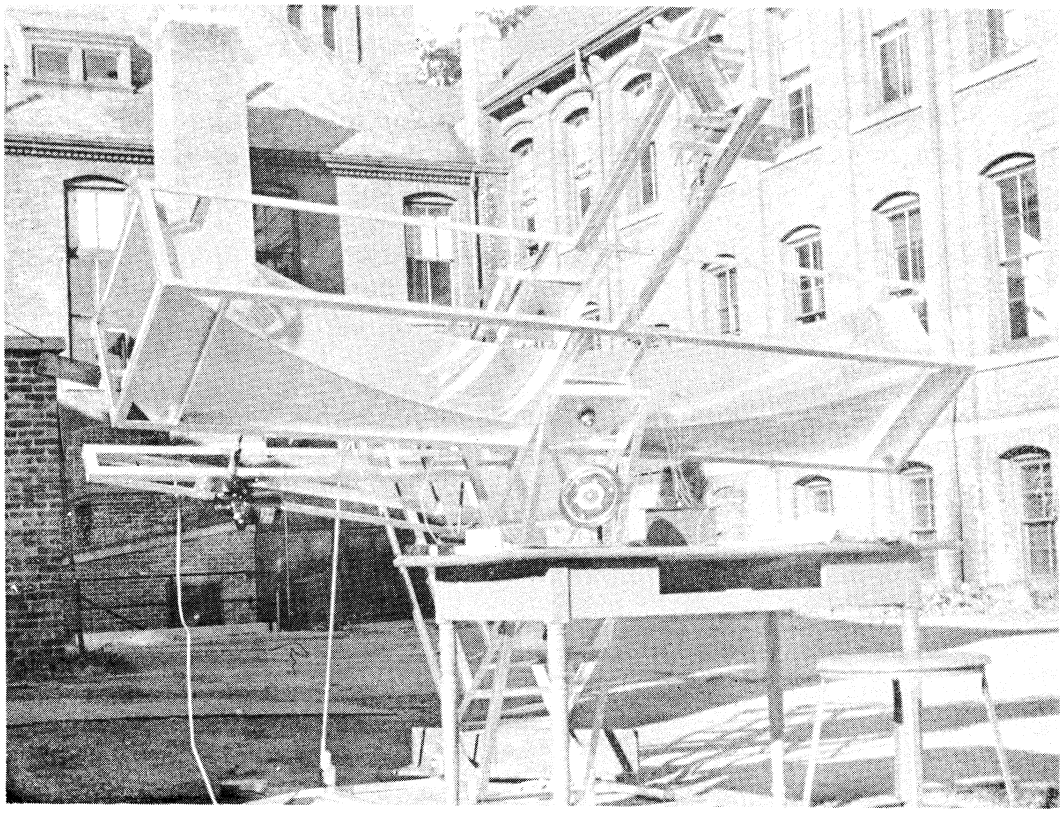

Plate I. Views of Solar Concentrator.

Figure c

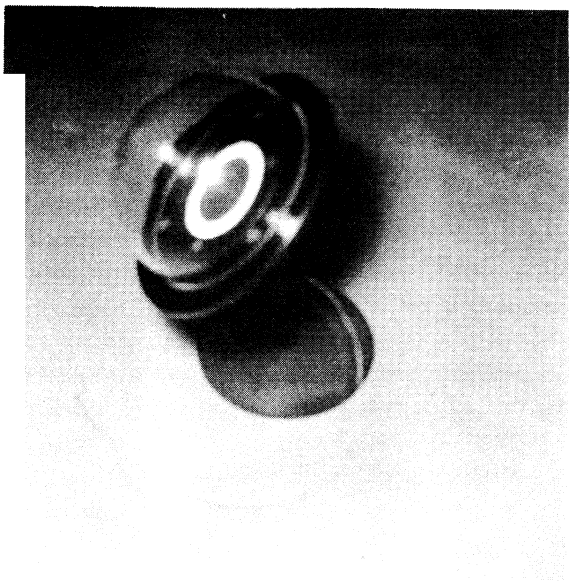

Plate II. Pyrheliometer

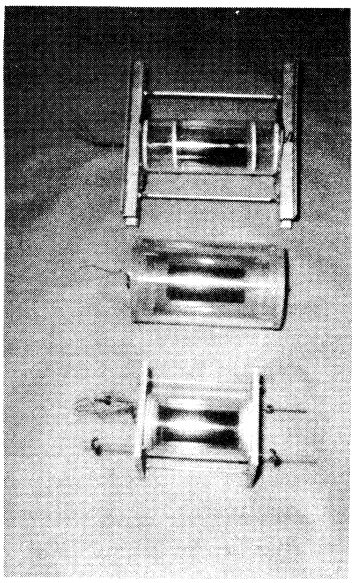

Plate III. Target Assembly #2, #1, #3.

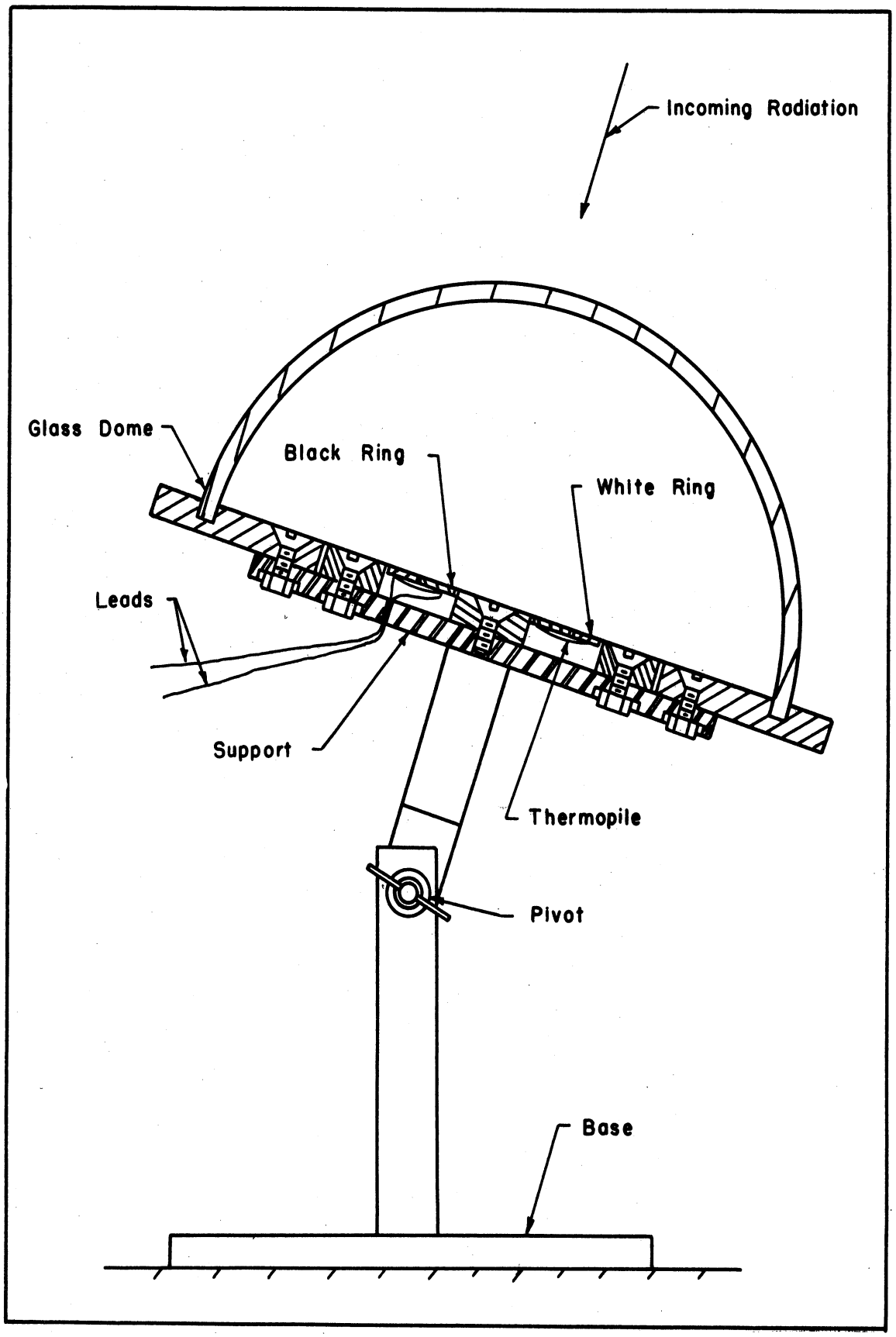

Figure 11. Solar Pyrheliometer.

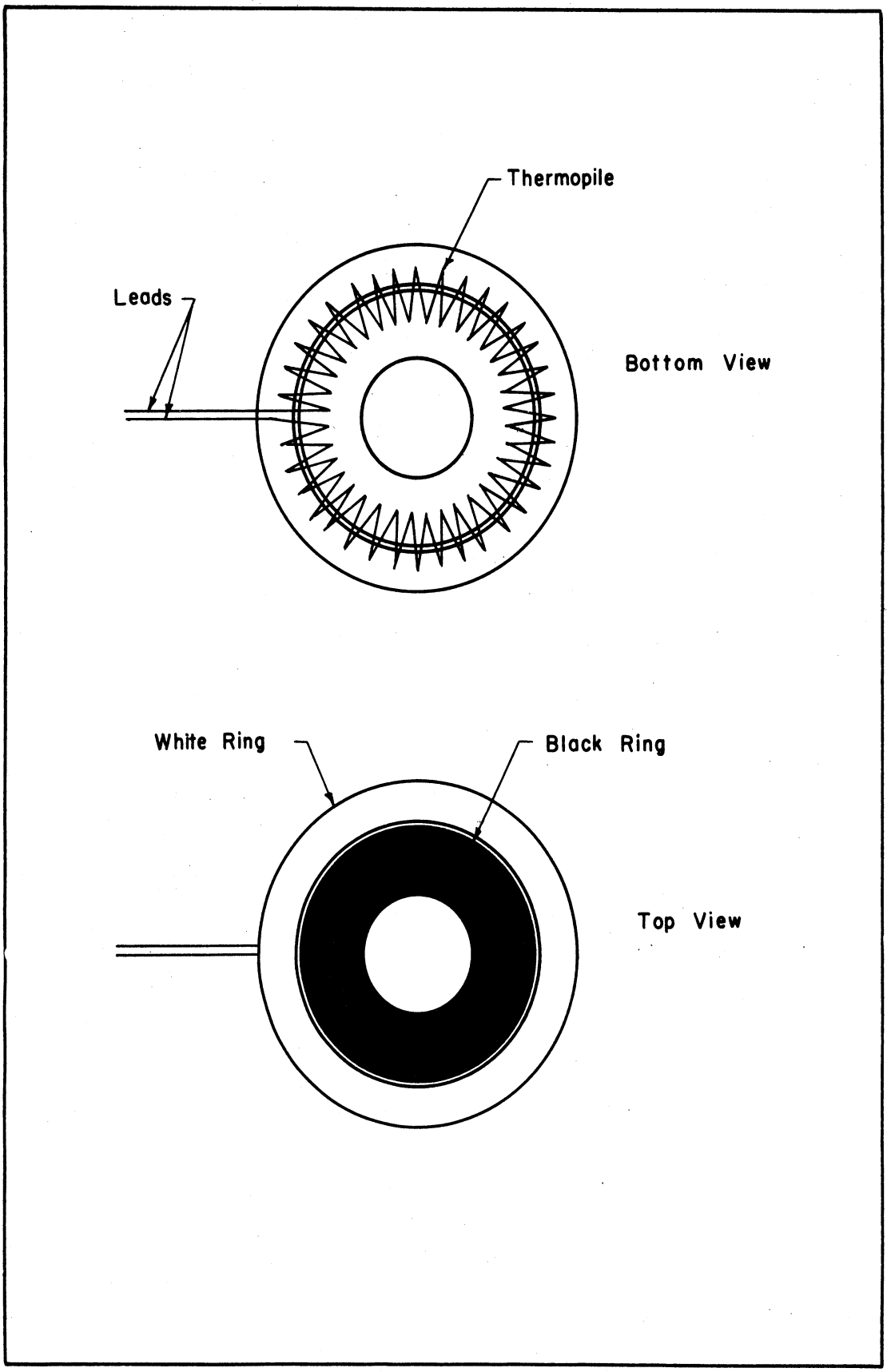

Figure 12. Thermopile Details.

room temperature, so that when receiving radiation from a hot source such as the sun, the black ring heats up to a different equilibrium temperature than the white ring. The temperature difference produces an e.m.f. of from 8 to 10 millivolts under bright sunlight.

The remaining parts shown in Figure 11 of the pyrheliometer are for convenience, or to aid constancy of readings. The glass hemisphere is placed over the rings to keep the wind from directly cooling the rings. The diameter of the cover was made over twice the diameter of the largest ring so that "the caustic curve caused by reflection of light from its internal surface does not fall on either of the rings."(10)

The pyrheliometer is pivoted to permit readings to be made with the ring surface normal to the sun's rays.

The pyrheliometer was calibrated at the United States Bureau of Standards in the Bureau's 9-foot standard illumination sphere. The calibration was done by Mr. Norman Foster, instrumental engineer of the United States Weather Bureau in Washington, D.C. The pyrheliometer develops 5.60 millivolts per gram calorie per minute centimeter^2 at 85°F. According to Mr. Foster, the calibration is within 1% of the true value.

The pyrheliometer is used in the following way. The ring surfaces are placed normal to the sun's radiation and a reading is made after equilibrium is reached. This reading when multiplied by the constant of the instrument is the total radiation in Btu/hr ft^2.

---

(10) Ibid.

The sky or diffuse radiation is obtained by shading the rings with a disk that just shadows the rings from the sun. When equilibrium is reached, this reading when multiplied by the instrument constant is the sky radiation in Btu/hr ft^2. By subtracting the sky radiation from the total radiation, the direct sun radiation in Btu/hr ft^2 is determined.

Solar Concentrator

The solar concentrator is a device that converges the radiation received on a large area to a smaller one. The solar concentrator in this experiment accomplished the converging by having a polished aluminum mirror formed in the shape of a parabolic cylinder. A solar concentrator of this type must perform the following functions: support itself, allow for aiming at the sun, be able to track the sun in its east-west movement across the sky, provide the shape for the mirror, and finally, hold the target and target assembly in a position fixed with reference to the mirror. In order to explain this solar concentrator more fully, the discussion has been divided into four categories: framework, aiming and tracking, mirror shape, and target assemblies.

Framework

The entire apparatus rests on a semi-flexible webbed base made of arc-welded 1" x 1" x 1/8" angle. At the south end of the base, as shown in Figure 13, two plates are welded to the base that together with pairs of nuts, bolts, and washers form pivot "C". At the north end of the base, in Figure 13, two smaller plates are welded to the base. These allow the two slide rods to pivot as frame "B" is rotated about pivot "C".

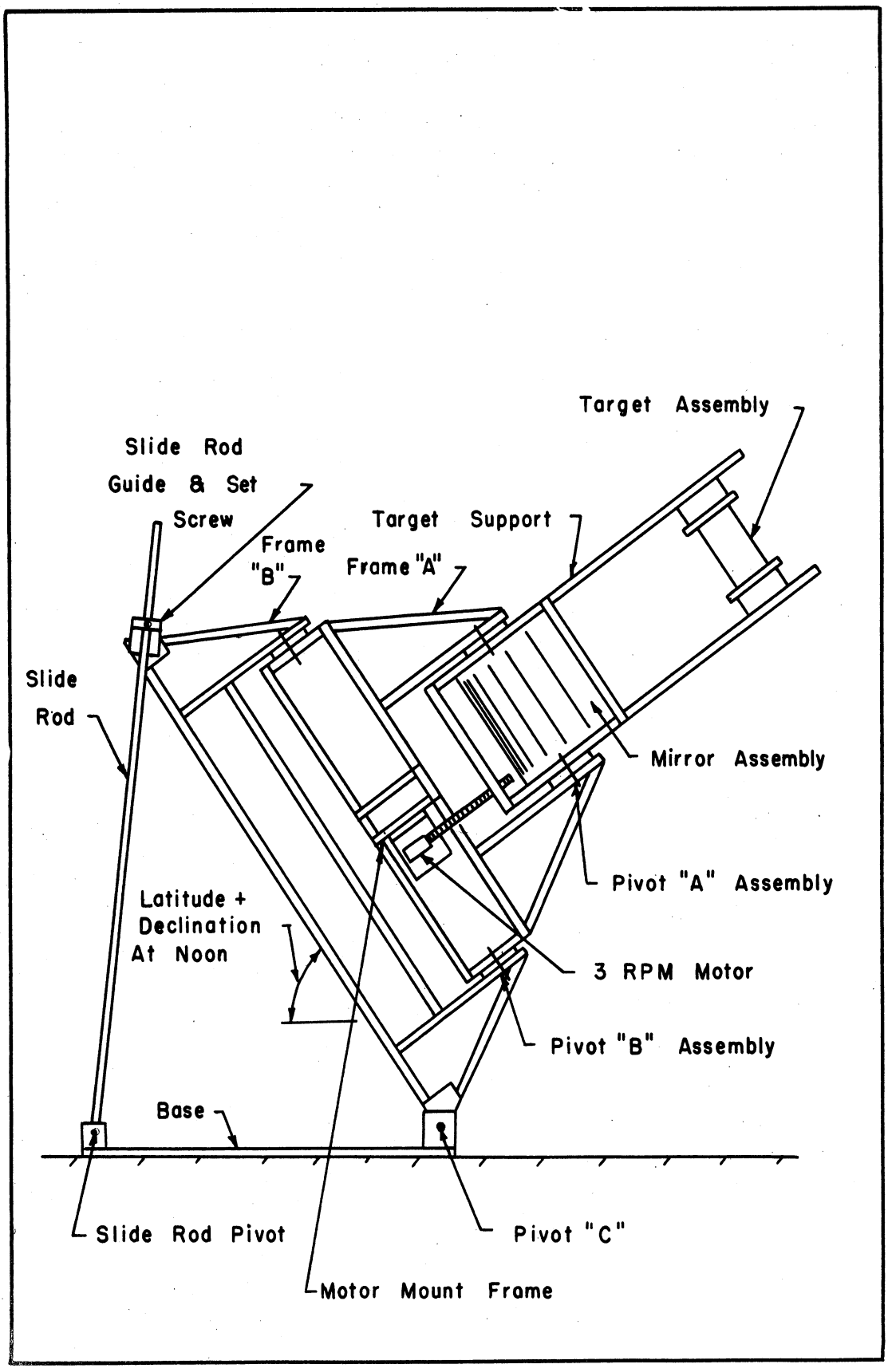

Figure 13. Solar Parabolic Concentrator.

The two slide rods which pivot about the slide rod pivot allow adjustments to be made in the angle that frame "B" makes with the horizon. When the angle is correct, it can be maintained by tightening a setscrew in each of the two slide rod guides.

Frame "B" pivots about pivot "C". It supports frame "A" through pivot "B" assembly. The frame is made of 1" x 1" x 1/8" arc-welded angle. At either end two sets of two plates are welded. At the lower end the plates form the bearing surface with the two bolts through pivot "C". At the upper end the two plates provide, with two bolts, the means for attaching the slide rod guides to frame "B". Proceeding toward the focus are the pivot "B" assemblies.

Each pivot "B" assembly consists of an 8" x 8" x 1/2" bearing plate arc-welded to frame "B", and a similar plate welded to frame "A". Between the bearing plates, a bearing of 6" diameter and 1/2" thick is placed. The assembly is held together by a 3/4" x 4" semi-finished nut and bolt. This bolt provides the axis of rotation and a locking device, since by tightening the nut, the pivot assembly will lock by friction.

Pivoting about pivot "B" is frame "A". This pivot allows frame "A" to have the correct hour angle to the sun and allows the motor to rotate the mirror about pivot "A" for small deflections. Frame "A" is made of arc-welded 1" x 1" x 1/8" angle. It holds the motor mount frame, and toward the target it positions the pivot "A" assemblies. Each pivot "A" assembly is identical to the pivot "B" assembly and provides the axis for the motor to turn the mirror assembly and target assembly independent of the rest of the solar concentrator.

The mirror assembly that pivots about pivot "A" consists of 1" x 1" x 1/8" angle arc-welded into a box shape of dimensions 96" x 20" x 14". The mirror form, which is made of marine plywood 1" thick and 96" long, is cut to the shape of the parabola $y = 15/2304\ x^2$. The form was undercut the thickness of the metal in the direction of the axis of symmetry to give the correct shape to the outer metal surface. The mirror is a piece of 10 gage aluminum sheet 96" long and 12" wide. This gives a mirror diameter (aperture) of 85.2" and a focal length of 38.4". The relative aperture (n) is 2.22 (n = D/f) where D is the diameter and f is the focal length.

The target support consists of two sets of two angles arc-welded so as to have a slot. There is one set to each side of the mirror assembly aiming in the direction of the axis of symmetry of each edge parabola. The slot permits the target assembly to be moved in and out of the region of intense radiation.

Aiming and Tracking

In order to follow the sun across the sky, two types of apparent motion of the sun must be allowed for. The first is the north-south march of the sun. It is given by (δ) called declination, which is the angluar distance measured from the equator to the sun along the hour circle through the sun.(11) This motion on an hourly basis is insignificant. It varies from 59 seconds of arc per hour at the equinoxes to approximately 0 seconds per hour at the solstices.(12) This means that

(11) Harry Bouchard, Surveying (Scranton, International Textbook Co., 1947), pp. 440-441.

(12) W. and L. E. Gurley, 1958 Gurley Ephemeris (Gurley Engineering Instruments, Troy, N.Y., 1958), pp. 41-53.

the declination can be allowed for once a day and then forgotten.

The other, more significant motion, is the apparent east-west motion of 15° per hour. This motion is accomplished by placing a 3 rpm motor, which turns the mirror assembly about pivot "A" (see Figure 13), at a distance of 34.4" from the center line of the pivots "A" and "B". This motor is attached through a flexible coupling of rubber to a 1/4-20 NC-2 x 11" thread. For small deflections on either side of the starting position, of Figure 13, the mirror assembly and focus turn at a rate of 15° per hour. About six inches of screw are used, which allows a run of 40 minutes before resetting.

To follow the sun exactly, the rotation should be around an axis parallel to the earth's axis of rotation. To establish this axis at any latitude requires that from a north-south horizontal line, an angle equal to the latitude (L) must be made from north horizon toward the zenith. In addition, to insure that the sun's rays are perpendicular to the mirror, an angle equal to the declination (δ) must be made from the axis of rotation and this requires an axis at right angles to the axis of rotation. Since this would add to the weight and complexity of the concentrator, the extra axis was omitted and the apparatus was set on the angle that aimed it directly at the sun. On the worst day for this method at the solstices at noon there would be a 1°48' error after one hour in tracking the sun due to rotation of the mirror at an angle of 23°27' to the correct axis. At the equinoxes the error is 0 since the δ is 0. Since the runs were all of 20 to 30 minutes duration, this does not appear to be a serious drawback.

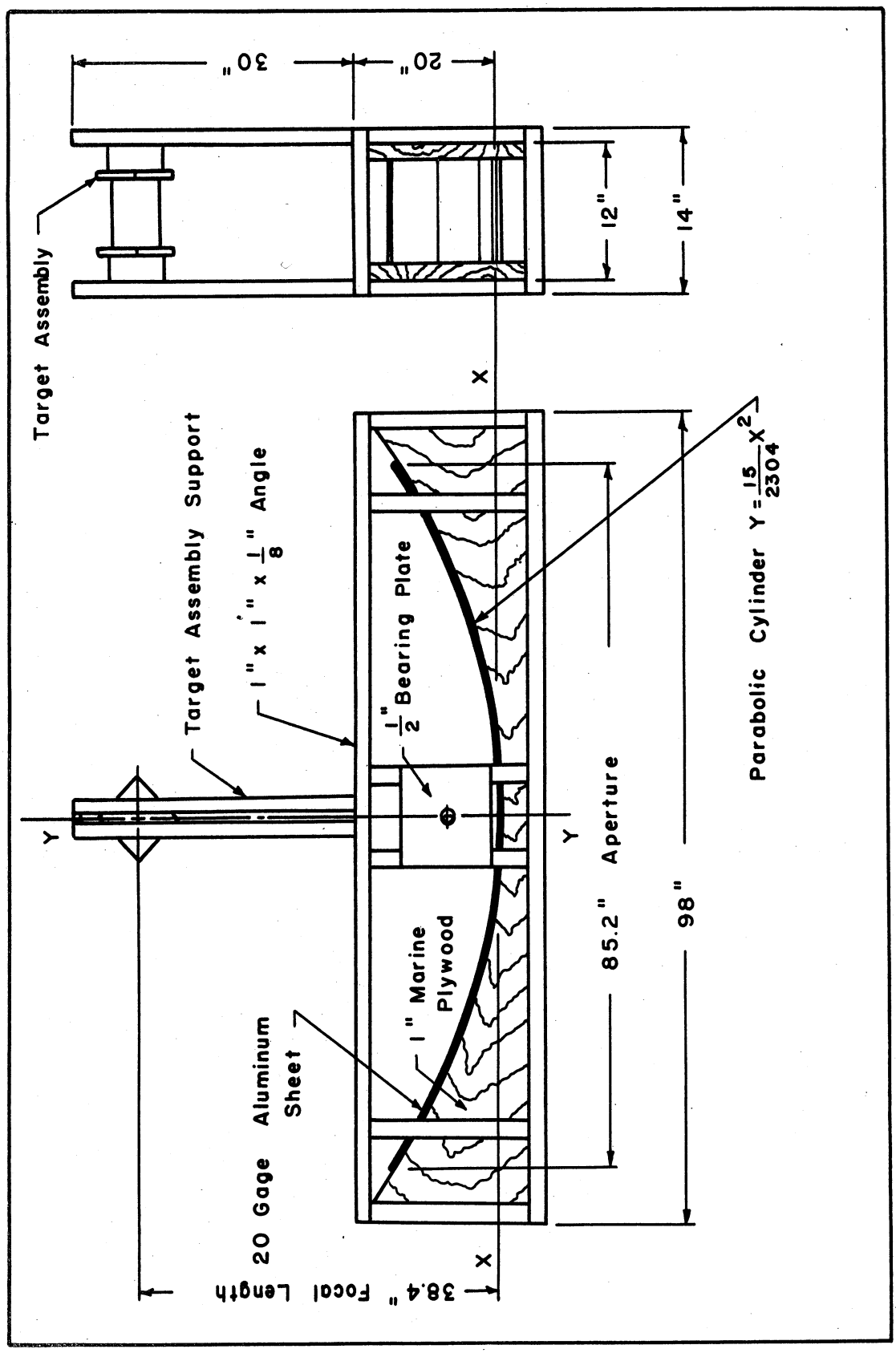

Figure 14. Mirror Assembly.

Mirror Shape

It has long been known that a two-dimensional parabola will reflect through its point focus all rays from infinity that are aprallel to the parabola's axis of symmetry. Similarly, a parabolic cylinder in three-dimensional space will reflect through its line focus all rays from infinity that are parallel to the parabolic cylinder's plane of symmetry. In comparing the cylinder and paraboloid for concentration, the paraboloid is superior since if two mirrors, a parabolic cylinder, and a paraboloid of revolution have the same relative aperture, the concentrating power of the paraboloid is the square of that of the cylinder.(13) However, on the basis of fabrication, the cylinder has some advantage, since it is singly curved and a thin sheet of metal will adapt to its shape without distortion, whereas the paraboloid of revolution must be deformed by pressure when made from a plane sheet.

A parabolic cylinder was built. The equation of the surface used was

$$y = \frac{15}{2304} x^2 = \frac{1}{4f} x^2$$

y = inches from vertex of parabola in the direction of the plane of symmetry

x = inches from vertex of parabola at right angles to the plane of symmetry

f = focal length, inches

This parabola has a focal length of $\frac{2304}{4x15} = 38.4$ inches. Since the aperture (D) is 85.2 inches, the relative aperture (n)(n = D/f) is 2.22 and has an ideal image on a flat plate of .884 inches. In the actual test all the targets used were larger than the minimum image size.

(13) Nathan Robinson, "Solar Machines," Proceedings of the World Symposium on Applied Solar Energy (Menlo Park, Stanford Research Institute, 1956), pp. 48-49.

Target Assembly

There were three types of target assemblies used in the tests. The target assembly provides: a means of attaching the target to the rest of the concentrator, an envelope around the target, and finally the target itself.

Target assembly no. 1 was a preliminary apparatus. It consisted of a steel cylinder 5-1/8" long and 2-3/16" in diameter with closed ends and painted with a flat black paint. The target guide (see Figure 15) was of wood. Three iron-constantan thermocouples were placed within the surface of the cylinder 120° apart. The target was surrounded by a plexiglass cylinder, 10" long and 5-9/16" in diameter and 3/8" thick, which had the ends closed with stepped plexiglass plugs. Each step of the plug was 3/8" thick. These plugs were provided with threaded holes to allow for attaching to the target support. During the first test, the target reached a temperature of about 500°F. but the plexiglass began to soften and to change shape, so the assembly was discarded.

Target assembly no. 2 (see Figure 16) consisted of a pyrex cylinder 10" long, 4" in diameter, and 1/8" thick. The pyrex cylinder was closed on either end by a square steel plate 5" x 5" x 1/4". This plate was grooved to allow for inserting the pyrex cylinder. Sealing wax was put around the groove circumference on both plates to make the assembly vacuum tight. A fitting was inserted in one plate to permit a vacuum pump to evacuate the target assembly. Four asbestos spacers were placed within the pyrex cylinder to position the target and reduce heat loss through the ends. There were three targets used in this assembly. These were positioned

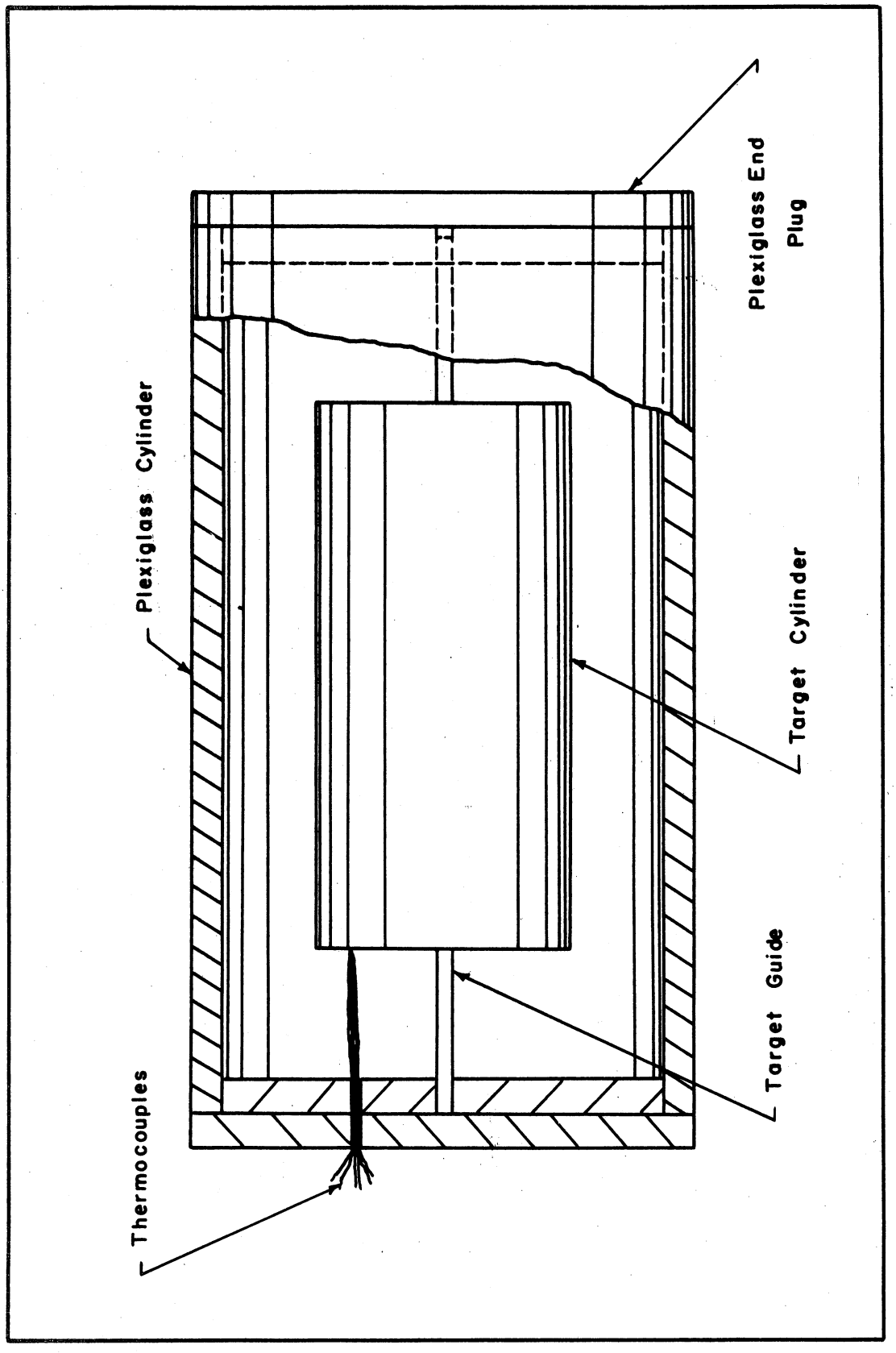

Figure 15. Target Assembly #1.

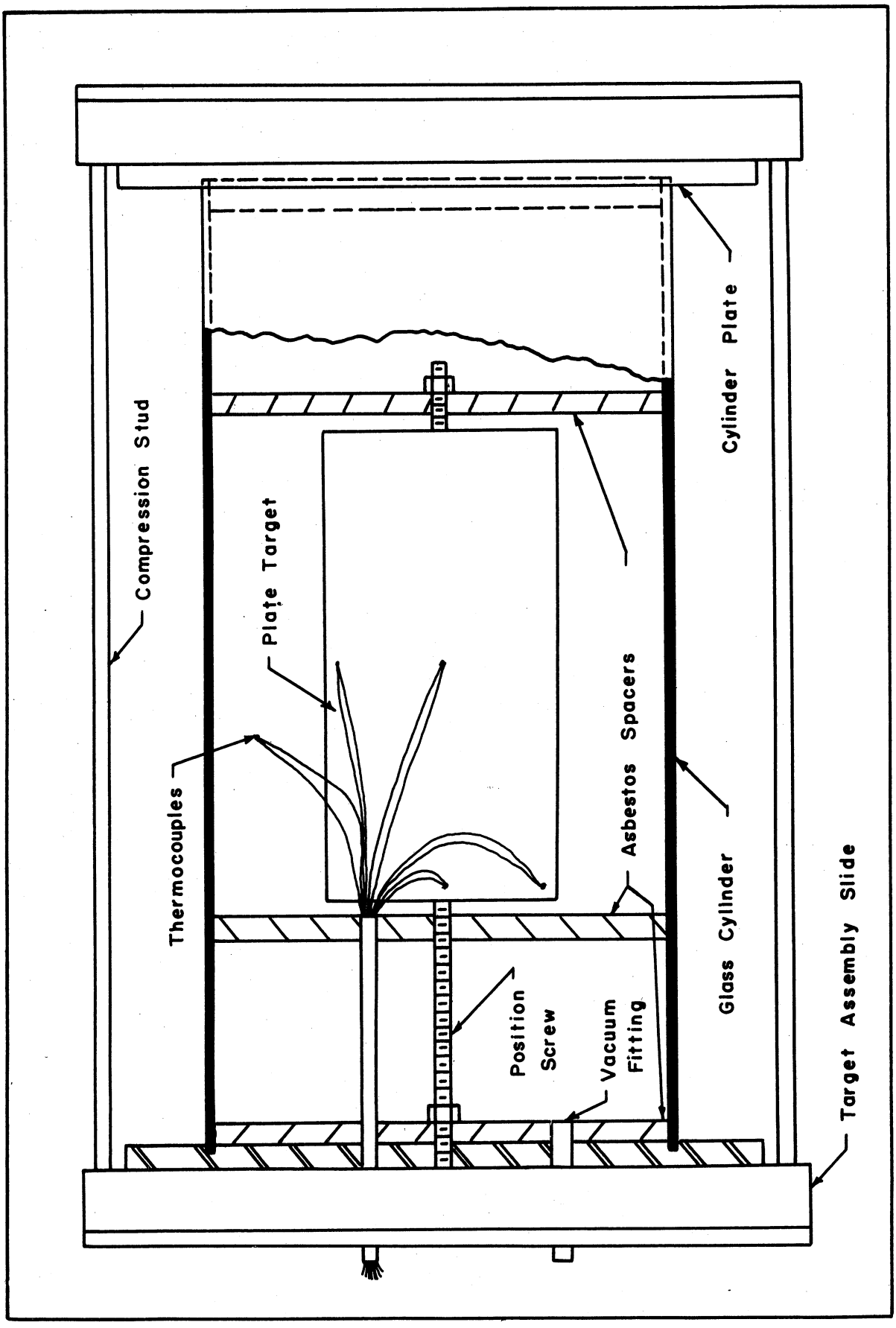

Figure 16. Target Assembly #2.

by screwing in the position screw on either side of the focus. The three targets in order of testing were: A flat steel plate 5-1/32" long x 2-3/4" wide x 1/8" thick and equipped with four thermocouples; a steel cylinder 5-1/8" long x 2-3/16" in diameter with closed ends and with three thermocouples; and 90° steel angle 5-1/8" x 1-17/32" x 1/8" with four thermocouples. The targets were blackened by placing them in an oxy-acetylene flame that was burning with insufficient oxygen.

In addition to the thermocouples in the targets, one thermocouple was positioned in the region midway between the target and the glass cylinder. Also, one thermocouple was placed touching the inside of the glass cylinder and one thermocouple was placed touching the outside of the glass cylinder. The thermocouple exit tube through one plate was filled with sealing wax to insure the assembly was vacuum tight. The assembly was held together by brass compression studs that were bolted to the target assembly slides, and these in turn were bolted to the target supports.

Target assembly no. 3 (see Figure 17) was used to test the effect of additional glass covers. It consisted of three pyrex cylinders of 4", 3 1/2" and 3" in diameter and lengths of 6 1/2", 6" and 5 1/2" respectively. Each was 1/8" thick. The target was a flat plate 4 1/2" long and 2-3/16" wide and 1/8" thick and blackened by an oxygen-deficient oxy-acetylene flame. The pyrex cylinders were positioned on concentric asbestos disks that were attached to an aluminum backed square asbestos plate that was 6" x 6" x 1/8". The assembly was attached to the target support by four support studs. Thermocouples were placed in the target, in the air between the target and the smallest diameter pyrex cylinder,

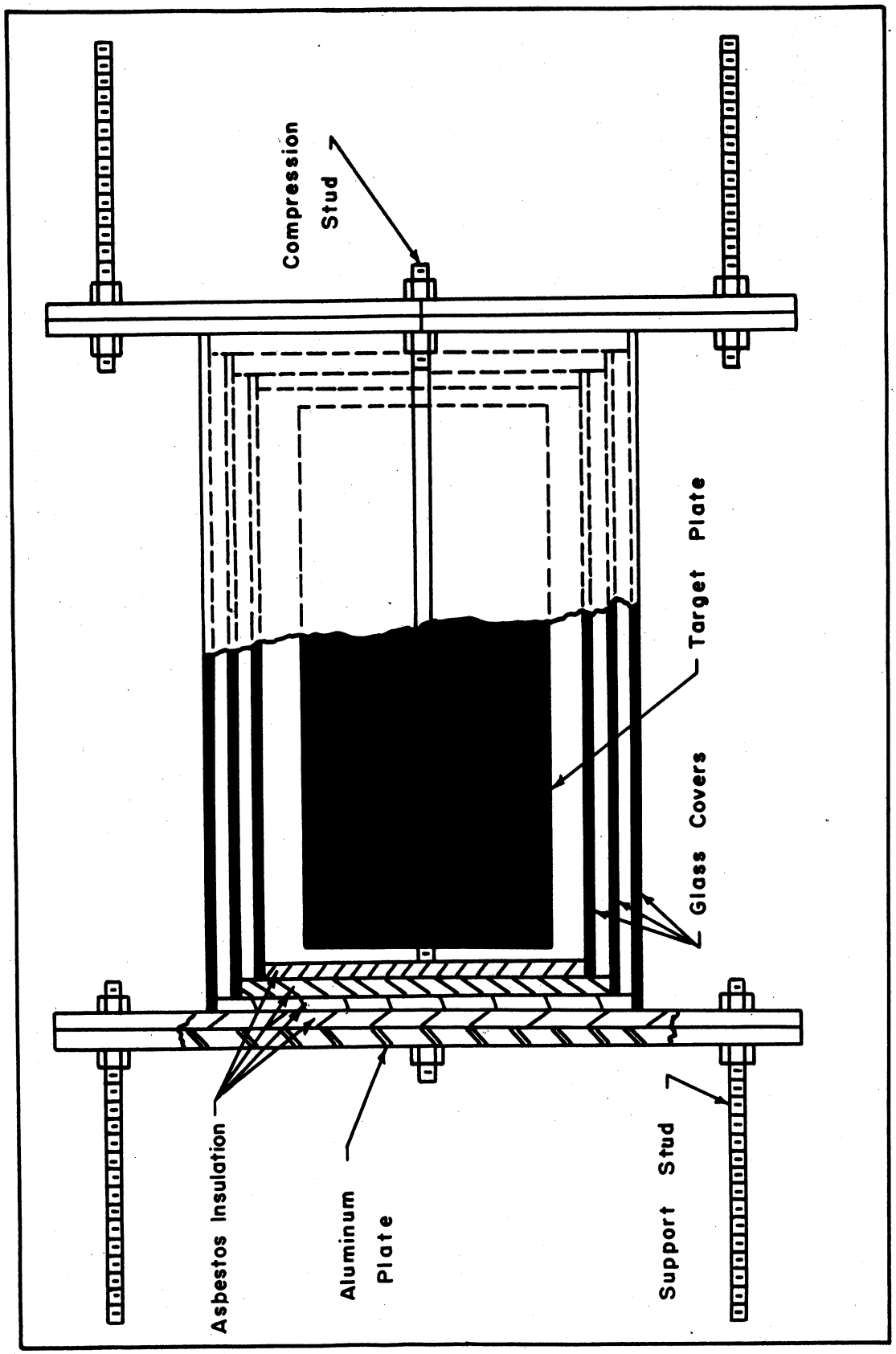

Figure 17. Target Assembly #3.

and in the air spaces between the three cylinders. In addition, thermocouples were placed touching the inside and outside of every cylinder. None of the thermocouples are shown in Figure 17.

APPENDIX

Ideal Maximum Concentration Ratio

For a solar concentrator with a perfect mirror aimed at the sun, the time rate of radiation in Btu/hr falling on the mirror equals the time rate of radiation in Btu/hr reaching the target area.

$$Q_m = Q_t \tag{1}$$

This could be written as

$$\frac{Q_m}{A_{nm'}} \times A_{nm'} = \frac{Q_t}{A_{tr}} \times A_{tr} \tag{2}$$

Rearranging yields

$$\frac{\frac{Q_{tr}}{A_{tr}}}{\frac{Q_m}{A_{nm'}}} = \frac{A_{nm'}}{A_{tr}} = \text{concentration} = C \tag{3}$$

Thus the concentration ratio C is equal to the time rate of radiation per unit area of target receiving radiation divided by the time rate of radiation per unit of normal mirror area.

Maximum Concentration for Flat Plate Target
(Approximation for small n)

Under the assumption that all rays from the sun hit the mirror very near the mirror axis of symmetry, an approximate maximum concentration ratio can be developed as follows. The concentration is

$$C = \frac{A_{nm'}}{A_{tr}} \tag{1}$$

For a target and mirror of length L Equation (1) is

$$C = \frac{D \times L}{d \times L} = \frac{D}{d} \tag{2}$$

Where d is the least width of a flat plate that will just contain all of the sun's image. From the figure it is seen that

$$\tan \frac{\alpha}{2} = \frac{\frac{d}{2}}{f} \tag{3}$$

or

$$d = 2f \tan \frac{\alpha}{2} \tag{4}$$

Thus Equation (2) becomes

$$C = \frac{D}{2f \tan \frac{\alpha}{2}} \tag{5}$$

The relative aperture n of a mirror is defined by

$$n = \frac{D}{f} \tag{6}$$

Thus the concentration becomes

$$C = \frac{n}{2\tan \frac{\alpha}{2}} \tag{7}$$

Since the sun subtends an angle of $\alpha \sim 32'$ Equation (7) becomes

$$C = 107.53n \tag{8}$$

This equation gives approximate answers that are good only for small n, and gives the maximum concentration obtainable for a target that uses all of the energy falling on the mirror.

Maximum Concentration for a Cylindrical Target
(Exact for all n)

The concentration is determined by the widest solar image that falls on the target cylinder at the focus. The largest image comes from the extreme edge of the mirror; thus if the mirror and target have a length of L

$$C = \frac{A_{nm'}}{A_{tr}} = \frac{D \times L}{\pi d' L} = \frac{D}{\pi d'} \tag{1}$$

The equation of the mirror parabola is

$$x^2 = 4fy \tag{2}$$

For conditions at the edge of the mirror that determine the cylinder diameter of the target $D = 2x_m$ or

$$(\frac{D}{2})^2 = 4fy_m \tag{3}$$

or

$$y_m = \frac{D^2}{16f} = \frac{nD}{16} \tag{4}$$

From the figure it is seen

$$\sin\frac{\alpha}{2} = \frac{\frac{d'}{2}}{\ell_m} \tag{5}$$

or

$$d' = 2\ell_m \sin\frac{\alpha}{2} \tag{6}$$

However, ℓ_m at the extreme section of the mirror is equal to

$$\ell_m = \sqrt{x_m^2 + (f-y_m)^2} = \sqrt{\frac{D^2}{4} + (f-y_m)^2} \tag{7}$$

$$\ell_m = \sqrt{4fy_m + f^2 - 2fy_m + y_m^2} \tag{8}$$

$$\ell_m = (f + y_m) = (f + \frac{nD}{16}) = f(1 + \frac{n^2}{16}) \tag{9}$$

Thus the concentration becomes

$$C = \frac{D}{\pi d'} = \frac{D}{\pi 2\ \ell_m \sin\frac{\alpha}{2}} = \frac{D}{\pi 2f(1+\frac{n^2}{16})\sin\frac{\alpha}{2}} \tag{10}$$

$$C = \frac{n}{2\pi(1+\frac{n^2}{16})\sin\frac{\alpha}{2}} \tag{11}$$

or

$$C = \frac{107.53n}{\pi(1+\frac{n^2}{16})} \tag{12}$$

To find the n for maximum concentration, take the derivative of C with respect to n and set it equal to 0

$$C = \frac{An}{(1+\frac{n^2}{16})} \tag{13}$$

$$\frac{dC}{dn} = 0 = A\left[-1(n)(1+\frac{n^2}{16})^{-2}(2n)+(1+\frac{n^2}{16})^{-1}\right] \tag{14}$$

$$0 = \frac{-2n^2}{16} + 1 + \frac{n^2}{16} \Big/ (1+\frac{n^2}{16})^2 \tag{15}$$

or

$$\frac{2n^2}{16} = 1 + \frac{n^2}{16}$$

$$n^2 = 16$$

$$n = \pm 4 \tag{16}$$

The -4 has no significance; thus, the maximum concentration obtainable for a mirror with a cylindrical target that receives all of the radiation from a mirror has an n of 4. Thus, the maximum concentration of any mirror with a cylindrical target is

$$C = \frac{107.53 \times 4}{\pi(1+\frac{4^2}{16})} = \frac{215.06}{\pi} \tag{17}$$

Maximum Concentration for a Flat Plate Target - Approximation for Medium n

The concentration is determined by the widest solar image that falls on the target at the focus. As in the case of a cylindrical target, the largest image comes from the extreme edge of the mirror; thus, if the mirror and target have a length of L

$$C = \frac{A_{nm'}}{A_{tr}} = \frac{DxL}{d''xL} = \frac{D}{d''} \tag{1}$$

In the figure, γ_1 is an angle of 89°44' and γ_2 is an angle of 90°16'. If γ_1 and γ_2 can be approximated by 90°, then from the figure we get

$$\cos\beta = \frac{\frac{d'}{2}}{\frac{d''}{2}} = \frac{d'}{d''} \tag{2}$$

The concentration becomes

$$C = \frac{D\cos\beta}{d'} \tag{3}$$

on the mirror surface

$$x^2 = 4fy \tag{4}$$

or when at the position that gives the largest image

$$x_m^2 = 4fy_m = (\frac{D}{2})^2 \tag{5}$$

$$y_m = \frac{D^2}{16f} = \frac{nD}{16} \tag{6}$$

In dealing with ℓ

$$\ell^2 = x^2 + (f-y)^2 = 4fy + f^2 - 2fy + y^2 \tag{7}$$

$$\ell = f+y \tag{8}$$

At the largest image

$$\ell_m = f+y_m = (f + \frac{nD}{16}) = f(1+\frac{nD}{16f})$$

$$\ell_m = f(1 + \frac{n^2}{16}) \tag{9}$$

Also

$$\tan\frac{\alpha}{2} = \frac{\frac{d'}{2}}{\ell} \tag{10}$$

and

$$d'_m = 2\ \ell_m \tan\frac{\alpha}{2} \tag{11}$$

β_m for largest image is determined at the edge of the mirror

$$\cos\beta_m = \frac{f-y_m}{\ell_m} = \frac{f-\frac{nD}{16}}{f(1+\frac{n^2}{16})} = \frac{(1-\frac{n^2}{16})}{(1+\frac{n^2}{16})} \tag{12}$$

Therefore

$$C = \frac{D}{2f(1+\frac{n^2}{16})\tan\frac{\alpha}{2}} \times \frac{(1-\frac{n^2}{16})}{(1+\frac{n^2}{16})} \tag{13}$$

Thus, the approximate concentration for a flat plate is given by

$$C = \frac{n(1-\frac{n^2}{16})}{2(1+\frac{n^2}{16})\tan\frac{\alpha}{2}} = \frac{107.53\ n(1-\frac{n^2}{16})}{(1+\frac{n^2}{16})} \tag{14}$$

To find the maximum concentration possible, take the derivative of C with respect to n and set it equal to 0; thus

$$\frac{dC}{dn} = 0 = \frac{1}{2\tan\frac{\alpha}{2}}\left[n(1-\frac{n^2}{16})(-2)(1+\frac{n^2}{16})^{-3}(\frac{2n}{16}) + (1+\frac{n^2}{16})^{-2}(1-\frac{3n^2}{16})\right] \tag{15}$$

or

$$0 = \frac{-\frac{4n^2}{16}\left(1-\frac{n^2}{16}\right)+\left(1+\frac{n^2}{16}\right)\left(1-\frac{3n^2}{16}\right)}{\left(1+\frac{n^2}{16}\right)^3} \quad (16)$$

$$0 = -\frac{4n^2}{16} + \frac{4n^4}{256} + 1 - \frac{3n^2}{16} + \frac{n^2}{16} - \frac{3n^4}{256} \quad (17)$$

$$n^4 - 96n^2 + 256 = 0 \quad (18)$$

It follows then

$$n^2 = 16(3 \pm \sqrt{8}) \quad (19)$$

$$n = \pm \sqrt[4]{3 \pm \sqrt{8}} \quad (20)$$

Throwing aside answers giving minus relative apertures

$$n = \sqrt[4]{3 \pm \sqrt{8}} \quad (21)$$

or

$$n = 1.65,\ 9.64 \quad (22)$$

The n of 9.64 gives a minus concentration and dropping this solution one obtains the optimum n to be

$$n = 1.65 \quad (23)$$

Putting this n in Equation (14) one obtains

$$C = \frac{1.65}{2\tan\frac{\alpha}{2}} \times \frac{\left(1 - \frac{1.65^2}{16}\right)}{\left(1 + \frac{1.65^2}{16}\right)} \cong \frac{1}{2\tan\frac{\alpha}{2}} \quad (24)$$

$$C = 107.53 \quad (25)$$

Maximum Concentration for a Flat Plate Target - Exact Derivation for All n

The concentration is determined by the widest solar image that falls on the target at the focus. As in previous cases, the largest image comes from the extreme edge of the mirror. However, the envelope of all solar images is formed by the light that travels along the angle $\beta + \alpha/2$, since these rays form a longer image on a flat target placed perpendicular to the axis of symmetry. Thus, it is seen from the figure

$$C = \frac{A_{nm'}}{A_{tr}} = \frac{DxL}{d'''xL} = \frac{D}{d'''} \tag{1}$$

but at the edge of the mirror

$$\tan(\beta_m + \frac{\alpha}{2}) = \frac{\frac{D}{2} + \frac{d'''_m}{2}}{f-y_m} = \frac{D}{2(f-y_m)} + \frac{d'''_m}{2(f-y_m)} \tag{2}$$

and

$$\tan\beta_m = \frac{D}{2(f-y_m)} \tag{3}$$

therefore

$$d'''_m = 2(f-y_m)\left[\tan(\beta_m + \frac{\alpha}{2}) - \tan\beta_m\right] \tag{4}$$

and the concentration becomes

$$C = \frac{D}{2(f-y_m)\left[\tan(\beta_m + \frac{\alpha}{2}) - \tan\beta_m\right]} \tag{5}$$

at the edge of the mirror

$$x_m^2 = 4fy_m \tag{6}$$

and

$$y_m = \frac{x_m^2}{4f} = (\frac{D}{2})^2 \times \frac{1}{4f} = \frac{D^2}{16f} = \frac{nD}{16} \tag{7}$$

Thus

$$(f-y_m) = f-\frac{nD}{16} = f-\frac{nfD}{16f} = f(1-\frac{n^2}{16}) \tag{8}$$

Substitution in Equation (5) yields

$$C = \frac{D}{2f(1-\frac{n^2}{16}) \quad \tan(\beta_m + \frac{\alpha}{2}) - \tan\beta_m} \tag{9}$$

This may be written

$$C = \frac{n}{2(1-\frac{n^2}{16}) \left[\frac{\tan\beta_m + \tan\frac{\alpha}{2}}{1 - \tan\beta_m \tan\frac{\alpha}{2}} - \tan\beta_m\right]} \tag{10}$$

or

$$C = \frac{n\left[1-\tan\beta_m\tan\frac{\alpha}{2}\right]}{2(1-\frac{n^2}{16})\left[\tan\beta_m + \tan\frac{\alpha}{2} - \tan\beta_m + \tan^2\beta_m\tan\frac{\alpha}{2}\right]} \tag{11}$$

This in turn may be written

$$C = \frac{n\left[1-\tan\beta_m\tan\frac{\alpha}{2}\right]}{2\tan\frac{\alpha}{2}(1-\frac{n^2}{16})\left[1+\tan^2\beta_m\right]}$$

$$C = \frac{n\left[1-\tan\beta_m\tan\frac{\alpha}{2}\right]}{2\tan\frac{\alpha}{2}(1-\frac{n^2}{16})\left[\frac{1}{\cos^2\beta_m}\right]} \tag{12}$$

From the figure it is seen

$$\cos^2\beta_m = \frac{(f-y_m)^2}{(\ell_m)^2} = \frac{(1-\frac{n^2}{16})^2}{(1+\frac{n^2}{16})^2} \tag{13}$$

and

$$\tan\beta_m = \frac{D}{2(f-y_m)} = \frac{D}{2f(1-\frac{n^2}{16})} = \frac{n}{2(1-\frac{n^2}{16})} \tag{14}$$

Thus

$$C = \frac{n\left[1-\frac{n\tan\frac{\alpha}{2}}{2(1-\frac{n^2}{16})}\right]}{2\tan\frac{\alpha}{2}\,(1-\frac{n^2}{16})\,\frac{(1+\frac{n^2}{16})^2}{(1-\frac{n^2}{16})^2}} \tag{15}$$

or

$$C = \frac{n(1-\frac{n^2}{16})\left[1-\frac{n\tan\frac{\alpha}{2}}{2(1-\frac{n^2}{16})}\right]}{2\tan\frac{\alpha}{2}(1+\frac{n^2}{16})^2} \tag{16}$$

or

$$C = \frac{n\left[1-\frac{n^2}{16}-\frac{n}{2}\tan\frac{\alpha}{2}\right]}{2\tan\frac{\alpha}{2}\,(1+\frac{n^2}{16})^2} \tag{17}$$

This may be written as

$$C = \frac{107.53\,n\left[1-\frac{n^2}{16}-\frac{n}{430.12}\right]}{(1+\frac{n^2}{16})^2} \tag{18}$$

To find the best concentration possible for any mirror having a flat plate target in Equation (18), set the derivative of C with respect to n equal to 0

$$C = \frac{A\left[n - \frac{n^3}{16} - \frac{n^2}{4A}\right]}{\left(1+\frac{n^2}{16}\right)^2} \tag{19}$$

Let $A = \frac{1}{2\tan\frac{\alpha}{2}}$

$$\frac{dC}{dn} = 0 = A\left[\left(n - \frac{n^3}{16} - \frac{n^2}{4A}\right)(-2)\left(1+\frac{n^2}{16}\right)^{-3}\left(\frac{2n}{16}\right)+\left(1+\frac{n^2}{16}\right)^{-2}\left(1-\frac{3n^2}{16} - \frac{2n}{4A}\right)\right] \tag{20}$$

or

$$0 = \frac{\left(n - \frac{n^3}{16} - \frac{n^2}{4A}\right)\left(\frac{-4n}{16}\right)+\left(1+\frac{n^2}{16}\right)\left(1-\frac{3n^2}{16} - \frac{2n}{4A}\right)}{\left(1+\frac{n^2}{16}\right)^3} \tag{21}$$

which reduces to

$$\frac{n^4}{256} + \frac{n^3}{32A} - \frac{6n^2}{16} - \frac{2n}{4A} + 1 = 0 \tag{22}$$

or

$$n^4 + \frac{8n^3}{A} - 96n^2 - \frac{128n}{A} + 1 = 0 \tag{23}$$

The pertinent optimum n is

$$n \sim 1.645 \tag{24}$$

This is seen to differ only a little from the approximate solution.

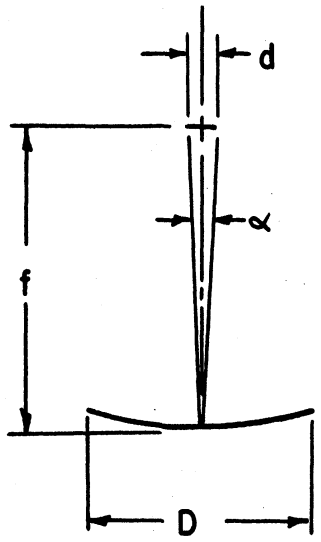

Figure 18. Ideal Maximum Concentration Ratio (Approximation for small n).

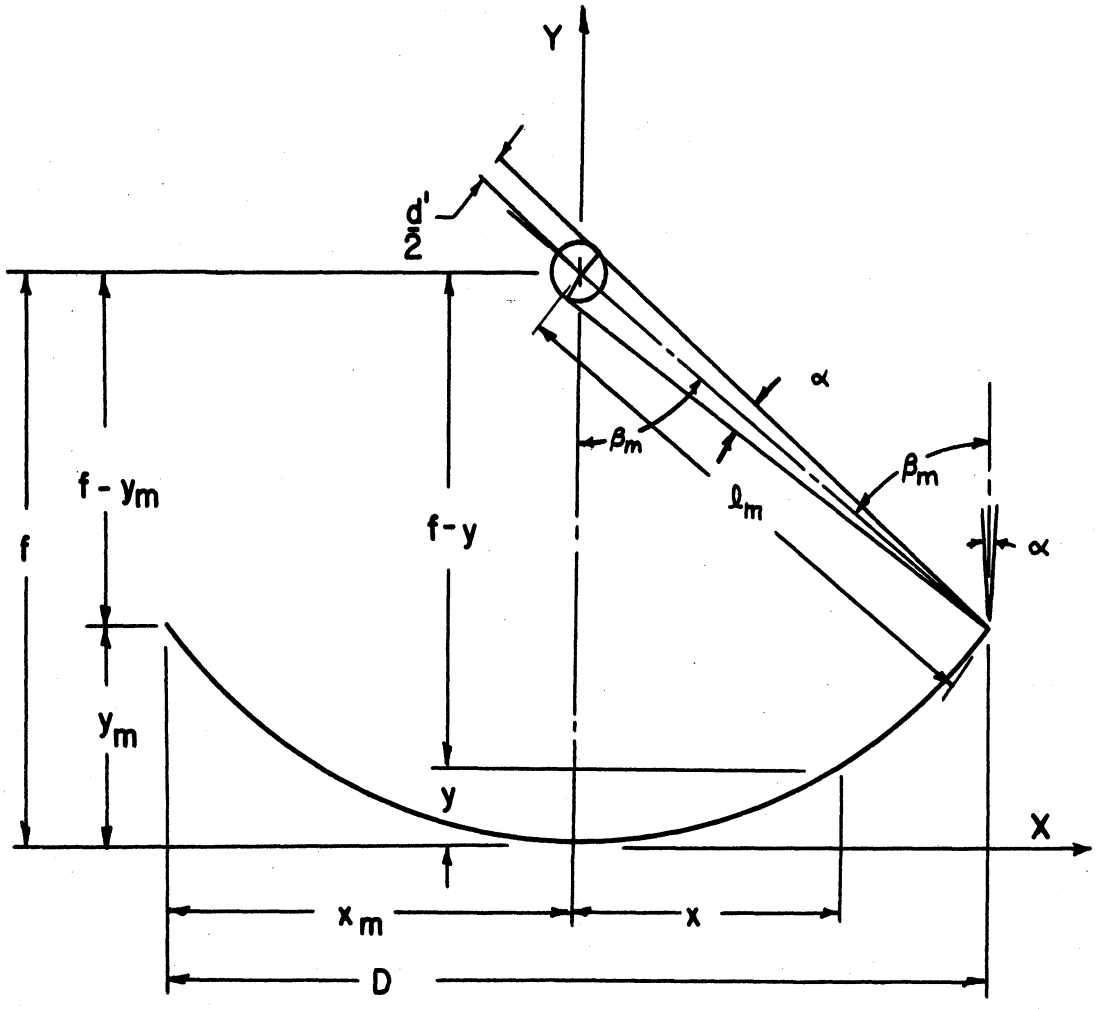

Figure 19. Maximum Concentration Ratio for a Cylindrical Target (Exact for all n).

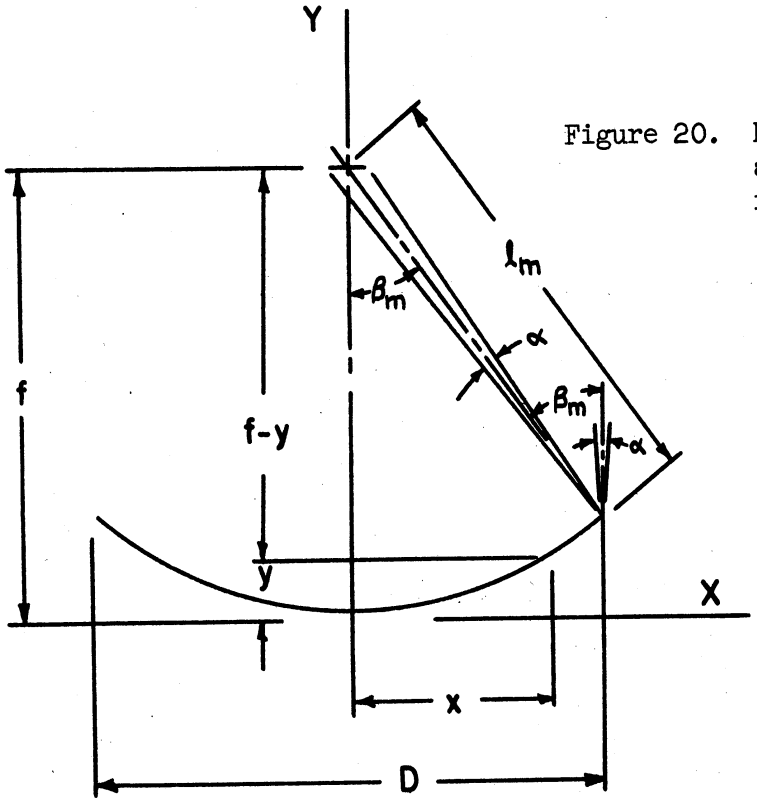

Figure 20. Maximum Concentration Ratio for a Flat Plate Target (Approximation for medium n).

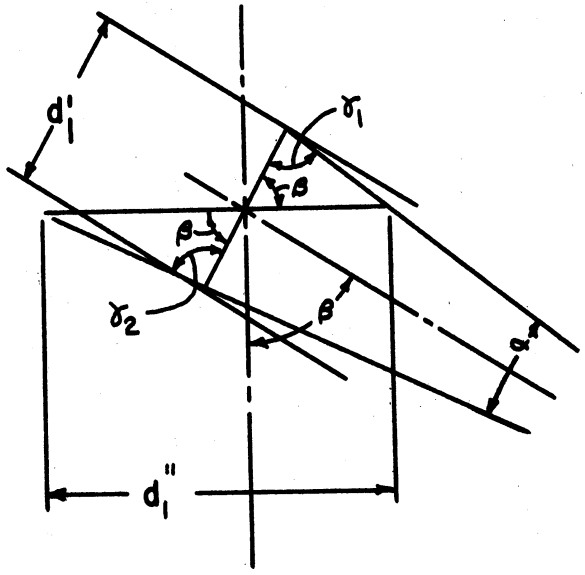

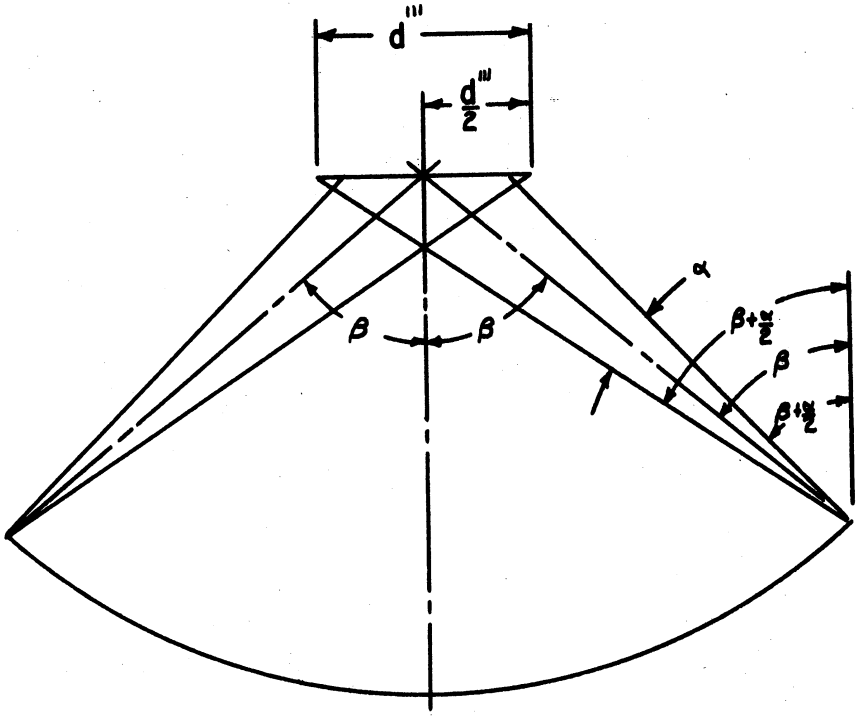

Figure 21. Maximum Concentration Ratio for a Flat Plate Target (Exact for all n).

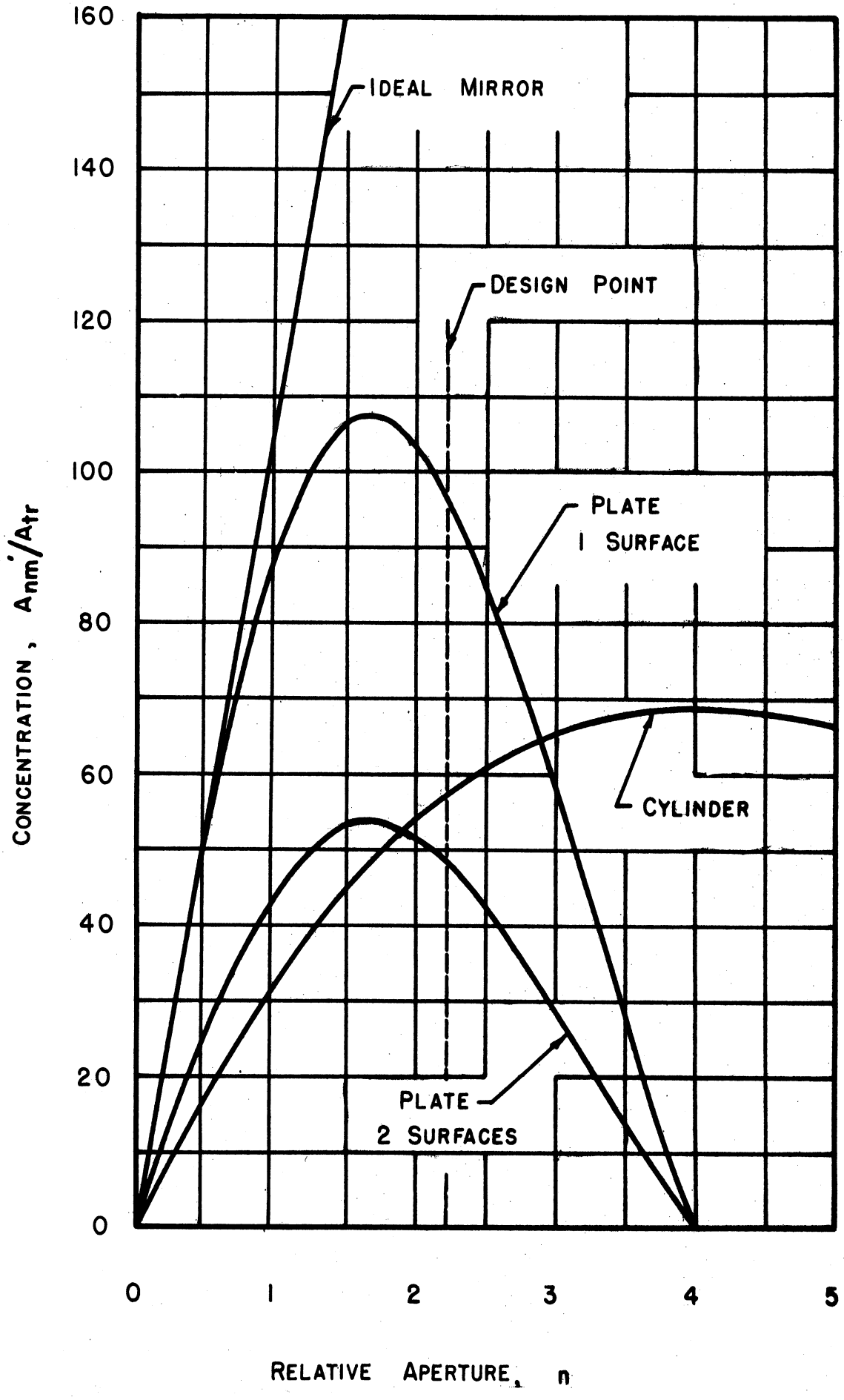

Figure 22. Concentration vs. n.

NOMENCLATURE (Mirror)

$A_{nm'}$ = Area of mirror normal to radiation without target, ft^2

A_{tr} = Area of target receiving radiation, ft^2

C = Concentration, dimensionless

D = Diameter of mirror, ft

d = Ideal diameter of image at the focus, ft

d' = Diameter of image at the focus formed by radiation from the mirror falling on a plane normal to the radiation, ft

d" = Diameter of solar image formed by rays coming from the mirror approaching a flat plate in the focus at an angle of β, ft

$\frac{d'''}{2}$ = Half diameter of solar image formed by rays coming from the mirror approaching a flat plate at the focus between the angle of β and $\beta + \frac{\alpha}{2}$, ft

f = Focal length of mirror, ft

L = Length of mirror, ft.

ℓ = Distance from any point on mirror to focus, ft

m = Subscript denoting maximum (y_m maximum y)

n = Relative aperture ($n = \frac{D}{f}$), dimensionless

Q_m = Rate of radiation falling on mirror, Btu/hr

Q_t = Rate of radiation falling on target, Btu/hr

x = Coordinate of mirror in direction of diameter, ft

y = Coordinate of mirror in direction of axis of symmetry, ft

α = Angle subtended by diameter of sun $\sim$ 32 minutes

β = Angle of incidence of ray to the normal of the mirror surface

γ = Supplementary angle to the angle of incidence of a solar image emanating from the mirror surface measured at the extremity of solar image from a plane normal to the angle β

δ = Declination

BIBLIOGRAPHY

Abbott, C. G., "Solar Power from Collecting Mirrors," Solar Energy Research (University of Wisconsin Press), 1955, pp. 91-95.

Bouchard, Harry, Surveying (Scranton, International Textbook Co.) 1947, pp. 440-441.

Brooks, F. A., "Notes on the Spectral Quality and Measurement of Solar Radiation," Solar Energy Research (University of Wisconsin Press), 1955, pp. 19-29.

Brooks, F. A., Solar Energy and Its Uses for Heating Water, California Bulletin 602 (University of California, Berkeley, California), 1936.

Conn, W. M., "Solar Furnaces for Attaining High Temperatures," Solar Energy Research (University of Wisconsin Press), 1955, pp. 163-167.

Crabb, George A., Jr., Solar Radiation Studies in Michigan, Technical Bulletin 222 (Michigan State College, East Lansing, Michigan), 1950.

Crain, R. W., Sr., Crain, R. W., Jr., Vincent, G. W., Reese, B. O., "A Solar Radiation Apparatus " Conference on Solar Energy--the Scientific Basis (University of Arizona), 1955.

Dietz, Albert G. H., "Diathermanous Materials and Properties of Surfaces," Space Heating with Solar Energy, Proceedings of a course symposium (Massachusetts Institute of Technology), 1950, pp. 25-43.

Duwez, Pol, Tietz, Thomas E., Loh, Eugene, Hiester, Nevin K., Operation and Use of a Lens Type Furnace," Conference on Solar Energy--the Scientific Basis (University of Arizona), 1955.

Farber, J., "Utilization of Solar Energy for the Attainment of High Temperatures," Solar Energy Research (University of Wisconsin Press), 1955, pp. 157-161.

Ghai, M. L., "Small Solar Power Plants," Solar Energy Research (University of Wisconsin Press), 1955, pp. 81-83.

Gurley, W. and Gurley, L. E., 1958 Gurley Ephemeris (Gurley Engineering Instruments, Troy, New York), 1958, pp. 41-53.

Hand, I. F., Pyrheliometers and Pyrheliometric Measurements, United States Department of Commerce, 1946.

Hottel, Hoyt C. and Woertz, B. B., "The Performance of Flat Plate Solar Heat Collectors," Transactions American Society of Mechnaical Engineers, 1942, 64, 91-104.

Hynek, J. Allen, "The Use of Optical Systems in the Utilization of Solar Energy," The Ohio Journal of Science (Ohio State University and Ohio Academy of Science, Columbus, Ohio), September, 1953, pp. 314-319.

Jakob, Max, Heat Transfer (John Wiley & Sons, New York), 1955, Vol. 1.

Jordan, Richard C., "Mechanical Energy from Solar Energy," World Symposium on Applied Solar Energy (Phoenix, Arizona), 1955, pp. 81-101.

Kimball, H. H. and Hobbs, H. E., "A New Form of Thermoelectric Recording Pyrheliometer," Monthly Weather Review, Vol. 51, No. 5, W. B. 806, May, 1923, pp. 239-242.

Marks, Linonel S., Mechanical Engineers Handbook (McGraw-Hill Book Co., New York), 1951.

McAdams, W. H., Heat Transmission (McGraw-Hill Book Co., New York), 1954.

Nash, Harry, International Rectifier News RN-955 (International Rectifier Corporation, El Segundo, California), August-September, 1955.

Parmalee, G. V. "A.S.H.V.E. Research on Heat Flow Through Glass and Its Application to Space Heating with Solar Energy," Space Heating with Solar Energy, Proceedings of a course symposium, Massachusetts Institute of Technology), 1950, pp. 44-57.

Robinson, Nathan, "Solar Machines," World Symposium on Applied Solar Energy (Phoenix, Arizona), 1955, pp. 43-61.

Technical Data "Pyrex" Brand Chemical Glass No. 7740 (Corning Glass Works, Corning, New York).

The Eppley Pyrheliometer, Bulletin No. 2 (The Eppley Lab., Inc., Newport, Rhode Island).

Trombe, Felix, "High Temperature Furnaces," World Symposium on Applied Solar Energy (Phoenix, Arizona), 1955, pp. 63-72.

Trombe, Felix, "Development of Larger Scale Solar Furnaces," Solar Energy Research (University of Wisconsin Press), 1955, pp. 169-171.